ISSN: 2712-0570
UDC: 72

AGG+

AGG+ Journal for Architecture, Civil Engineering, Geodesy and Related Scientific Fields / АГГ+ часопис за архитектуру, грађевинарство, геодезију и сродне научне области

2025_Special

Earthquake Engineering

University of Banja Luka, Faculty of Architecture, Civil Engineering and Geodesy
Универзитет у Бањој Луци, Архитектонско-грађевинско-геодетски факултет

University of Banja Luka I Faculty of Architecture, Civil Engineering and Geodesy
ISSN 2712-0570 I UDC 72

AGG+

2025

Special Issue

Earthquake Engineering

AGG+ Journal for Architecture, Civil Engineering, Geodesy and Related Scientific Fields
АГГ+ часопис за архитектуру, грађевинарство, геодезију и сродне научне области

Publisher
University of Banja Luka, Faculty of Architecture, Civil Engineering and Geodesy

Cover
Dubravko Aleksić (design)
Cover photo: @corelens via Canva.com

Proofreading
Jelena Pažin

Circulation 300
ISSN 2712-0570 (Print)
ISSN 2303-6036 (Online)

Print: Vilux Banja Luka

aggplus.aggf.unibl.org

University of Banja Luka I Faculty of Architecture, Civil Engineering and Geodesy
ISSN 2712-0570 I UDC 72

AGG+

2025

Special Issue

Earthquake Engineering

AGG+ Journal for Architecture, Civil Engineering, Geodesy and Related Scientific Fields
АГГ+ часопис за архитектуру, грађевинарство, геодезију и сродне научне области

Gordana Broćeta
University of Banja Luka, Faculty of Architecture, Civil Engineering and Geodesy,
gordana.broceta@aggf.unibl.org

Anđelko Cumbo
University of Banja Luka, Faculty of Architecture, Civil Engineering and Geodesy,
andjelko.cumbo@aggf.unibl.org

INTRODUCTION BY GUEST EDITORS

Earthquakes remain among the most unpredictable and destructive natural hazards, capable of causing widespread human suffering and extensive material damage. Recent seismic events in Türkiye, Syria, and Morocco have once again underscored the devastating consequences of inadequate structural resilience, highlighting the urgent need for improved seismic risk mitigation. Closer to home, the ongoing subduction of the Adriatic microplate beneath the Eurasian Plate continuously stresses the crust of the Western Balkans, generating persistent seismicity across the region. The 2020 Petrinja earthquake in Croatia serves as a stark reminder that our own terrain is not exempt from such hazards. In this context, the imperative to design and construct seismically resilient infrastructure emerges as both a scientific responsibility and a societal necessity.

Developing such resilience demands more than strict adherence to seismic design codes; it requires continuous refinement of national regulations and engineering methodologies, aligned with European frameworks—particularly the Eurocodes. This effort must be underpinned by reliable site-specific seismic inputs, comprehensive geotechnical and structural databases, accurate typology classifications, and the integration of advanced modeling techniques.

This special issue presents six contributions from the fields of civil engineering and geodesy, each addressing seismic hazard from a distinct yet complementary perspective. Together, they illustrate the value of interdisciplinary cooperation in confronting seismic vulnerability with both computational innovation and empirical precision.

In the article “On Simplified Approaches of Seismic Analysis of Tunnels,” E. Zlatanović et al. assess widely used free-field deformation methods alongside Wang’s soil–structure interaction formulations for tunnel design under seismic loading. Through comparative 1D and 2D simulations, the study finds that although these simplified methods tend to conservatively overestimate shear strains and internal forces, they nonetheless provide a transparent and dependable foundation for practical engineering design.

The paper “Numerical Modeling of Tunnel Excavation and Support Using the Deconfinement Method for Static and Seismic Conditions,” by Z. Zafirovski et al., applies the (1–β) deconfinement technique within PLAXIS 2D to simulate staged excavation and support performance under combined loading conditions. Their parametric study confirms a direct relationship between increased deconfinement ratios and rising displacements and internal forces, supporting the method’s reliability for tunnel lining design.

In “The Effect of Masonry Infill Model Selection on the Seismic Response of Reinforced Concrete Frame Structures,” A. Cumbo et al. compare bare frames and various infill configurations to assess seismic response. The findings reveal that non-isolated infill significantly modifies dynamic behavior, introducing soft-story mechanisms and amplifying base shear forces. The authors advocate for updated code provisions and design simplifications using diagonal strut models to ensure both safety and practical implementation.

The study “Environmental Impact Assessment and Seismic Hazard Analysis: Petrinja 2020 Experience,” by B. Kordić et al., synthesizes field observations, GNSS data, InSAR imagery, and paleoseismic trenching to characterize the surface rupture features of the 2020 Mw 6.2 Petrinja earthquake. By identifying the Petrinja–Pokupsko Fault as the principal seismogenic structure, the authors emphasize the necessity of regionally coordinated geological and geophysical investigations to refine hazard models across national borders.

The paper “Modeling Tectonic Movements Using the Kalman Filter on GNSS Coordinate Time Series,” by V. Janković et al., integrates Kalman filtering with seasonal-trend models to analyze GNSS time

series from Japan. Capturing complex horizontal displacements and coseismic offsets during the 2011 Tōhoku earthquake, the study demonstrates the robustness of filtered GNSS trajectories in mapping crustal deformation and informing seismic risk assessments.

Finally, “Tectonic Geodesy as Supplement Data in Seismology,” by T. Đukanović et al., focuses on GNSS observations from the SRJV station in Sarajevo, which indicate a northeastward motion of approximately 28 mm/year. Highlighting the sparse spatial distribution of geodetic instrumentation in Bosnia and Herzegovina, the authors call for a densified GNSS network and better integration with seismic and geological data to support hazard mapping and earthquake-resilient urban development.

Taken together, these six contributions establish a dynamic dialogue between civil engineering and geodesy on the topic of earthquake resilience. The geographic focus on the Western Balkans – particularly Bosnia and Herzegovina – adds both urgency and relevance, as this region lies within a high-risk seismic zone shaped by complex tectonic interactions. The collective scientific value of this issue lies in its ability to unify multiscale insights ranging from conservative yet practical equations for tunnel design, through nonlinear structural modeling and staged excavation simulations, to high-rate GNSS data for crustal motion monitoring and fault characterization.

Together, these studies forge a coherent toolbox for seismic hazard assessment: benchmarking simplified tunnel design methods against advanced soil–structure interaction models; validating deconfinement-based simulations for staged excavation; and clarifying how infill assumptions reshape seismic demand in reinforced concrete frames. Field-to-satellite analyses of the 2020 Petrinja earthquake, Kalman-filtered GNSS time series from Japan, and GNSS network evaluations for Bosnia and Herzegovina collectively demonstrate that high-resolution geodetic data are indispensable for quantifying ground deformation before, during, and after seismic events. By bridging the scale from tunnel lining stresses to plate-boundary dynamics, the papers underscore the importance of aligning simplified engineering rules with data-driven geophysical models to improve seismic hazard assessments and regulatory frameworks.

Ultimately, this issue advances the state of practice toward performance-based, geo-referenced earthquake engineering that is both computationally efficient and empirically grounded.

EDITORS’ BIOGRAPHIES

Gordana Broćeta

Gordana Broćeta, PhD, earned her master's and doctoral degrees in the field of Building Materials and Structures at the Faculty of Architecture, Civil Engineering, and Geodesy of the University of Banja Luka, where she currently works as a lecturer with the title of associate professor. She has gained extensive experience in designing concrete composites, as well as in examining and assessing the condition of concrete structures. Her scientific research focuses on influential factors that affect various aspects of the durability of concrete structures.

Anđelko Cumbo

Anđelko Cumbo, PhD, earned his doctoral degree at the Faculty of Civil Engineering and Architecture at the University of Niš and obtained his master's degree at the Faculty of Technical Sciences at the University of Novi Sad. He has gained several years of professional experience in the design, assessment, and examination of bridge and building structures. In his research work, he focuses on the development of computational modelling for the analysis of complex composite structures, as well as the analysis and modelling of structures under strong earthquakes. This includes the behaviour and strengthening of retrofitted and older structures. He has published scientific and professional papers in recognized journals and conferences in these fields.

Aerial view of tunnel with trains - Erie Railway, Otisville Tunnel, Sanitarium Road to Otisville Road, Otisville, Orange County, NY. Photographer: Boucher, Jack, 1968. Source: https://www.loc.gov/pictures/item/ny1220.photos.121395p/ (Wikimedia Commons)

University of Banja Luka I Faculty of Architecture, Civil Engineering and Geodesy
ISSN 2712-0570 I UDC 72

2025
Special Issue

Earthquake Engineering

AGG+ Journal for Architecture, Civil Engineering, Geodesy and Related Scientific Fields
АГГ+ часопис за архитектуру, грађевинарство, геодезију и сродне научне области

002-028 **Categorisation** I Review scientific paper
DOI I 10.61892/AGG202502004Z
Paper received I 19/02/2024
Paper accepted I 23/04/2024

Elefterija Zlatanović
University of Niš, Faculty of Civil Engineering and Architecture, Serbia,
elefterija.zlatanovic@gaf.ni.ac.rs

Zoran Bonić
University of Niš, Faculty of Civil Engineering and Architecture, Serbia,
zoran.bonic@gaf.ni.ac.rs

Nemanja Marinković
University of Niš, Faculty of Civil Engineering and Architecture, Serbia,
nemanja.marinkovic@gaf.ni.ac.rs

Nikola Romić
University of Niš, Faculty of Civil Engineering and Architecture, Serbia,
nikola.romic@gaf.ni.ac.rs

ON SIMPLIFIED APPROACHES OF SEISMIC ANALYSIS OF TUNNELS

Review scientific paper
DOI 10.61892/AGG202502004Z
Paper received I 19/02/2024
Paper accepted I 23/04/2024

* corresponding author

Elefterija Zlatanović *
University of Niš, Faculty of Civil Engineering and Architecture, Serbia, elefterija.zlatanovic@gaf.ni.ac.rs

Zoran Bonić
University of Niš, Faculty of Civil Engineering and Architecture, Serbia, zoran.bonic@gaf.ni.ac.rs

Nemanja Marinković
University of Niš, Faculty of Civil Engineering and Architecture, Serbia, nemanja.marinkovic@gaf.ni.ac.rs

Nikola Romić
University of Niš, Faculty of Civil Engineering and Architecture, Serbia, nikola.romic@gaf.ni.ac.rs

ON SIMPLIFIED APPROACHES OF SEISMIC ANALYSIS OF TUNNELS

ABSTRACT

Overview of current progress in the field of seismic regulations for the design of tunnel structures revealed that, despite significant progress in research work on seismic analysis of tunnels over the past few decades, however, a deficiency of systematic and precisely defined rules for the seismic design of tunnels still exists even in the most developed societies. Precisely for this reason, a great effort has recently been made in this research field in terms of finding simple approaches of the seismic analysis of tunnels that could be implemented in design codes and thus serve designers in everyday engineering practice. The response of tunnel structures to earthquake excitation is primarily conditioned by the strain field in the surrounding ground. The simplest approach in seismic analysis of tunnels is based on the assumption that deformations in the circular tunnel are identical to the deformations of the ground induced by seismic waves in its natural state, without tunnel excavation (the so-called "free-field deformation approach"). In addition, seismic design of tunnel structures taking into account the effects of soil–structure interaction is becoming increasingly important nowadays, because the effects of the interaction between the structure and the surrounding gorund can cause greater external forces on the tunnel structure (the so-called "soil–structure interaction approach"). The present study considers the most frequently used simple analytical expressions, regarding the idealised tunnel geometry and ground properties, for calculating the relevant design soil shear strain that occurs between the depths that correspond to the tunnel crown and the invert, on the one hand, and for determining the seismically induced forces in the tunnel lining taking into account the soil–structure interaction effects, on the other hand. Furthermore, in order to evaluate the ability of the analytical expressions to simulate the most important aspects of the seismic behaviour of tunnels, numerical analyses were also carried out by one-dimensional free-field ground response analysis in the code EERA and by the simplified dynamic soil–structure interaction analysis in the software ANSYS, respectively. Lastly, the results obtained by the simple analytical and numerical approaches were evaluated, considering the main soil types – stiff soil with good properties and soft saturated soil with poor properties.

Keywords: *circular tunnel, earthquake, design codes, seismic analysis, simplified approaches*

1. INTRODUCTION

Traffic infrastructure, of which tunnels are integral parts, is considered of great significance when considering the risk of strong earthquakes. The availability of roads affects the speed and extent of emergency measures to be taken in emergency and relief operations immediately after an earthquake. Furthermore, earthquake-induced damage to infrastructure may seriously affect the earthquake-affected region's economy due to the time required to restore network functionality. In addition, underground structures are often located beneath densely populated urban areas. Considering all abovementioned facts, tunnel structures require very high standards regarding their stability, safety, and reliability [1]. In this regard, in the following part, a brief overview of the current progress in the field of seismic regulations for the design of tunnel structures is presented.

After the Hyogoken Nanbu (Kobe) Earthquake in 1995, which was the first case of serious damage to modern underground structures caused by an earthquake**, earthquake-resistant design regulations in Japan** were revised by defining two levels of design: low-to-moderate earthquakes and strong earthquakes. In the "Standard Specifications for Tunneling" [2], published by the Japan Society of Civil Engineers, mountain tunnels, shield tunnels, and cut-and-cover tunnels are discussed. According to "Standard Specifications for Concrete Structures - Design" [3], it is recommended to consider the usage of structures and materials designed to increase flexibility, with an aim to maintain the required seismic behaviour of underground structures. Therefore, especially for the seismic analysis of shield tunnels, based on the seismic deformation method, calculation approaches using the bedded-beam model [4] with appropriate ground springs and structural joint- springs are proposed with the use of elastic analysis.

Despite the fact that **seismic design regulations in the United States of America** are highly developed, there is still a lack of adequate codes in the field of seismic design of tunnels. Recommendations of the American Society of Civil Engineers provided within the code ASCE/SEI 7-10 “Minimum Design Loads for Buildings and Other Structures” [5], are not dealing with tunnel structures (Chapter 15 "Seismic design requirements for non-building structures" states that underground lines and their appurtenances are not included in the scope of requirements for non-building structures). For tunnel structures, Chapter 13 of the "Technical Manual for the Design and Construction of Road Tunnels" [6], proposed by the Federal Highway Administration, provides good practice. It provides a general procedure for the seismic design and analysis of underground structures based primarily on the ground deformation method, which is the opposite of the inertial force approach typical for aboveground structures. Consequently, tunnel structures should be designed to conform the surrounding ground deformations. Yet, this procedure is only a recommendation, it is not a standard or regulation.

Standards for the seismic design of structures in the countries of the European Union are presented within Eurocode 8. The European Standard EN 1998-4 “Eurocode 8: Design of structures for earthquake resistance – Part 4: Silos, tanks, and pipelines” specifies the principles and rules for the seismic design of aboveground and underground pipeline systems, storage tanks, and silos of different types and uses [7]. Moreover, in the European Standard EN 1998-5 “Eurocode 8: Design of structures for earthquake resistance: Foundations, retaining structures, and geotechnical aspects” [8], as part 5 of the European Seismic Regulation, requirements, criteria, and rules are defined for the design of various earthquake-resistant foundation systems and retaining structures, as well as for the

seismically induced soil–structure interaction. However, provisions related to the seismic design of tunnels are not provided for in these standards.

The **seismic design code in the Russian Federation** SP14.13330.2014 [9] are the newest version of the previous seismic design code SniP II-7-81. Unlike European standards, it represent a single document embracing everything from foundation structures to fire protection. Section 7.9 of the code is dedicated to tunnel structures, recommending the application of the corresponding type of tunnel lining depending on the level of seismicity, as well as the use of anti-seismic expansion joints. Given the calculation procedure, in Section 8.4 the effect of earthquakes is defined to some extent through the appropriate dynamic coefficients.

Design standards in the Republic of Serbia are prepared in accordance with the aforementioned European norms and accompanying documents. In the field of seismic design, there are SRPS EN 1998-4 [10] and SRPS EN 1998-5 [11], and they are related to the corresponding European norms. Consequently, as in the case of Eurocode 8, the SRPS standards and guidelines do not specifically deal with the issue of seismic design of underground structures. The "Collection of Yugoslav regulations and standards for engineering constructions" [12] was previously published, in which a draft version of the "Regulations on technical rules for the design and calculation of engineering structures in seismic areas" was created as part of the "Actions on structures" section. This version of the regulations provided a methodology for determining the seismic pressure of the ground on underground and buried structures. It was the beginning of raising awareness about the importance of aseismic design of tunnel structures, as well as the beginning of placing this issue within the framework of standards. Despite this concept, which at that time represented a great advance in the standardisation practice, unfortunately, this draft version remained at the level of ideas and proposals and never entered into force.

On the basis of the presented short review on the current standards and codes for aseismic design of structures, it can be concluded that there is a deficiency of systematic and precisely defined rules for the seismic design of tunnels. It is obvious that even in the most developed societies there is a noticeable discrepancy between the currently valid regulations for tunnel structures, especially with regard to earthquake activity, and the requirements for the design and construction of safe and cost-effective underground structures. Moreover, considering twin-tunnels, it should be noted that research on the mutual influence of closely located tunnels, where the aspect of their minimum seismically safe distance should be of utmost importance, is still at an initial level [13]–[15]. Accordingly, it should be said that we have a serious task ahead of us. This study attempted to improve this situation, as it deals with the review and evaluation of simple approaches to the seismic analysis of single tunnels that could be considered in seismic design codes for tunnels and thus serve in daily engineering practice.

2. METHODS OF SEISMIC RESPONSE ANALYSIS OF TUNNELS

Tunnel structures have characteristics by which their seismic behaviour differs from most aboveground structures, such as their complete constraint by the surrounding medium (soil or rock) and their considerable length. Aboveground structures are designed to accommodate the inertial forces induced by ground accelerations with focus on inertial effects of the structure itself (Seismic Force Method), which is completely opposite to the

design of tunnels, in which case seismic design loads are defined by stresses and strains imposed on the tunnel structure by the surrounding ground (Seismic Deformation Method).

The seismic response of underground structures may be assessed using two approaches: the "*free-field deformation approach*" and the "*soil–structure interaction approach*" [16]. These two approaches include different sub-methods with different levels of approximation, which depends on the design stage, as well as knowledge of geological conditions and geotechnical parameters. Regarding the types of analyses, they may be grouped into three categories: "*pseudo-static*", "*simplified dynamic*", and "*full (detailed) dynamic analysis*", depending on the desired level of complexity related to the selected model, soil characterisation, and seismic input description.

2.1. FREE-FIELD DEFORMATION APPROACH

The simplest approach is the so-called the "free-field ground deformation" approach. The term "free-field deformation" refers to ground deformations caused by seismic waves in the absence of tunnel excavations or structures, meaning that this approach does not take into consideration the interaction between the underground structure and the surrounding ground. However, it can provide a simple and fast first-order estimate of the predicted structure deformation. So the essence of the procedure is that free-field ground deformations due to the seismic event are evaluated and the underground structure is designed to accommodate these deformations.

Given the level of approximation, deformations of the structure using this approach may be overestimated or underestimated, which primarily depends on the stiffness of the structure relative to the ground stiffness. The results are satisfactory for the cases of low levels of shaking, the tunnel structure in a rock medium, or when the tunnel structure is flexible in comparison with the surrounding ground (such as the case of a tunnel in a rock medium, in which case the stiff surrounding ground deformations cannot be affected considerably by the stiffness of the structure). Yet, in many other cases, particularly in the case of soft soils, this method yields conservative design, since free-field deformations in soft soils are in general quite large.

2.1.1. Closed-form elastic solutions for circular tunnels (pseudo-static analysis)

Simplified closed-form elastic solutions are fruitful for obtaining an initial assessment of tunnel deformations. These simplified methods are based on the assumption that the seismic wave field is a field of plane waves, which have the same amplitudes at all locations along the tunnel's length and differ only in their arrival time. Thus, the complex three-dimensional wave propagation and scattering that lead to differences in wave amplitudes along the tunnel's length are not taken into consideration, although this ground motion incoherence may enlarge stresses and deformations in the tunnel's longitudinal direction. Therefore, the results of analyses based on the plane wave propagation assumptions have to be interpreted with a great caution.

The component that has the most significant effect upon the tunnel lining under the action of earthquakes is the ovaling deformation (ovalisation), with vertically propagating shear S-waves being predominant form of seismic loading that causes these types of deformations. The results of the ovaling deformation are cycles of additional stress concentrations with alternating compressive and tensile stresses in the tunnel lining, whereby the following critical modes are possible:

- compressive dynamic stresses added to the compressive static stresses can locally exceed the compressive strength of the tunnel lining;
- tensile dynamic stresses subtracted from compressive static stresses can locally reduce the bending strength of the tunnel lining, with a tendency for the resulting stresses to be tensile.

The ovalisation is usually simulated under the two-dimensional plane strain condition. The resulting free-field ground shear distortion can be expressed as a shear distribution, i.e. a shear strain profile as a function of depth. The simplest way of ovaling deformation estimation is based on the assumption that the deformations in the circular tunnel are identical to the free-field ground deformations, thus neglecting the soil–tunnel structure interaction. The circular tunnel–ground shearing can be modelled in two ways [16]:

1) As a continuous medium without the presence of a tunnel (i.e. non-perforated ground presented in Fig. 1(a)), whereby the circular tunnel distortion or diametric strain can be calculated as:

$$\frac{\Delta d_{free-field}}{d} = \pm\frac{\gamma_{max}}{2} \tag{1}$$

where γ_{max} is the maximum free-field ground shear strain and d is a diameter of the tunnel. It is obvious that, in this case, the maximum diametric strain of the circular section is solely a function of the maximum free-field shear strain. This assumption is reasonable in the case when the ovaling stiffness (i.e. stiffness against distortion) of the lined tunnel is identical to the stiffness of the surrounding ground.

2) The circular tunnel distortion or diametric strain is calculated under the assumption of an unlined tunnel (i.e. perforated ground in Fig. 1 (b)):

$$\frac{\Delta d_{free-field}}{d} = 2\gamma_{max}(1-\nu_{gr}) \tag{2}$$

where ν_{gr} is Poisson ratio of the ground. In this case, apart from the maximum free-field shear strain, the maximum diametric strain is related to the Poisson ratio of the ground as well. This assumption is convenient in the case when the ovaling stiffness of the lined tunnel is very small compared to the surrounding ground, i.e. for circular tunnels in rock media or stiff soils.

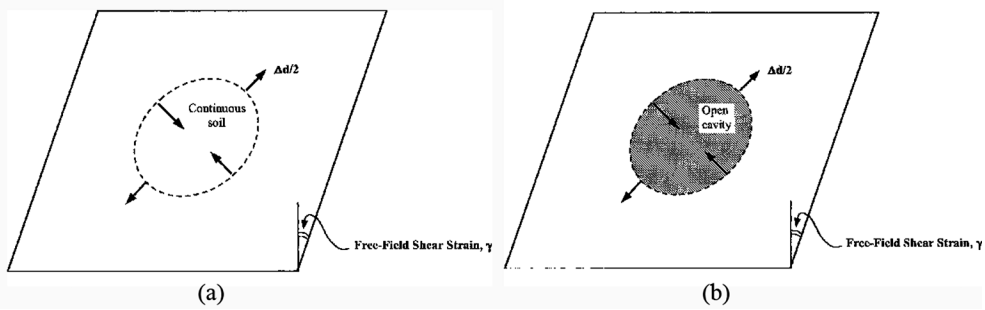

Figure 1. *Free-field shear distortion (circular shape): (a) non-perforated ground; (b) perforated ground [16]*

Both Eq. (1) and Eq. (2) assume the non-existence of the tunnel lining, thus neglecting the tunnel–ground interaction. In a free field, the perforated ground will reach a much higher distortion than the non-perforated ground, with distortion sometimes two or three times greater. This is an appropriate distortion criterion for a tunnel lining of a lower stiffness in comparison with that of the surrounding ground. The deformation equation for the non-perforated ground, on the other hand, will be reasonable when the stiffness of the tunnel lining is identical to that of the surrounding ground. A tunnel lining with stiffness higher than that of the surrounding ground (i.e., when a tunnel is built in a soft or very soft soil) will experience distortions less than those given by Eq. (1).

2.1.2. Earthquake-induced maximum soil shear strain γ_{max}

Considering the fact that the transient deformation of the soil during the action of an earthquake cannot be measured directly, it is common practice to indirectly calculate the peak deformations of the soil using simplified expressions derived under the assumption of propagation of plane waves in a homogeneous medium. The maximum shear strain in the free field is expressed as [16]:

$$\gamma_{max} = \frac{V_{S,max}}{C_S} \tag{3}$$

where $V_{S,max}$ is the peak particle (peak ground) velocity associated with shear S-wave and C_S is the apparent (effective) shear wave propagation velocity (i.e., maximum mass velocity in the ground). The values of C_S can be obtained on the basis of *in situ* and laboratory tests. The effective shear wave propagation velocity is related to the effective shear modulus of the ground G_{gr} according to the following expression:

$$C_S = \sqrt{\frac{G_{gr}}{\rho_{gr}}} \tag{4}$$

where ρ_{gr} is the mass density of the ground.

The expression in Eq. (3) has an extensive application in engineering practice, since it enables a simple estimation of design stresses. Despite its simplicity, a number of input quantities that are not easy to determine are however required, such as incidence angle, apparent wave propagation velocity, predominant wave type, etc. Accordingly, it can be used only in situations where the assumptions of its derivation are met (e.g., one-dimensional plane harmonic propagation of waves in a homogeneous medium). In addition to wave propagation characteristics, there are also effects that are not taken into account in this expression, such as spatial incoherence, site effects, as well as near-fault effects.

2.1.3. Relevant earthquake-induced soil shear strain at the tunnel depth γ_{rel}

In the seismic analysis of tunnel structures, the peak ground strain during an earthquake is not relevant for the appearance of pressures on the tunnel structure, but the soil shear strain occurring between the depths associated with the tunnel crown and the invert. Data on strong ground motion at the depths of concern for tunnel structures are usually not available. Accordingly, the design ground motions include depth-dependent attenuation effects (i.e., ground motion generally decreases with depth). Table 1 and the expression in Eq. (5) can be used to find a relationship between the ground motion at ground surface and the ground motion at the corresponding depth:

Table 1. *Ratios of ground motion at depth to motion at the ground surface [17]*

Tunnel depth [m]	Ratio of ground motion at a tunnel depth to motion at the ground surface
≤ 6	1.0
6–15	0.9
15–30	0.8
> 30	0.7

$$a_{S,depth} = (\text{coefficient from Table 1}) \cdot a_{S,max} \quad (5)$$

where $a_{S,max}$ is the peak particle (peak ground) acceleration.

Earthquake-induced damage to tunnel structures is primarily correlated with particle velocity and displacement, not acceleration. Existing attenuation relationships are usually applicable to estimate peak ground surface acceleration; however, they can also be used to estimate peak ground velocity and displacement. In the case where site-specific data are not available, based on Tables 2 and 3 and the known peak ground acceleration, the peak velocity and displacement can be obtained, respectively. In all the presented tables, the types of sediments represent the following shear wave velocity ranges: in rock medium $C_S \geq 750$ m/s, in stiff soil $C_S = 200–750$ m/s, and in soft soil $C_S < 200$ m/s. It should be noted that the given ratios of peak ground velocity to peak ground acceleration are less certain with regard to soft soils [17].

Table 2. *Ratios of peak ground velocity to peak ground acceleration at surface in rock and soil [17]*

Moment magnitude Mw	***Ratio of peak ground velocity [cm/s] to peak ground acceleration [g]***		
	Distance from source to site[km]		
	0–20	**20–50**	**50–100**
Rock			
6.5	66	76	86
7.5	97	109	97
8.5	127	140	152
Stiff soil			
6.5	94	102	109
7.5	140	127	155
8.5	180	188	193
Soft soil			
6.5	140	132	142
7.5	208	165	201
8.5	269	244	251

Accordingly, the particle (ground) velocity at the tunnel depth would be:

$$V_{S,depth} = (\text{value from Table 2 [cm/s/g]}) \cdot a_{S,depth}\ [\text{g}] \quad (6)$$

Table 3. *Ratios of peak ground displacement to peak ground acceleration at surface in rock and soil [17]*

Moment magnitude Mw	***Ratio of peak ground displacement [cm] to peak ground acceleration [g]***		
	Distance from source to site [km]		
	0–20	**20–50**	**50–100**
Rock			
6.5	18	23	30
7.5	43	56	69
8.5	81	99	119
Stiff soil			
6.5	35	41	48
7.5	89	99	112
8.5	165	178	191
Soft soil			
6.5	71	74	76
7.5	178	178	178
8.5	330	320	305

Analogously, the particle (ground) displacement at the tunnel depth is calculated by the following formula:

$$D_{S,depth} = (\text{value from Table 3 [cm/g]}) \cdot \ a_{S,depth}\ [\text{g}] \tag{7}$$

Finally, the relevant soil shear strain γ_{rel} at the depth of the longitudinal central axis of the tunnel, induced by the propagation of seismic shear S-waves, is given by the following expression:

$$\gamma_{rel} = \frac{V_{S,depth}}{C_S} \tag{8}$$

2.1.4. One-dimensional seismic site response analysis (simplified dynamic analysis)

This method aims to calculate the earthquake-induced acceleration, shear stress, strain, and maximum ground displacements in a range of depths related to the tunnel section, between the tunnel crown and the invert, using a one-dimensional (1D) free-field seismic site response (SSR) analysis. In doing so, both the time history of the acceleration and the site characteristics are taken into consideration, whereas the effects of the tunnel–ground interaction are still not taken into account.

Seismic waves, emanating from the source, may travel even tens of kilometers through the rock medium and usually less than 100 m through the overlying soil. Nevertheless, soil can contribute significantly to the ground surface motion characteristics. A major issue in the ground response analysis is determination of the response of the soil deposit to the motion of the underlying bedrock. As presented in Fig. 2(a), the motion of the surface of the soil deposit is called the *free surface motion*, the motion of the base of the soil deposit (which at the same time represents the motion of the top of the bedrock) is called the *bedrock motion*, whereas the motion of the bedrock exposed at the ground surface is called the *rock outcropping motion*. In the case when the soil deposit does not exist (as presented in Fig. 2(b)), the motion of the top of the bedrock is called the *bedrock outcropping motion* [18].

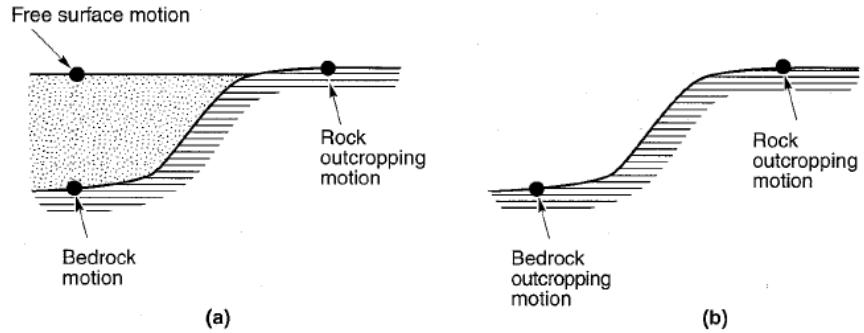

Figure 2. *Nomenclature in the ground response analysis: (a) soil deposit overlying bedrock; (b) no soil deposit overlying bedrock [18]*

After a fault occurs below the ground surface, seismic body waves travel away from the source in all directions. On their path to the ground surface, the waves reach boundaries between two geological materials of different characteristics and are being reflected and refracted. Considering that the propagation velocities of seismic waves in shallow soil media are mostly lower than the velocities in the underlying media of greater depths, inclined seismic waves that strike horizontal layer boundaries tend to be reflected in a more vertical direction. During the travel of seismic waves towards the ground surface, they are bent in an almost vertical direction (Fig. 3) due to manifold refractions. In one-dimensional ground response analyses, all boundaries are assumed to extend infinitely in the horizontal direction (typically a distance several times the total depth to the bedrock) and the response of soil deposits is assumed to be primarily induced by vertically propagating S-waves (SH- or SV-waves) travelling from the underlying bedrock.

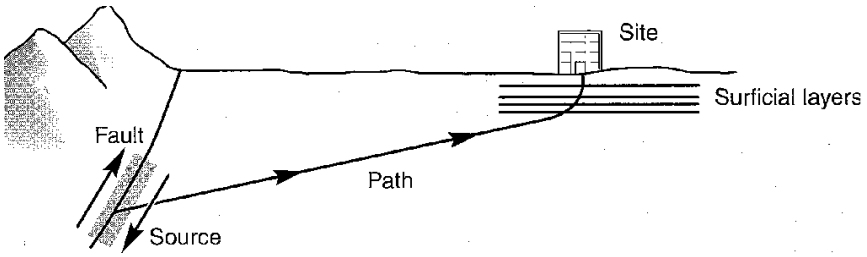

Figure 3. *Multiple refraction of seismic waves that produces near-vertical wave propagation near the ground surface [18]*

Many computer programs are available for 1D wave propagation analysis: SHAKE [19], EERA - Equivalent-linear Earthquake site Response Analysis [20], NERA - Nonlinear Earthquake site Response Analysis [21], DEEPSOIL [22], SPECFEM 1D [23] based on the Spectral Element method (SEM).

Ground response analysis is based on the application of the so-called transfer functions, by the virtue of which a variety of output quantities (i.e., response parameters, such as displacement, velocity, acceleration, shear stress, and shear strain) can be related to an input motion parameter (i.e., bedrock acceleration). This approach relies on the principle of superposition, and therefore it is reasonable to be used exclusively in linear analysis. The principle is as follows:

- The known input quantity (time history of bedrock motion) is represented by a Fourier series, using the Fast Fourier Transform (FFT).
- Each term in the Fourier series of the bedrock motion is being multiplied by the transfer function in order to obtain the output quantity (Fourier series of the ground surface motion).
- The ground surface motion is being expressed in the time domain based on the inverse Fast Fourier Transform.
- Based on this, the transfer function defines for each frequency in the bedrock input motion whether it is amplified or deamplified owing to the presence of the soil deposit.

2.2. SOIL–STRUCTURE INTERACTION APPROACH

The soil–structure interaction (SSI) effects have recently become an indispensable part of the analysis and design of tunnels under earthquake conditions, because it has been proven that the effects of the interaction between the tunnel structure and the surrounding ground may result in greater external forces acting on the structure. The presence of the structure considerably modifies the free-field ground motion, leading to a different seismic response of the tunnel lining. The interaction effects are manifested in the form of kinematic interaction and inertial interaction, which most often act in combination. The kinematic interaction occurs due to the inability of the tunnel to follow ground motion due to its higher stiffness compared to ground stiffness and has been proven to be of primary importance. The inertial interaction is often considered less important and could be ignored as the tunnel structure inertia is negligible compared to the surrounding ground inertia [25].

Tunnel–ground interaction under seismic action is considerably more complex compared to that of aboveground structures. In the case of aboveground structures only foundations are exposed to the soil–structure interaction effects, whereby the vibrations of the ground particles imposed to the foundations are being transmitted to the structure above the ground surface. When it comes to tunnel structures, on the other hand, the soil–structure interaction is induced along the entire structural contour, whereby the form of interaction depends primarily on the type of construction procedure, that is, on the excavation methodology and installation technology of the tunnel support system. The effect of an earthquake on the tunnel–ground interaction depends on a number of parameters, such as the peak ground acceleration, the intensity and duration of the earthquake, and the relative stiffness between the tunnel and the surrounding ground. Thus, in the case of a rigid liner in a soft soil, the soil cannot produce tunnel deformation; however, in the case of a flexible liner, there is an interaction between the liner and the surrounding soil.

There are a number of approaches that allow dynamic soil–structure interaction to be taken into account when designing a tunnel structure. In these approaches, for simplicity, it is assumed that the soil behaves as a linear elastic or viscoelastic material and is perfectly connected to the tunnel structure (the so-called no-slip condition). However, in reality, the bond between the soil and the structure is rarely of a perfect nature, as slippage or even separation in the contact surface may occur (the so-called full slip condition), which is especially typical in the case of tunnels in very soft soils or under strong earthquakes. In most cases, there is a partial slip condition (owing to large deformations of the soil, the soil–structure interaction decreases with increasing relative displacements between the soil and the structure). Therefore, it is always recommended to consider both extreme cases (no-slip condition and full slip condition) and apply the more critical one.

2.2.1. Simplified analytical SSI approach for circular tunnels (pseudo-static analysis)

In pseudo-static approach, tunnel and soil analysis are separated. The seismic input is represented by the peak strain amplitude. This quantity is calculated according to simplified formulae based on the simple assumption of the propagation of plane harmonic S-waves in a homogeneous, isotropic, elastic medium. After that, its action on the tunnel lining under static conditions is considered. In doing so, the influence of the shape and stiffness of the tunnel on the seismic behaviour of the ground is not taken into account.

The simplified analytical approach, proposed by Wang [25], is based on the theory of an elastic beam on an elastic foundation, by which the effects of the tunnel–ground interaction are considered under quasi-static conditions. The solution refers to circular tunnels, the most critical deformation pattern of which is ovalisation (distortion, shearing) of the circular cross-section of the tunnel, caused by shear S-waves that propagate in planes perpendicular to the longitudinal axis of the tunnel. Ovalisation is usually simulated under the two-dimensional plane-strain condition. Such an approach is justified for the following reasons: (1) the typical cross-sectional dimensions of the tunnel liner are small compared to the wavelengths of the predominant ground motion that induces the ovaling deformation; (2) the effects of inertia in the tunnel lining and the surrounding soil as a result of the dynamic effects of the interaction between the soil and the structure are relatively small. Furthermore, the solution is based on the assumption that the soil behaves in a linear elastic manner. For the case of *no-slip* tunnel–ground interface condition (perfect bond, rigid contact, or rough interface) that considers the continuity of stresses and displacements and no relative shear displacements of the ground and tunnel liner at the common interface, the expressions for the bending moment *M* and thrust (axial force) *T* (Fig. 4) according to the Wang's solution, in terms of an angle θ measured counterclockwise with respect to the axis of the tunnel spring line, are:

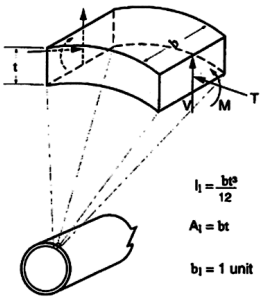

***Figure 4**. Circumferential tunnel lining forces and moments induced by seismic waves propagating perpendicular to tunnel longitudinal axis [16]*

$$M(\theta) = \pm\frac{1}{12}K_1 G_{gr} d^2 \cdot \gamma_{rel} \cos\left[2\left(\theta + \frac{\pi}{4}\right)\right] \Rightarrow M_{max} = \pm\frac{1}{6}K_1 \frac{E_{gr}}{1+\nu_{gr}} r^2 \cdot \gamma_{rel} \quad (9)$$

$$T(\theta) = \pm\frac{1}{2}K_2 G_{gr} d \cdot \gamma_{rel} \cos\left[2\left(\theta + \frac{\pi}{4}\right)\right] \Rightarrow T_{max} = \pm K_2 \frac{E_{gr}}{2(1+\nu_{gr})} r \cdot \gamma_{rel} \quad (10)$$

where:

$$K_1 = \frac{12(1-\nu_{gr})}{2F+5-6\nu_{gr}} \tag{11}$$

$$K_2 = 1 + \frac{F\left[(1-2\nu_{gr}) - (1-2\nu_{gr})C\right] - \frac{1}{2}(1-2\nu_{gr})^2 + 2}{F\left[(3-2\nu_{gr}) + (1-2\nu_{gr})C\right] + C\left(\frac{5}{2} - 8\nu_{gr} + 6{\nu_{gr}}^2\right)^2 + 6 - 8\nu_{gr}} \tag{12}$$

$$C = \frac{E_{gr}(1-{\nu_{lin}}^2)r}{E_{lin}t_{lin}(1+\nu_{gr})(1-2\nu_{gr})} \tag{13}$$

$$F = \frac{E_{gr}(1-{\nu_{lin}}^2)r^3}{6E_{lin}I_{lin}(1+\nu_{gr})} \tag{14}$$

$$\frac{\Delta d_{lin}}{d} = \pm\frac{1}{3}K_1 F \cdot \gamma_{rel} \tag{15}$$

In the above given equations, r is the tunnel radius, d is the tunnel diameter, t_{lin} denotes the thickness of the tunnel lining, I_{lin} is moment of inertia of the tunnel lining (per unit width) for circular tunnel, ν_{lin} is the Poisson ratio of the lining, E_{lin} is the elasticity modulus of the lining, , $\Delta d_{lin}/d$ is the diametric strain of the lining, ν_{gr} is the Poisson ratio of the soil, E_{gr} is the elasticity modulus of the soil, $G_{gr} = \rho_{gr} \cdot {C_S}^2$ is the soil shear modulus (it relates the velocity of propagation of shear waves in the ground C_S to the mass density of the ground ρ_{gr}), γ_{rel} is the relevant free-field shear strain (i.e., the mean value of the free-field shear strain in the depth range corresponding to the tunnel crown and the invert), K_1 stands for the moment response coefficient, K_2 represents the thrust response coefficient.

In order to understand the significance of tunnel lining stiffness, there are two dimensionless parameters that relate the stiffness of the tunnel and the surrounding ground. The first is the compressibility ratio C, as a measure of the compressive stiffness of the ground in relation to the tunnel lining under the free-field uniform or symmetrical loading conditions (vertical soil stress = horizontal soil stress), and it reflects the circular stiffness of the tunnel–ground system (i.e., resistance to compression). The second is the flexibility ratio F, which is a measure of the shear stiffness of the ground with respect to the tunnel lining under the free-field antisymmetric loading condition (horizontal ground stress equal, but opposite in sign, to the vertical ground stress in the free-field), and it reflects the radial stiffness of the tunnel–ground system (i.e., resistance to ovalisation). Of these two ratios, the flexibility ratio is suggested to be more important, as it reflects the ability of the tunnel lining to resist shearing deformations imposed by the surrounding ground (for more details, see [26]).

The above presented analysis procedures can be reasonably applied to tunnel linings with sufficiently large burial depths (the so-called deeply embedded tunnels), so that the boundary conditions of free surface at the top of the soil and bedrock at the bottom of the soil, have a negligibly small effect on soil–structure interaction. As shown by Wang [25], these boundary effects could be considered negligible in the case of circular tunnel linings with a ratio $h/d > 1.5$ (where h is the distance from the free surface, as well as the bedrock, to the mid-height of the lining, and d is the outer diameter of the lining). Furthermore, these solutions are adequate for cast-in-place concrete tunnel linings or shield tunnel linings

composed of prefabricated-concrete segments, i.e. for cases when the linings are placed in soils with lower values of the modulus of elasticity compared to the modulus of the tunnel lining, that is, for the case of linings in soft soils when the effects of soil–structure interaction are particularly pronounced.

Although the given solutions were proposed several decades ago, they are still the most commonly used analytical solutions today. The main reason lies in the fact that the problem of soil–tunnel structure interaction under the influence of earthquakes has not been fully investigated and known until now, and according to the author's knowledge, there has been no evident progress in this regard during the past decade or two. In addition, the literature dealing with the effect of earthquakes on tunnel structures is quite rare, and therefore presenting analytical solutions based on the theory of elasticity is fruitful, in order to see the basic assumptions and limitations that are essential in these solutions. Finally, advanced numerical analyses using contemporary software are rather complex and time-consuming, and are therefore focused on case-specific studies. The simplified approaches mentioned above, on the other hand, allow relatively quick and simple analysis and provide reasonable results for the needs of engineering practice.

2.2.2. Simplified dynamic SSI analysis

In a simplified dynamic SSI analysis, soil strains over a range of depths corresponding to the tunnel section (i.e., at depths between the tunnel crown and the invert) are calculated by one-dimensional (1D) free-field seismic site response (SSR) analysis and after that applied to the tunnel lining, under pseudo-static conditions as was the case with the previously explained simplified solution. By that, both the time history acceleration and the characteristics of the site are taken into account, but the kinematic soil–structure interaction is still not taken into account. Furthermore, the effects of compressional waves are also ignored, given that solely shear waves are considered, with propagation in vertical planes causing shear deformations.

Contemporary technological development has contributed to the development of a large number of software, which are based on the principles of the finite element method (FEM) and which are suitable for conducting a simplified dynamic SSI analysis, whether it is a specialised software for SSI analysis (PLAXIS, FLAC, COMSOL, GEFDYN, FLUSH, SASSI, HOPDYNE) or a general software (ANSYS, ADINA, ABAQUS, DYNAFLOW). (All the mentioned software can also perform a full dynamic analysis, in which the seismically induced increase in force in the tunnel lining is directly obtained as the output quantity of the corresponding numerical model selected for the simulation of the shaking of the coupled tunnel–ground system; in addition to the acceleration time history and site characteristics, kinematic and dynamic interactions are also taken into account).

3. PROPERTIES OF THE GROUND AND THE TUNNEL IN THE PRESENT STUDY

The circular cross-section tunnel structure was considered to be placed in a soil layer of 30 m in thickness, which lay over a relatively stiff bedrock. An outer tunnel radius of 3.0 m was considered, while the lining thickness was 0.3 m. The overburden depth was 12 m and a centre of the tunnel was at the depth of 15 m.

The physical properties of the tunnel lining and the soil material surrounding the tunnel are shown in Figure 5. Given that the effects of soil–structure interaction depend on the

relationship between the stiffness of the soil and the lining, in the present study a stiff soil is considered a soil in good condition, while soft saturated soil is used as an example of soil in poor condition.

The shear wave velocity profiles $C_S(z)$ are depicted in Figure 5 by vertical lines (solid line in the case of stiff soil in good condition (Fig. 5(a)) and dashed line in the case of soft saturated soil in poor condition (Fig. 5(b)). These lines present the so-called "equivalent velocity", which is the mean value of the soil shear wave velocity, needed to perform a one-dimensional seismic site response linear analysis. In the considered cases, an average shear wave velocity profile of 250 m/s for stiff soil and 110 m/s for soft soil was used in the study.

With regard to the soil shear modulus, it is in a linear analysis of a constant nature with respect to a constant value of the shear wave velocity. The modulus value in the case of stiff soil was $G_{gr} = G_{max} = 120$ MPa and for soft soil it was $G_{gr} = G_{max} = 21$ MPa (after Eq. (4)). The value of the damping coefficient is also constant given the linear analysis, and $D_{gr} = D_0 = 1\%$ was taken for stiff soil deposit, whereas $D_{gr} = D_0 = 2.5\%$ was considered for soft soil material.

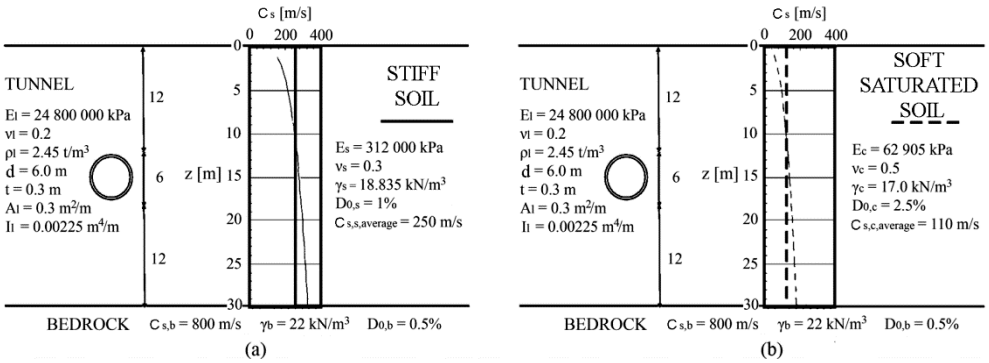

***Figure 5**. Properties of the tunnel and the soil: (a) stiff soil; (b) soft saturated soil [27]*

4. COMPARISON OF ANALYTICAL AND NUMERICAL ANALYSIS RESULTS WITH REGARD TO DESIGN SOIL SHEAR STRAIN EVALUATION IN SEISMIC ANALYSIS OF TUNNELS

In the following study, both pseudo-static and simplified dynamic analysis methods were considered for the evaluation of the relevant (design) soil shear strain in seismic analysis of tunnels, regarding the idealised tunnel geometry and ground properties. In the quasi-static approach, the soil shear strain induced by shear body waves was calculated using the most frequently applied expressions, whereas in the simplified dynamic analysis the soil shearing was determined by performing a one-dimensional free-field ground response analysis in the corresponding programme. A comparison of the results of these two approaches, considering both good and poor soil conditions with linear elastic behaviour assumption, is performed, and the significant mutual differences are evaluated.

4.1. ONE-DIMENSIONAL SSR LINEAR ANALYSIS

The SSR analysis was performed using the programme EERA (Equivalent-linear Earthquake site Response Analysis) [20], which is integrated with the MS-Excel spreadsheet programme.

This programme allows performing 1D linear or equivalent linear SSR analyses, considering horizontally layered subsoils with vertical propagation of horizontal shear waves (SH-waves). The behaviour of the horizontal soil layer is simulated by the Kelvin–Voigt solid, with shear modulus and viscous damping characterising the properties of soil layers. Solving the wave propagation equations is done in the frequency domain (FD).

In the EERA programme, the bedrock can be simulated as rigid (by selecting the option "inside"), or as elastic (by selecting the option "extract", which assigns its properties to the last soil layer). For the sake of transforming the signal from the outcropping rock to the bedrock placed at the bottom of the soil layer, an appropriate transfer function is applied to the input signal, thus taking into account the transfer of shear stress between the bedrock and the overlying layer [18].

In these analyses, the soil conditions and soil behaviour were modelled in accordance with Figure 5. The seismically induced free-field soil deformations were calculated assuming that the soil behaviour is linearly elastic, and consequently, the soil shear modulus and damping coefficient are constant and do not depend on the shear level during the analysis.

In this study, the time history acceleration record of the 1995 Kobe Earthquake in Japan was considered, as this earthquake was the most destructive event for underground infrastructure in recorded history. In view of the fact that there is no recorded acceleration of strong ground motion at the depths where the tunnels are being built, the existing accelerogram recorded on the free surface was scaled to 0.25 g, thus accounting for the attenuation of the strong ground motion with depth [18]. The acceleration time history used in the SSR analyses (magnitude *Mw* = 6.5, distance from source to site = 26.4 km) is illustrated in Figure 6. The maximum value of the input acceleration time history was 0.251 g (2.46 m/s^2) and it occurred approximately 7.3 s after the start of earthquake excitation. The given earthquake acceleration input was applied to the bottom boundary of the soil model, whereby the bedrock was simulated as rigid by choosing the option "inside".

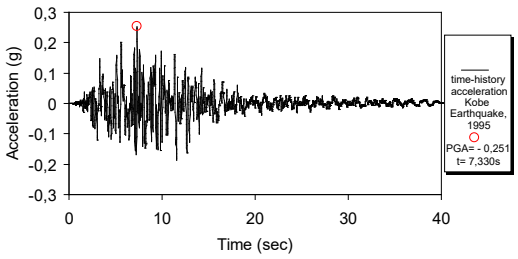

Figure 6. *Scaled accelerogram of the 1995 Kobe Earthquake in Japan used in the study [27]*

Analyses of the soil response to seismic motion enabled the calculation of the maximum values of acceleration and shear strains in the soil for the both considered cases, stiff soil and soft saturated soil, which is shown in the following diagrams (Fig. 7). With regard to Figure 7(a), concerning the given input motion, maximum ground acceleration value for the case of soft soil deposit is 1.45g, whereas in case of soft saturated soil peak ground acceleration is 0.76g. Consequently, the stiff soil column resulted in a higher peak ground acceleration compared to the value obtained for the saturated soft soil, in which case the accelerations were considerably lower along the depth of the soil column. This is in agreement with the property of soft saturated soil in terms of a higher damping ratio due

to worse soil conditions, and therefore the soil ability to absorb more of the energy of the seismic wave, which ultimately results in significantly lower ground acceleration values.

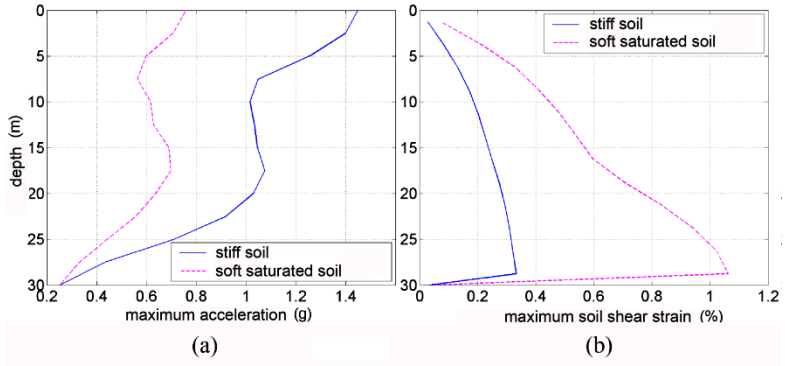

Figure 7 . *Profiles for stiff soil and soft saturated soil: (a) maximum acceleration; (b) maximum soil shear strain [27]*

4.2. COMPARATIVE STUDY OF ANALYTICAL AND NUMERICAL RESULTS

4.2.1. Evaluation of relevant (design) soil shear strain: pseudo-static approach

Parameters of the earthquake and soil:

- *Mw* = 6.5, distance from source to site = 26.4 km;
- Maximum ground particle acceleration at the free surface (stiff soil): $a_{S,max}$ = 1.45g;
- Maximum ground particle acceleration at the free surface (soft saturated soil): $a_{S,max}$ = 0.76g.

Stiff soil

Estimation of ground motion at the depth of the tunnel (according to Eq. (5) and Table 1):

$$a_{S,depth} = (\text{coefficient from Table 1}) \cdot a_{S,max} = 0.85 \cdot a_{S,max} = 0.85 \cdot 1.45\text{g} = 1.23\text{g}\,.$$

Determination of peak particle (peak ground) velocity at the depth of the tunnel (according to Eq. (6) and Table 2):

$$V_{S,depth} = (\text{value from Table 2}) \cdot a_{S,depth} = 102\ \frac{\frac{\text{cm}}{\text{s}}}{\text{g}} \cdot 1.23\text{g} = 125.5\ \frac{\text{cm}}{\text{s}} = 1.25\ \frac{\text{m}}{\text{s}}.$$

Computation of the relevant (design) soil shear strain (according to Eq. (8)):

$$\gamma_{rel} = \frac{V_{S,depth}}{C_S} = \frac{1.25\ \frac{\text{m}}{\text{s}}}{250\ \frac{\text{m}}{\text{s}}} = 0.005 = 0.5\%\,.$$

Soft saturated soil

Estimation of ground motion at the depth of the tunnel (according to Eq. (5) and Table 1):

$$a_{S,depth} = (\text{coefficient from Table 1}) \cdot a_{S,max} = 0.85 \cdot a_{S,max} = 0.85 \cdot 0.76\text{g} = 0.65\text{g}\,.$$

Determination of peak particle (peak ground) velocity at the depth of the tunnel (according to Eq. (6) and Table 2):

$$V_{S,depth} = (\text{value from Table 2}) \cdot a_{S,depth} = 132\ \frac{\frac{\text{cm}}{\text{s}}}{\text{g}} \cdot 0.65\text{g} = 85.8\ \frac{\text{cm}}{\text{s}} = 0.858\ \frac{\text{m}}{\text{s}}.$$

Computation of the relevant (design) soil shear strain (according to Eq. (8)):

$$\gamma_{rel} = \frac{V_{S,depth}}{C_S} = \frac{0.858\frac{\text{m}}{\text{s}}}{110\ \frac{\text{m}}{\text{s}}} = 0.0078 = 0.78\%\,.$$

4.2.2. Evaluation of relevant (design) soil shear strain: simplified dynamic approach

Linear EERA analysis revealed that for the considered stiff soil profile and input seismic data, ground acceleration value at the tunnel axis level is 1.03g. In case of soft saturated soil, ground acceleration at the tunnel spring line location is 0.64g (Fig. 7(a)). Accordingly, the numerically obtained values compare reasonably well with those computed by simplified expressions within pseudo-static approach.

The soil shear deformations are shown in Figure 7(b). Based on the given diagrams, the relevant value of soil shear deformation was also calculated, as the average value of soil shear deformation within the space that will be occupied by the tunnel structure, between the crown and the invert of the tunnel. The maximum value of soil shear deformation for the case of stiff soil deposit is 0.33%, whereas for the case of soft saturated soil it is 1.06%. The average value of the shear deformation of the soil at the location of the tunnel, i.e. in the range of depths between the tunnel crown and the invert, is 0.24% in stiff soil and 0.57% in soft saturated soil. Consequently, the shear deformations of the soil for the case of soft saturated soil are considerably higher, given the weaker properties of the soil in terms of the presence of water, higher damping values, and a higher share of seismic wave energy absorption.

4.2.3. Comparative analysis of the obtained results

The relevant (design) values of seismically induced soil shear strain, obtained by analytical (pseudo-static) approach and numerical (simplified dynamic) approach, considering both the stiff subsoil and the soft saturated subsoil are set side-by-side in Table 4.

Table 4. *Comparison of pseudo-static and simplified dynamic approaches for relevant soil shear strain evaluation concerning stiff soil and saturated soft soil deposits*

Soil	**Stiff soil**			**Soft saturated soil**		
approach / *relevant shear strain*	***Analytical (pseudo-static)***	***Numerical (simplified dynamic)***	***Analytical vs. Numerical***	***Analytical (pseudo-static)***	***Numerical (simplified dynamic)***	***Analytical vs. Numerical***
γ_{rel}	0.005	0.0024	52%	0.0078	0.0057	27%

According to the comparison of the obtained results, the conclusion that arises is that the pseudo-static analytical expressions generally provide a higher soil shear strain than that obtained by the simplified dynamic linear analysis. This conclusion holds particularly true for the case of stiff soil deposits, since the former approach yields prediction of the strain level closer to the simplified dynamic analysis for the case of soft soil deposit, thus implying that simplified relations based on quasi-static approach are in a better agreement with poorer soil properties, such as loose sand or water-saturated clay, which have lower values of the compressional and flexural stiffness.

It can be summarised that pseudo-static analysis can result as more conservative in estimating the strain level in comparison with the simplified dynamic analysis approach, thereby overestimating forces in the tunnel lining to an extent. However, from the aspect of engineering practice, simple analytical expressions are very useful and the results obtained in this way can be considered to be on the side of safety.

5. COMPARISON OF ANALYTICAL AND NUMERICAL ANALYSIS RESULTS WITH REGARD TO SEISMICALLY INDUCED INTERNAL LINING FORCES BASED ON SSI APPROACH

In order to assess the seismically induced tunnel–ground interaction effects, given the main soil classes, stiff and soft soils, an analysis was performed based on a comparison of the results obtained by a simplified analytical approach and a simplified numerical model. Based on that, the ability of the analytical and numerical models in simulating the most significant aspects of the interaction effects was evaluated, along with the most significant factors that affect the tunnel–ground interaction under an earthquake action.

5.1. DETERMINATION OF SEISMICALLY INDUCED TUNNEL LINING FORCES ACCORDING TO ANALYTICAL EXPRESSIONS

Firstly, on the basis of the previously presented analytical expressions for seismically induced tunnel lining forces that takes into account the kinematic tunnel–ground interaction effects, proposed by Wang [25], the maximum values of tunnel lining internal forces M_{max} and T_{max} were calculated for the case of no-slip condition.

5.1.1. Stiff soil

Based on Figures 4 and 5(a), and according to Eqs. (14), (13), (11), (12), (9), and (10), respectively:

Flexibility ratio:

$$F = \frac{E_{gr}(1-{\nu_{lin}}^2)r^3}{6E_{lin}I_{lin}(1+\nu_{gr})} = \frac{312000(1-0.2^2)3.0^3}{6\cdot 24.8\cdot 10^6\cdot 0.00225(1+0.3)} = 18.581\,.$$

Compressibility ratio:

$$C = \frac{E_{gr}(1-{\nu_{lin}}^2)r}{E_{lin}t_{lin}(1+\nu_{gr})(1-2\nu_{gr})} = \frac{312000(1-0.2^2)3.0}{24.8\cdot 10^6\cdot 0.3(1+0.3)(1-2\cdot 0.3)} = 0.232\,.$$

Moment response coefficient K_1:

$$K_1 = \frac{12(1-\nu_{gr})}{2F+5-6\nu_{gr}} = \frac{12(1-0.3)}{2\cdot 18.581+5-6\cdot 0.3} = 0.208\,.$$

Thrust response coefficient K_2:

$$K_2 = 1 + \frac{18.581[(1-2\cdot 0.3)-(1-2\cdot 0.3)0.232] - \frac{1}{2}(1-2\cdot 0.3)^2 + 2}{18.581[(3-2\cdot 0.3)+(1-2\cdot 0.3)0.232] + 0.232\left(\frac{5}{2}-8\cdot 0.3+6\cdot 0.3^2\right)^2 + 6 - 8\cdot 0.3} = 1.152\,.$$

Maximum moment due to S-waves (for the relevant (design) value of earthquake induced soil shear strain obtained by 1D SSR analysis (γ_{rel} = 0.0024)):

$$M_{max} = \frac{1}{6}K_1\frac{E_{gr}}{1+\nu_{gr}}r^2\cdot\gamma_{rel} = \frac{1}{6}0.208\frac{312000}{1+0.3}3.0^2\cdot 0.0024 = 179.8\ \text{kNm}\,.$$

Maximum tangential thrust due to S-waves (for the relevant (design) value of earthquake induced soil shear strain obtained by 1D SSR analysis (γ_{rel} = 0.0024)):

$$T_{max} = K_2\frac{E_{gr}}{2(1+\nu_{gr})}r\cdot\gamma_{rel} = 1.152\frac{312000}{2(1+0.3)}3.0\cdot 0.0024 = 995.6\ \text{kN}\,.$$

5.1.2. Soft saturated soil

Based on Figures 4 and 5(a), and according to Eqs. (14), (13), (11), (12), (9), and (10), respectively:

Flexibility ratio:

$$F = \frac{E_{gr}(1-{\nu_{lin}}^2)r^3}{6E_{lin}I_{lin}(1+\nu_{gr})} = \frac{62905(1-0.2^2)3.0^3}{6\cdot 24.8\cdot 10^6\cdot 0.00225(1+0.5)} = 3.247\,.$$

Compressibility ratio (in Eq. (14), the Poisson's ratio was set to 0.49, because a value of 0.5 will result in an infinite value of the ratio):

$$C = \frac{E_{gr}(1-{\nu_{lin}}^2)r}{E_{lin}t_{lin}(1+\nu_{gr})(1-2\nu_{gr})} = \frac{62905(1-0.2^2)3.0}{24.8\cdot 10^6\cdot 0.3(1+0.49)(1-2\cdot 0.49)} = 0.812\,.$$

Moment response coefficient K_1:

$$K_1 = \frac{12(1-\nu_{gr})}{2F+5-6\nu_{gr}} = \frac{12(1-0.5)}{2\cdot 3.247+5-6\cdot 0.5} = 0.706\,.$$

Thrust response coefficient K_2:

$$K_2 = 1 + \frac{3.247[(1-2\cdot 0.5)-(1-2\cdot 0.5)0.812] - \frac{1}{2}(1-2\cdot 0.5)^2 + 2}{3.24[(3-2\cdot 0.5)+(1-2\cdot 0.5)0.812] + 0.812\left(\frac{5}{2}-8\cdot 0.5+6\cdot 0.5^2\right)^2 + 6 - 8\cdot 0.5} = 1.231\,.$$

Maximum moment due to S-waves (for the relevant (design) value of earthquake induced soil shear strain obtained by 1D SSR analysis (γ_{rel} = 0.0057)):

$$M_{max} = \frac{1}{6} K_1 \frac{E_{gr}}{1+\nu_{gr}} r^2 \cdot \gamma_{rel} = \frac{1}{6} 0.706 \frac{62905}{1+0.5} 3.0^2 \cdot 0.0057 = 252.6 \text{ kNm} .$$

Maximum tangential thrust due to S-waves (for the relevant (design) value of earthquake induced soil shear strain obtained by 1D SSR analysis (γ_{rel} = 0.0057)):

$$T_{max} = K_2 \frac{E_{gr}}{2(1+\nu_{gr})} r \cdot \gamma_{rel} = 1.231 \frac{62905}{2(1+0.5)} 3.0 \cdot 0.0057 = 440.2 \text{ kN} .$$

5.2. A SIMPLIFIED NUMERICAL FINITE ELEMENT MODEL

In the present study, a two-dimensional (2D) simplified dynamic linear analysis was carried out using the finite element (FE) based commercial software ANSYS [28], by employing a continuous FE model. The idealisations, on which the performed analysis was based, were as follows: (1) it was assumed that the soil surrounding the tunnel is a homogeneous, isotropic, elastic half-space; (2) it was assumed that the behaviour of the tunnel lining is linearly elastic; (3) two-dimensional analyses under the plane-strain condition were conducted, which separated the transverse response from the longitudinal response, thus assuming uniform properties of the soil and the tunnel structure along the length of the tunnel.

With an aim to minimise boundary effects, the soil was modelled in such a way that the outer boundaries extended a distance > 4*d* (*d* being the tunnel diameter). Therefore, the width of the mesh was selected to be 54 m, whereas its height was 30 m, which is in accordance with the thickness of the soil deposit overlying the bedrock. The ground was modelled by plane-strain solid elements with two degrees of freedom (U_x, U_y) at each node, whereas the tunnel was modelled by beam elements with three degrees of freedom (U_x, U_y, ROT_z). The FE mesh consisted of 368 triangular solid elements with six nodes and 36 beam elements with two nodes. The ANSYS free-meshing algorithm was used, along with mesh refinement in the vicinity of the tunnel. To simulate the no-slip condition, the tied degrees-of-freedom boundary condition was applied along the joint surface of the tunnel lining and the surrounding ground, thereby assuming the compatibility of the lining and ground displacements and constraining the nodes on the two sides of the different meshes to deform identically [29]. Displacements in the vertical and horizontal directions were fixed at the bottom of the FE mesh, thus modelling rigid bedrock beneath the soil deposit. The upper horizontal boundary of the FE model, which simulated the ground surface, was considered free.

All 2D simplified dynamic analyses presented herein were preceded by static analyses to verify the model under static conditions as well. In performing static analyses, on the one hand, in order to restrict horizontal displacements along the vertical boundaries of the model, supports in the form of rollers were used. In performing dynamic analyses, on the other hand, the vertical displacements were constrained along the lateral boundaries of the model. The seismic loading was simulated under simple shear conditions, obtained by means of 1D SSR analysis in the code EERA. Even though such simplified approaches cannot adequately simulate the variations of soil stiffness and strength that occur during an earthquake and do not take into account any dynamic tunnel–ground interaction effects, however, they usually provide a reasonable assessment of the earthquake load.

Considering the stiff soil, the maximum calculated values of displacements at the tunnel section were 2.43 cm at the level of the crown of the tunnel and 1.67 cm at the level of the tunnel invert. Accordingly, the relative displacement between the crown and the invert of the circular tunnel cross-section is of lower value (0.76 cm), which led to less distortion (ovalisation) of the circular cross-section of the tunnel. In the case of soft saturated soil, as a result of significantly higher soil shear strain values, larger soil displacements occured (12.73 cm and 10.19 cm at the top and bottom of the tunnel, respectively), which imposed a larger relative displacement between the tunnel crown and invert (2.54 cm) compared to the stiff-soil case, and thus resulted in significantly greater ovalisation of the tunnel structure (Fig. 8).

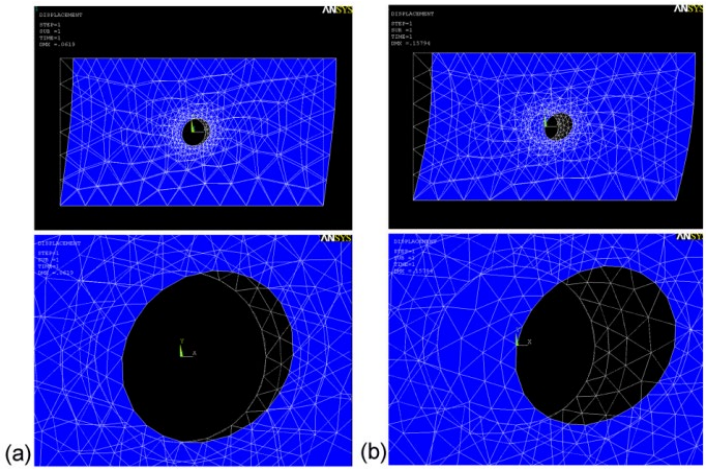

Figure 8. *Seismically induced ovalisation of the circular tunnel cross-section (displacements enlarged 25 times): (a) stiff soil; (b) soft saturated soil [27]*

5.3. COMPARISON OF THE ANALYTICAL AND NUMERICAL RESULTS

The obtained numerical results were compared to the analytical solutions, as presented by diagrams in Figure 9. Thrust (T) and bending moment (M) were determined in terms of the angle θ, which was measured counterclockwise with respect to the axis of the tunnel spring line.

Based on the obtained analytical and numerical results with regard to soils of good and poor conditions, it was observed that the magnitude of the thrust T has a much stronger effect on the stresses in the tunnel lining when compared to the bending moment M, which is typical for the no-slip assumption considered in the given analysis and in line with the findings of Hashash et al. [16].

When considering the distribution of thrust in the tunnel lining, it could be seen that the numerical results related to the soft saturated soil agree quite well with the Wang's analytical solution, whereas in the case of the stiff soil, the numerically obtained accumulated thrust provides a fairly consistent distribution pattern with, however, somewhat lower maximum values than those of the Wang's solution.

In terms of seismically induced bending moments, the numerical model accounting for the soft saturated soil predicted a distribution that conforms that obtained by the Wang's analytical approach. In the case of stiff soil, however, the numerically obtained distribution

is quite similar to that determined by the Wang's analytical solution, with slightly lower maximum values.

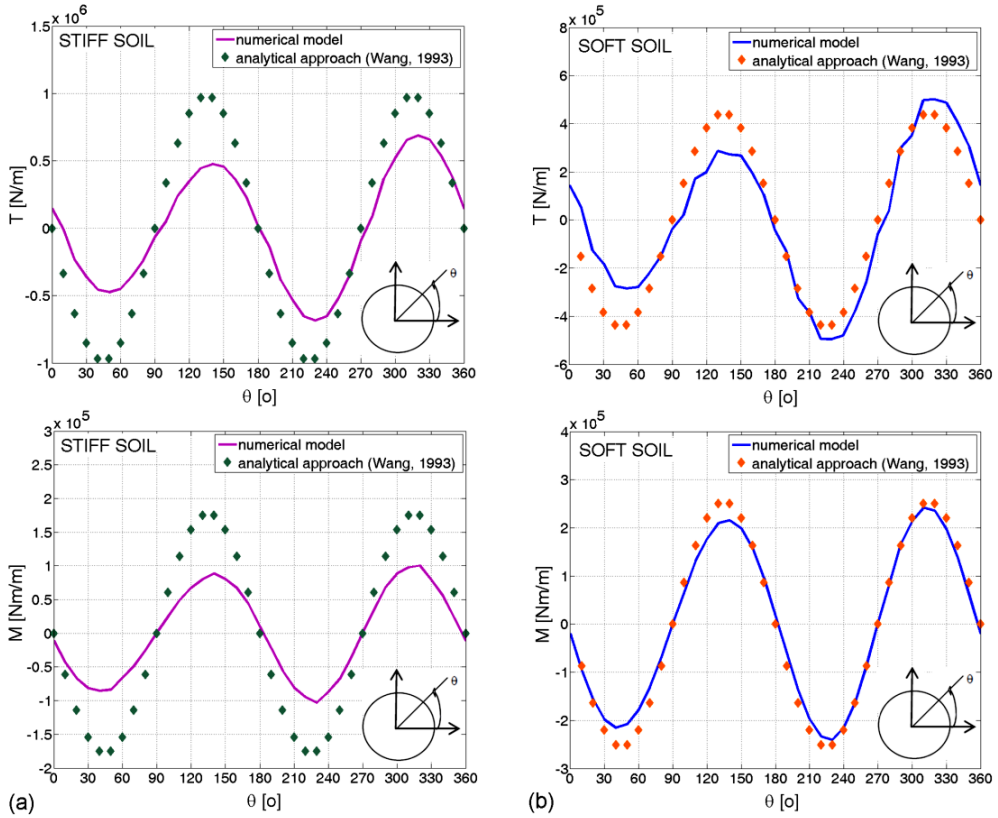

Figure 9. *Comparison of the analytical and numerical results: (a) stiff soil; (b) soft saturated soil [27]*

The maximum values of internal tunnel lining forces caused by the earthquake, obtained by the analytical and numerical models for the case of stiff soil and the case of soft saturated soil, are highlighted in Table 5.

Table 5. *Comparison of the analytical and numerical results related to the stiff soil and soft soil*

Soil	**Stiff soil**			**Soft saturated soil**		
approach / *force*	***Analytical (pseudo-static)***	***Numerical (simplified dynamic)***	***Analytical vs. Numerical***	***Analytical (pseudo-static)***	***Numerical (simplified dynamic)***	***Analytical vs. Numerical***
M_{max} **[kNm/m]**	180	103	≈ 40%	253	242	≈ 4%
T_{max} **[kN/m]**	996	687	≈ 30%	440	500	≈ 10%

A common conclusion that can be drawn from the results obtained according to the frequently used simplified analytical approach according to Wang and performed two-dimensional simplified dynamic linear finite element analysis is that Wang's analytical expressions more faithfully simulate soils of poorer properties and lower stiffness, such as, for example, loose sand or soft undrained clay.

It can also be summarised that pseudo-static analysis approach may give a more conservative assessment of internal tunnel lining forces compared to the simplified dynamic analysis approach. Here again, from the aspect of engineering practice, simple analytical expressions are very useful and the results obtained in this way can be considered to be on the side of safety.

Given the results shown above, a difference between the seismically induced internal tunnel lining forces for the case of stiff soil in relation to the case of soft saturated soil can be seen, which clearly implies the significance of the tunnel–ground interaction effects.

Axial forces (thrust) in the case of stiff soil deposit are of higher values compared to the case of soft saturated soil. This results from significantly higher values of soil shear stress, due to the fact that stiff soil has better characteristics, and therefore higher compressional and flexural stiffness, which results in lower internal tunnel lining forces. This finding is consistent with the observation of Hashash et al. [16], according to which earthquake-induced tunnel lining forces increase with a decrease in the compressibility and flexibility ratio of the soil in relation to the lining.

On the other hand, regarding the distribution of the bending moment, the results of both analytical and numerical approaches showed that the moment values are considerably higher in the case of soft saturated soil, which is affected by significantly weaker properties and lower shear stiffness of the soil, leading to larger soil shear deformations, and therefore to larger seismically induced soil displacements.

6. CONCLUDING REMARKS

The tunnel–ground interaction effects have recently become an indispensable part of the analysis and design of tunnels under earthquake conditions, as these effects between the structure and the surrounding soil may result in higher pressures acting on the structure. The tunnel basically reacts to soil deformations, where the level of tunnel deformation depends primarily on the ratio of the tunnel lining stiffness and the soil stiffness. In the seismic analysis of tunnel structures, the peak ground strain during an earthquake is not relevant for the appearance of pressures on the tunnel structure, but the soil shear strain that occurs in the range of depths that correspond to the tunnel crown and invert.

The present study considered the most frequently used simple analytical expressions, regarding the idealised tunnel geometry and ground properties. The presented analytical expressions refer to the calculation of the relevant (design) soil shear strain that occurs in the range of depths that correspond to the tunnel crown and invert, on the one hand, and of the seismically induced forces in the tunnel lining considering the tunnel–ground interaction effects, on the other hand. The latter, proposed by Wang, are presented as one of the still most commonly used analytical expressions today. Furthermore, in order to evaluate the ability of the analytical expressions to simulate the most important aspects of the seismic performance of tunnels, numerical analyses were also carried out by one-dimensional free-field ground response analysis in the programme EERA and by the simplified dynamic soil–structure interaction analysis in the software ANSYS, respectively. Lastly, the results obtained by the simple analytical and numerical approaches were evaluated, given the main soil classes, stiff and soft soils.

Based on the comprehensive comparison of the obtained results, the following most significant conclusions could be drawn:

- The pseudo-static analytical expressions generally provide a higher soil shear strain than that obtained by the 1D SSR linear analysis. This conclusion holds particularly true for the case of stiff soil deposits, since the former approach yields prediction of the strain level closer to the simplified dynamic analysis for the case of soft soil deposit. This finding implies that simplified relations based on quasi-static approach are in a better agreement with poorer soil properties, which have lower extensional and flexural stiffness values.
- A common conclusion that can be drawn from the results obtained according to the frequently used simplified analytical approach according to Wang and the performed two-dimensional simplified dynamic linear finite element analysis is that the Wang's analytical expressions more faithfully simulate soils of weaker properties and lower stiffness, such as, for example, loose sand or soft undrained clay.
- The pseudo-static analytical expressions proved to be more conservative in estimating the strain level in comparison with the simplified dynamic analysis approach, thereby overestimating forces in the tunnel lining to an extent.
- In addition, the simplified analytical approach according to Wang resulted in a more conservative assessment of tunnel lining internal forces compared to the simplified dynamic analysis approach.
- It can be summarised that, although simple analytical expressions, considering both the design value of the soil shear strain and the seismically induced internal lining forces, are shown to be conservative, they are very fruitful as they give rational results from the aspect of engineering practice, which are on the side of safety.

In the examined case study, soil is assumed to behave in the linear elastic manner. Soil, however, rarely behaves this way. A more accurate approach would consider the nonlinear behaviour of the soil, by which damping and attenuation of the soil material will be taken into consideration. Moreover, the interface between the lining and the surrounding soil can be taken as a partial or full slip condition, which is particularly adequate in the case of an earthquake excitation of high frequency, as well as in the case of shallow-embedded tunnels. Finally, the presented analyses do not take into consideration the nonlinear behaviour of the tunnel lining and the possible cracking of the lining, so the assessed internal lining forces may differ somewhat from the forces actually acting in the lining.

However, when it comes to analytical expressions suitable from the aspect of engineering practice, a very serious and challenging task lies ahead, because, on the one hand, they should be as realistic as possible and include as many relevant parameters as possible, whereas, on the other hand, they should remain sufficiently simple and understandable for a design engineer for whom they are primarily intended.

Acknowledgement. *The authors gratefully acknowledge the support of the Ministry of Science, Technological Development, and Innovations of the Republic of Serbia within the research project No. 451-03-65/2024-03/200095 (project TR36028: "Development and improvement of methods for analysis of the soil–structure interaction based on theoretical and experimental research").*

7. REFERENCES

[1] E. Zlatanović, V. Šešov, D. Lukić, Z. Bonić, N. Davidović, "State-of-the-art of seismic design codes for tunnels and underground structures", *Sci. J. Civ. Eng.*, Special Issue on the Occasion of 15 Years of SEEFORM, Faculty of Civil Engineering of University "Ss. Cyril and Methodius" of Skopje, vol. 8, no. 2, 2019, pp. 49-54, 2019. https://sjce.gf.ukim.edu.mk/wp-content/uploads/2022/04/volume-8-issue-2-state-of-the-art-of-seismic-design-codes-for-tunnels-and-underground-structures.pdf

[2] *Standard Specifications for Tunnelling*. Japanese Society of Civil Engineers (JSCE), Tokyo, Japan, 2006.

[3] *Standard Specifications for Concrete Structures: Design*. Japanese Society of Civil Engineers (JSCE), Tokyo, Japan, 2007.

[4] **E. Zlatanović,** G. Brođeta, N. Popović-Miletić, "Numerical modelling in seismic analysis of tunnels regarding soil–structure interaction"*, Fac. Uni., Series: Arch. and Civ. Eng.*, vol. 11, no. 3, pp. 251-267, 2013. https://doi.org/10.2298/FUACE1303251Z

[5] *ASCE/SEI 7-10 Standard: Minimum Design Loads for Buildings and Other Structures*. American Society of Civil Engineers (ASCE), Los Angeles, USA, 2010.

[6] *Technical Manual for Design and Construction of Road Tunnels – Civil Elements*. Publication No. FHWA-NHI-10-034, U.S. Department of Transportation, Federal Highway Administration (FHWA), Washington, DC, USA, 2009.

[7] *EN 1998-4 Eurocode 8: Design of Structures for Earthquake Resistance – Part 4: Silos, tanks, and pipelines*. European Committee for Standardisation (CEN), Bruxelles, Belgium, 2006.

[8] *EN 1998-5 Eurocode 8: Design of Structures for Earthquake Resistance – Part 5: Foundations, retaining structures, and geotechnical aspects*. European Committee for Standardisation (CEN), Bruxelles, Belgium, 2004.

[9] *SP14.13330.2014 Construction in Seismic Regions*. Federal Centre for Regulation, Standardisation, and Conformity Assessment of Technical Construction (FAUFCC), Moskva, Russia, 2014.

[10] *SRPS EN 1998-4 Eurocode 8: Design of Structures for Earthquake Resistance – Part 4: Silos, tanks, and pipelines*. Institute for standardisation of Serbia (ISS), Belgrade, Serbia, 2012.

[11] *SRPS EN 1998-5 Eurocode 8: Design of Structures for Earthquake Resistance – Part 5: Foundations, retaining structures, and geotechnical aspects*. Institute for standardisation of Serbia (ISS), Belgrade, Serbia, 2012.

[12] *Collection of Yugoslav regulations and standards for engineering structures*. Yugoslav Association of Structural Engineers (YASE), Belgrade, Serbia, 1995.

[13] E. Zlatanović, V. Šešov, D. Lukić, Z. Bonić, "Mathematical interpretation of seismic wave scattering and refraction on tunnel structures of circular cross-section", *Fac. Uni. Arch. Civ. Eng.*, vol. 18, no. 3, pp. 241-260, 2020. https://doi.org/10.2298/FUACE200422018Z

[14] E. Zlatanović, V. Šešov, D.Č. Lukić, Z. Bonić, "Influence of a new-bored neighbouring cavity on the seismic response of an existing tunnel under incident P- and SV-waves", *Earth. Eng. Struct. Dyn.*, vol. 50, no. 11, pp. 2980-3014, 2021. https://doi.org/10.1002/eqe.3497

[15] E. Zlatanović, V. Šešov, D.Č. Lukić, Z. Bonić, "Dynamic analysis of a deeply buried tunnel influenced by a newly-built adjacent cavity with a special emphasis on the minimum seismically safe tunnel distance", *Period. Polytech. Civ. Eng.*, vol. 66, no. 1, pp. 138-148, 2022. https://doi.org/10.3311/PPci.19001

[16] Y.M.A. Hashash, J.J. Hook, B. Schmidt, J.I.-C. Yao, "Seismic design and analysis of underground structures", *Tunnell. Underg. Sp. Tech.*, vol. 16, no. 4, pp. 247-293, 2001. https://doi.org/10.1016/S0886-7798(01)00051-7

[17] M.S. Power, D. Rosidi, J. Kaneshiro, *Vol. III Strawman: screening, evaluation, and retrofit design of tunnels*. Report Draft, National Center for Earthquake Engineering Research, Buffalo, New York, 1996.

[18] S.L. Kramer, *Geotechnical earthquake engineering*. Prentice Hall, 1996.

[19] P.B. Schnabel, J.L. Lysmer H.B. Seed, *SHAKE: A computer program for earthquake response analysis of horizontally layered sites*. Earthquake Engineering Research Center, Berkeley, California, 1972.

[20] J.P., Bardet, K., Ichii, C.H. Lin, *EERA – A computer program for Equivalent-linear Earthquake site Response Analyses of layered soil deposits*. University of Southern California, Los Angeles, California, 2000.

[21] J.P., Bardet, T. Tobita, *NERA – A computer program for Nonlinear Earthquake site Response Analyses of layered soil deposits*. University of Southern California, Los Angeles, California, 2001.

[22] Y.M.A. Hashash, D. Park, "Non-linear one-dimensional seismic ground motion propagation in the Mississipi embayment," *Eng. Geol.*, vol. 62, 185-206, 2001.

[23] Computational Infrastructure for Geodynamics (CIG), *SPECFEM 1D – An open-source software package for seismic wave propagation in a one-dimensional heterogeneous medium*. Princeton University, Princeton, New Jersey, 2002. http://www.princeton.edu/geosciences

[24] E. Zlatanović, M. Trajković-Milenković, D. Č. Lukić, S. Brčić, V. Šešov, "A comparison of linear and nonlinear seismic tunnel–ground interaction analyses", *Acta Geot. Slov.*, vol. 13, no. 2, pp. 27-42, 2016. http://www.fg.uni-mb.si/journal-ags/2016-2/article-3.asp

[25] J.-N. Wang, *Seismic Design of Tunnels: A State-of-the-Art Approach*. Monograph, monograph 7, Parsons, Brinckerhoff, Quade and Douglas, Inc., New York, 1993.

[26] E. Zlatanović, D. Lukić, V. Šešov, "Presentation of analytical solutions for seismically induced tunnel lining forces accounting for soil–structure interaction effects", *Build. Mater. Struct. (Gradjevinski materijali i konstrukcije)*, vol. 57, no. 1, pp. 3-28, 2014. https://doi.org/10.5937/grmk1401003Z

[27] E. Zlatanović, D.Č. Lukić, V. Prolović, Z. Bonić, N. Davidović, "Comparative study on earthquake-induced soil–tunnel structure interaction effects under good and poor soil conditions", *Eur. J. Envir. Civ. Eng.*, vol. 19, no. 8, pp. 1000-1014, 2015. https://doi.org/10.1080/19648189.2014.992548

[28] *ANSYS documentation, ANSYS Multiphysics*. Canonsburg, Pennsylvania. www.ansys.com.

[29] D.M. Potts, L. Zdravković, *Finite element analysis in geotechnical engineering: Theory*. Thomas Thelford, 1999.

AUTHOR'S BIOGRAPHIES

Assoc. Prof. Dr. Elefterija Zlatanović, Grad. Civ. Eng.

Completed doctoral studies in the field of geotechnical earthquake engineering at the Institute IZIIS of University of Skopje, N. Macedonia, within "SEEFORM PhD Programme" supported by DAAD. Employed at the Department of Construction Geotechnics at the Faculty of Civil Engineering and Architecture of University of Niš, Serbia, lecturing in Transportation Tunnels, Underground Structures, and Geotechnical Earthquake Engineering. Extensive experience in research work and project administration in the field of civil engineering geotechnics. SCOPUS citation 65, h-index 5.

Prof. Dr. Zoran Bonić, Grad. Civ. Eng.

Employed at the Faculty of Civil Engineering and Architecture of University of Niš, Serbia, lecturing in Foundation Engineering, Soil Mechanics, Slope Stability and Remediation, and Management of Geotechnical Risks. Highly experienced researcher with organisational and administrative skills on scientific projects in the field of civil engineering geotechnics. SCOPUS citation 131, h-index 6.

Assistant Nemanja Marinković, M.Sc. Civ. Eng., M.Sc. Geol. Eng.

A young researcher at the Faculty of Civil Engineering and Architecture of University of Niš, Serbia, teaching Engineering Geology, Soil Mechanics, and Underground Structures. Valuable experience in experimental research in the field of contemporary soil stabilisation techniques.

Assistant Nikola Romić, M.Sc. Civ. Eng.

A PhD student at the Faculty of Civil Engineering and Architecture of University of Niš, Serbia, teaching Soil Mechanics, Foundation Engineering, and SlopeStability and Remediation. Extensive experience in experimental and numerical research in the field of civil engineering geotechnics.

О УПРОШЋЕНИМ ПРИСТУПИМА СЕИЗМИЧКЕ АНАЛИЗЕ ТУНЕЛА

Сажетак: Прегледом актуелних сеизмичких стандарда за пројектовање тунела у свету и код нас утврђено је да, упркос значајном напретку у области принципа сеизмичке анализе тунела у последњих неколико деценија, чак и у најразвијенијим земљама још увек постоји недостатак систематских и прецизно утврђених правила сеизмичког пројектовања тунела. У овом раду размотрени су једноставни аналитички изрази, који се базирају на претпоставци идеализоване геометрије тунела и својстава тла, за одређивање меродавне вредности смичуће деформације тла која се јавља на делу између тунелског свода и инверта, са једне стране, и за срачунавање сеизмички индукованих сила у тунелској облози узимајући у обзир ефекте интеракције конструкције и тла, са друге стране. Такође, са циљем оцене аналитичких израза у погледу сагледавања најважнијих аспеката сеизмичког одговора тунела, спроведене су и нумеричке анализе једнодимензионалном анализом сеизмичког одзива тла у програму EERA и упрошћеном динамичком анализом интеракције тло–конструкција у софтверу ANSYS, респективно. На крају, извршено је поређење резултата добијених упрошћеним аналитичким и нумеричким приступима, уз разматрање два карактеристична случаја тла, чврстог тла добрих карактеристика и меког засићеног тла слабих карактеристика.

Кључне ријечи: кружни тунел, земљотрес, стандарди, сеизмичка анализа, упрошћени приступи

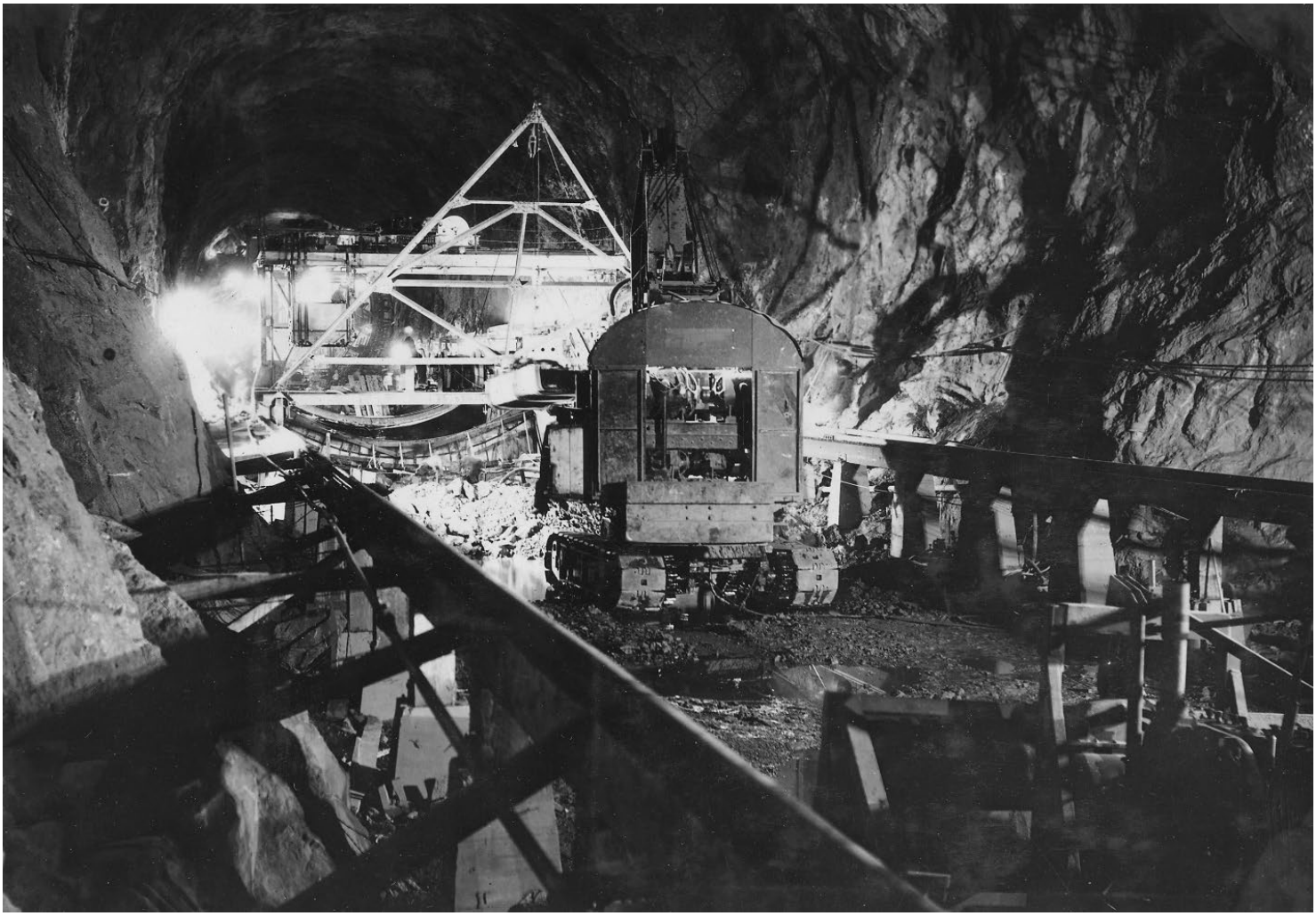

Photograph from Volume Two of a series of photo albums documenting the construction of Hoover Dam, Boulder City, Nevada, 1932. Source: National Archives and Records Administration, cataloged under the National Archives Identifier (NAID) 293677, Public domain, http://catalog.archives.gov/id/293677 (Wikimedia Commons)

University of Banja Luka I Faculty of Architecture, Civil Engineering and Geodesy
ISSN 2712-0570 I UDC 72

2025
Special Issue
Earthquake Engineering

AGG+ Journal for Architecture, Civil Engineering, Geodesy and Related Scientific Fields
АГГ+ часопис за архитектуру, грађевинарство, геодезију и сродне научне области

032-046 **Categorisation** I Original scientific paper
DOI I 10.61892/AGG202502019Z
Paper received I 25/03/2024
Paper accepted I 14/05/2024

Zlatko Zafirovski *
Ss. Cyril and Methodius University in Skopje, Faculty of Civil Engineering, North Macedonia, zafirovski@gf.ukim.edu.mk

Bojan Susinov
Ss. Cyril and Methodius University in Skopje, Faculty of Civil Engineering, North Macedonia, susinov@gf.ukim.edu.mk

Sead Abazi
Ss. Cyril and Methodius University in Skopje, Faculty of Civil Engineering, North Macedonia, sead@gf.ukim.edu.mk

Ivona Nedevska Trajkova
Ss. Cyril and Methodius University in Skopje, Faculty of Civil Engineering, North Macedonia, nedevska@gf.ukim.edu.mk

Riste Ristov
Ss. Cyril and Methodius University in Skopje, Faculty of Civil Engineering, North Macedonia, ristov@gf.ukim.edu.mk

Vasko Gacevski
Ss. Cyril and Methodius University in Skopje, Faculty of Civil Engineering, North Macedonia, gacevski@gf.ukim.edu.mk

Mihaela Daniloska
Ss. Cyril and Methodius University in Skopje, Faculty of Civil Engineering, North Macedonia, mihaela.daniloska98@gmail.com

Angela Naumceska
Ss. Cyril and Methodius University in Skopje, Faculty of Civil Engineering, North Macedonia, anaumceska50@gmail.com

NUMERICAL MODELING OF TUNNEL EXCAVATION AND SUPPORT USING THE DECONFINEMENT METHOD FOR STATIC AND SEISMIC CONDITIONS

Review scientific paper
DOI 10.61892/AGG202502004Z
Paper received | 25/03/2024
Paper accepted | 14/05/2024

* corresponding author

Zlatko Zafirovski *

Ss. Cyril and Methodius University in Skopje, Faculty of Civil Engineering, North Macedonia, zafirovski@gf.ukim.edu.mk

Bojan Susinov

Ss. Cyril and Methodius University in Skopje, Faculty of Civil Engineering, North Macedonia, susinov@gf.ukim.edu.mk

Sead Abazi

Ss. Cyril and Methodius University in Skopje, Faculty of Civil Engineering, North Macedonia, sead@gf.ukim.edu.mk

Ivona Nedevska Trajkova

Ss. Cyril and Methodius University in Skopje, Faculty of Civil Engineering, North Macedonia, nedevska@gf.ukim.edu.mk

Riste Ristov

Ss. Cyril and Methodius University in Skopje, Faculty of Civil Engineering, North Macedonia, ristov@gf.ukim.edu.mk

Vasko Gacevski

Ss. Cyril and Methodius University in Skopje, Faculty of Civil Engineering, North Macedonia, gacevski@gf.ukim.edu.mk

Mihaela Daniloska

Ss. Cyril and Methodius University in Skopje, Faculty of Civil Engineering, North Macedonia, mihaela.daniloska98@gmail.com

Angela Naumceska

Ss. Cyril and Methodius University in Skopje, Faculty of Civil Engineering, North Macedonia, anaumceska50@gmail.com

NUMERICAL MODELING OF TUNNEL EXCAVATION AND SUPPORT USING THE DECONFINEMENT METHOD FOR STATIC AND SEISMIC CONDITIONS

ABSTRACT

In this paper, an analysis of the phase construction of a tunnel with support in static and seismic conditions is made. The PLAXIS 2D software package was used for the problem's numerical modelling. A parametric analysis of the excavation using the deconfinement method (1-ß) was made on an actual tunnel with support in the excavation phase and primary lining with sprayed concrete and anchors. From the conducted analysis, it can be concluded that through the so-called method 1-β, i.e., the percentage enabled realisation of the deformations in the excavation, can successfully model the time needed to set up the support and obtain relevant parameters for dimensioning the elements of the lining for different load cases in static and seismic conditions and stages of performance.

Keywords: *tunnel, tunnel support, numerical modelling, deconfinement method.*

1. INTRODUCTION

This paper deals with tunnel excavation numerical analysis in static and seismic conditions using PLAXIS 2D software. The deconfinement method (1-ß) [1]-[3] was used for the parametric analysis of the excavation, which can simulate the tunnel's behaviour under different excavation conditions and duration until the support is placed.

The analysis is based on a case example of constructing an access tunnel to a hydrotechnical tunnel, which suffered certain damages during the operation phase, so its rehabilitation is needed. It concerns the Vlajnicki tunnel as part of the Mavrovo hydro system in Western Macedonia. Access to the rehabilitation parts is possible only through the construction of transverse entrances—in the case of tunnels, from where the necessary equipment will be brought in.

The Vlajnica tunnel is part of the main water supply from the Mavrovo dam reservoir to the Vrutok HPP, which has a total length of 3,163.00 m. It is intended to operate with flow Q=32 m^3/s and flow velocities of V=3.98 m/s, internal apparent diameter (clear opening) of 3,20 m, longitudinal slope of 3 ‰ and internal water pressure up to a maximum of 8 bar. The facility is of exceptional importance for HPP Mavrovo, especially for the operation of HPP Vrutok and HPP Raven, as well as for transporting water from the Shar and Jelov supply to the reservoir (reverse direction). During the construction of this tunnel, six access tunnels were excavated and built to increase the number of workplaces and reduce transport lengths.

2. METHODOLOGY

In this paper, an innovative numerical approach was used to analyse tunnel excavation, as it effectively simulates the percentage of deformation realised during the excavation phase and assesses the deformations and internal forces in the lining elements.

To improve the stability and maintain the self-support of the rock mass near the limits of the underground excavation, a primary support consisting of reinforced shotcrete and anchors was applied.

The analysis was performed for both static and seismic conditions and different values of the 1 – β parameter.

3. GEOLOGICAL, HYDROGEOLOGICAL AND SEISMIC CHARACTERISTICS OF THE LOCATION

The Vlajnicki tunnel passes through terrain with a different structure. According to its global geological-tectonic structure, it belongs to a geotectonic unit of the first rank in western Macedonia, more specifically, to the so-called Sharsko-Pelisterska zone.

The geological structure of the terrain mainly includes rocks of the Paleozoic age, represented by quartzites, schistose quartzites with ularitoschists, black clay schists, silicified black clay schists, chlorite schists, marbleised limestones, chloride schists, serpentinites less often and other rocks. It is significant for this environment to be significantly tectonically damaged with the presence of fault zones, faults, and increased cracking. This entire Paleozoic complex has undergone intense multi-grade tectonic shaping so that on the terrain today, they are represented as folds, cracks, and fault structures with the most different patterns and sizes.

Generally speaking, the black clay shale and chlorite shale are the most common for the whole tunnel, and the occurrences of more complex quartzites can be considered relatively impermeable to water, while the carbonate complex (marbles, limestones, and their mixtures) and very cracked hard environments have increased water permeability and often appear to have underground water in them.

During the excavation of the tunnel, no underground water appeared in the marbled limestones and quartzites, which indicates increased cracking and cavernousness in the limestones and quartzites, so that at this height, they had the function of a hydro-collector-conductor. Such sections are completely dry and, as an environment, are extremely water permeable. In the rest of the rocks, especially in the chloride shale, there was also water in the form of wetting or seepage. This heterogeneous engineering-geological composition of the environment was also reflected in the diversity of the strength-deformable characteristics of the rocks after the completion of the tunnel construction. Consolidation injection of the tunnel along its entire length was carried out on profiles with a mutual distance of 4 m and boreholes with a length of 0,5 m.

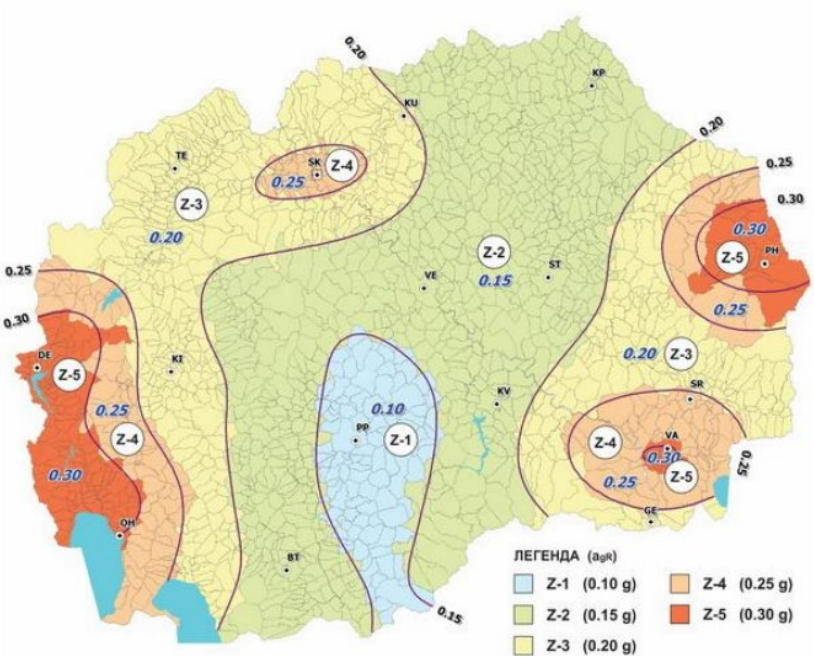

Figure 1. Seismic zoning map of Macedonia, ground-type A, Vs ≥ 800 m/s [4]. Adopted for National Annex to MKS EN 1998-1:2012 Eurocode 8

In terms of seismic characteristics, according to the seismicity map for a return period of 475 years (Figure 1), the location belongs to zone 3, with a seismicity coefficient of 0,2g.

4. GEOTECHNICAL PARAMETERS AND NUMERICAL ANALYSIS

In order to perform a geostatic calculation of the access tunnel, a numerical analysis was performed that determined the stress-deformation state of the soil masses from which the internal forces in the elements needed for the dimensioning of the lining will be obtained. The problem is modelled using the PLAXIS program package, based on FEM, which is

specialised for application to continuous soil environments for various geotechnical problems, giving a simple representation of the loads and the stress-strain state depending on the strength and deformable characteristics of the soil materials [5]. It is also possible to model structural elements: reinforced concrete, geosynthetics, etc. There are many models to define soil materials, and triangular surface isoparametric finite elements with 9-node and 15-node points are also available. For this calculation, a two-dimensional analysis of the planar state of deformations was performed, where the Mohr-Coulomb model approximates the soil as a continuous medium. At the same time, a linear elastic one was applied for the shotcrete and tunnel lining.

For the analysis's needs, the geometry of the models represented by the characteristic (representative) cross-section of the tunnel together with all its elements is defined first, while the soil materials from the surrounding environment are defined through their physical-mechanical strength and deformable characteristics.

Data from previous geotechnical research and tests were used to define appropriate environmental parameters. From there, the strength-deformable parameters shown in Table 1 were adopted (on the side of reliability due to the usual indeterminacy in constructing such structures).

Table 1. Adopted ground material parameters

Parameter	Symbol	Unit	Native ground material
Material model			Mohr - Coulomb
Conditions			Drained
Modulus of elasticity	Eref	[kPa]	50 000
Water-saturated volume weight	γsat	[kN/m3]	22
Natural state volume weight	γunsat	[kN/m3]	22
Poisson's ratio	ν	[/]	0.35
Cohesion	c	[kPa]	10
Angle of internal friction	φ	[°]	20
Dilation angle	ψ	[°]	0

Table 2. Adopted shotcrete parameters

Parameter	Symbol	Unit	Shotcrete
Material model			Linear Elastic
Axial stiffness	EA	[kN/m]	3150000
Bending stiffness	EI	[kN/m]	2625
Thickness	d	[cm]	10

Table 3. Adopted seismic parameters

Symbol	Seismic parameters
Kx	0.20 g
Ky	0.10 g

The analysis is done for a tunnel with primary support that includes anchors and shotcrete. The anchors are modelled with the embedded beam row option. Steel anchors with a diameter of Ø32 and a length of 2 m are adopted, and they are placed at a mutual distance of 2 m in the longitudinal direction. The shotcrete is modelled as a plate element; the adopted thickness is 10 cm (Table 2).

The tunnel construction in PLAXIS is analysed in several stages: excavation and placing the structural elements of the tunnel.

In PLAXIS 2D, it is possible to enter a Deconfinement value during staged construction (as 1-β) in the model explorer. This enables part of the stresses (β) in the soil polygon inside the tunnel to be retained as a support pressure.

The Deconfinement (1-β) method simulates the three-dimensional soil arching behaviour around an unsupported tunnel face using a 2D model, like PLAXIS 2D.

There are two ways to set this up in PLAXIS 2D:

- using the method of partial staged construction (setting the phase's general ΣMstage value to 1 – β);
- or using the Deconfinement option for a deactivated soil cluster.

A deconfinement value can be entered during staged construction as 1-β in the model explorer for any selected and deactivated soil cluster. This method intends to give similar results to those obtained using the partial staged construction (ΣMstage) method while bringing additional flexibility since different deconfinements can be applied to different tunnels or tunnel sections in the same phase.

Various methods are described in the literature for analysing tunnels constructed according to the New Austrian Tunnelling Method. One is the so-called Convergence confinement method or β-method. The idea is that the initial stresses pk acting around the location where the tunnel is to be constructed are divided into a part $(1 - \beta)p_k$ that is applied to the unsupported tunnel and a part βp_k that is applied to the supported tunnel (Figure 2). The β-value is an 'experience value,' which, among other things, depends on the ratio of the unsupported tunnel length and the equivalent tunnel diameter.

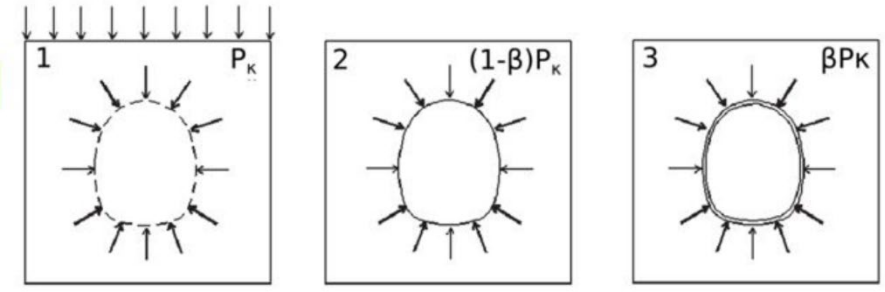

Figure 2. Schematic representation of the β-method for the analysis of NATM tunnels

This coefficient is given in percentages, and it can be explained in the simplest way as the percentage allowability of deformations of an unsupported excavation, while the tunnel support will accept the rest of the percentages of deformation.

The model helps determine soil stresses acting on the tunnel lining, which determines static quantities in the sections: bending moments and axial and transverse forces. The total

displacements, i.e., deformations, were also calculated, which defines the complete picture of the construction's response.

The geometry of the numerical model is given in Figure 3, where its discretisation with finite elements is also shown. The standard fixities option in Plaxis is used to set the model limits. The light opening of the tunnel is 3.2 m.

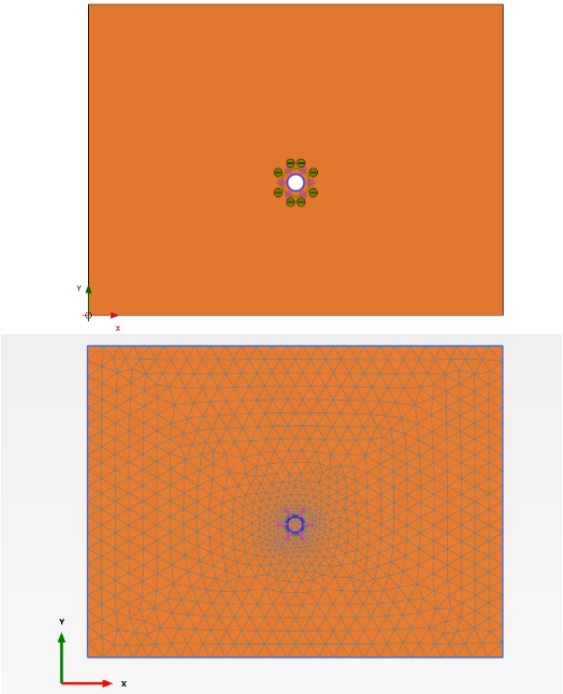

Figure 3. A view of the tunnel and the generated finite element mesh in PLAXIS

5. RESULTS

The following Figure 4 presents the deformations of the medium for two different coefficients 1 – ß.

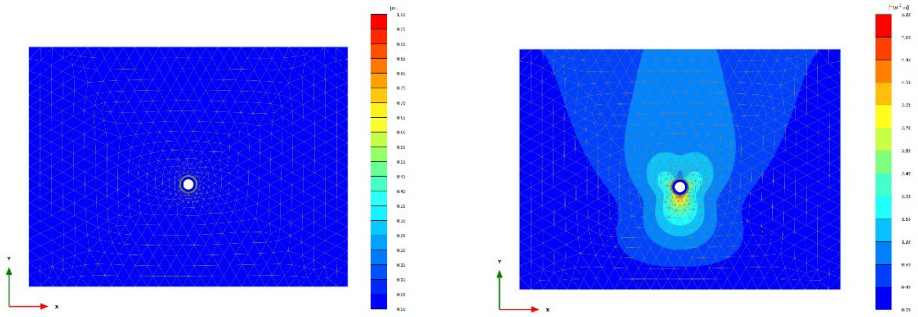

A) 1 – ß=0% B) 1 – ß=100%

Figure 4. Display of the tunnel deformations for different values of the coefficient 1–ß

From the diagram of deformations, it can be seen that for case 1 – ß=0 %, no deformations occurred after the excavation of the tunnel opening, while for case 1 – ß=100 %, all the deformations were realised before the support was installed.

The results are presented for all analysed values of 1-ß through tables and different relationships. In contrast, graphical outputs from the software are shown only from the phase where 1-ß= 100 %, aiming to best compare the results in static and seismic conditions (equivalent static).

Table 4. Maximum displacements of the local environment

1-ß	[%]	0	20	40	60	80	100
d seismic	[m]	0.2685	0.2686	0.2684	0.2681	0.268	0.2677
d static	[m]	0.000434	0.002014	0.004608	0.007152	0.00984	0.01272

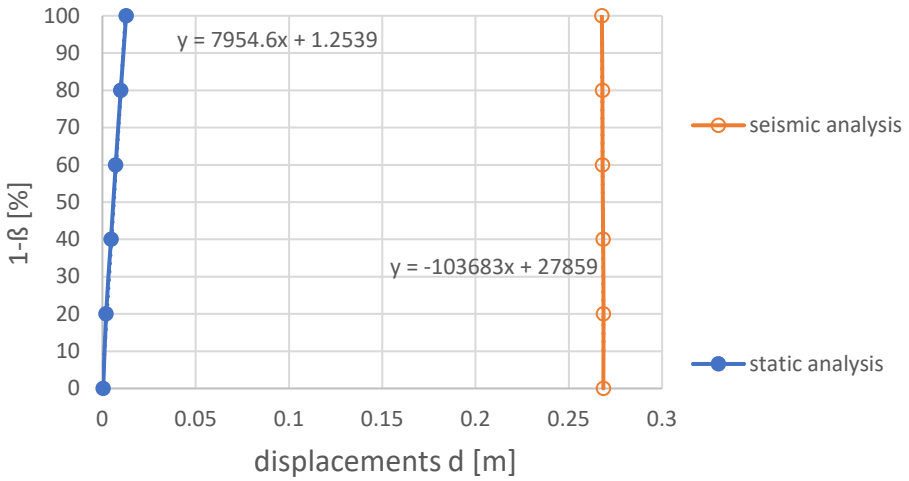

Figure 5. Dependence (1-ß) - d of the surrounding ground in both static and seismic conditions

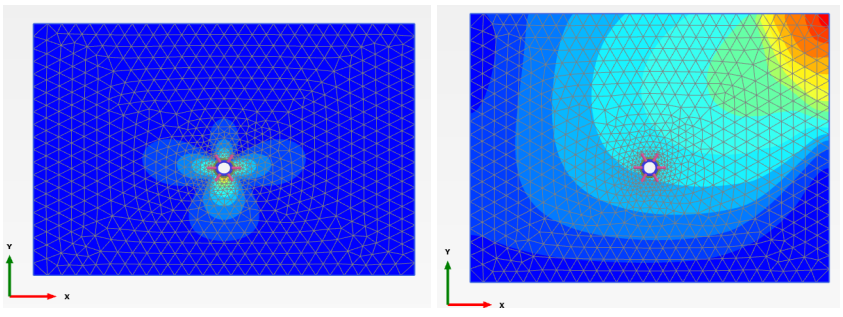

A) Static analysis *B) Seismic analysis*

Figure 6. Total displacement phase 1-ß= 100%

Based on the results presented in Table 4 and Figures 5 and 6, the deformations of the surrounding ground increase insignificantly with the increase of the coefficient 1-ß in static

conditions. In contrast, in seismic conditions, they are significantly larger and increase linearly with the increase of the coefficient 1-ß.

Table 5. Maximum deformation of the anchor

1-ß	[%]	0	20	40	60	80	100
d static	[m]	0.000434	0.001808	0.003562	0.005535	0.007534	0.009692
d seismic	[m]	0.09067	0.09104	0.0914	0.09181	0.09215	0.09256

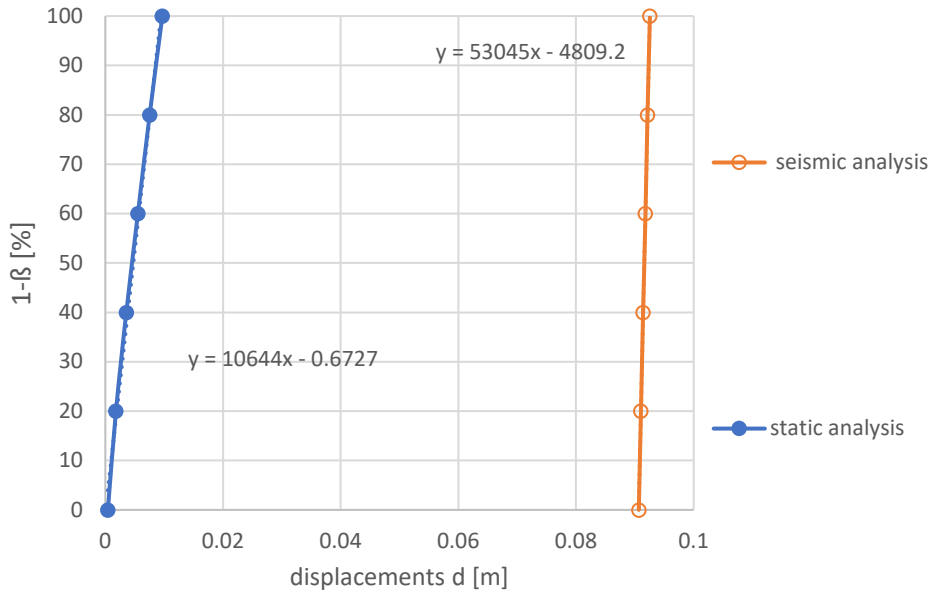

Figure 7. Dependence (1-ß) – d of the anchor in static and seismic conditions

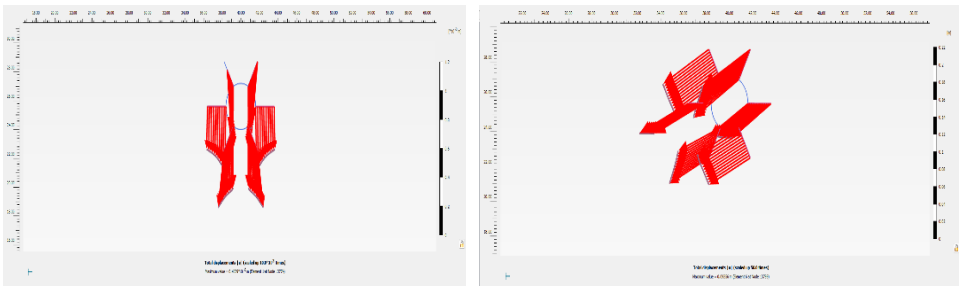

A) Static analysis B) Seismic analysis

Figure 8. Total displacement of an anchor phase 1-ß= 100%

Based on the results presented in Table 5 and Figures 7 and 8, the deformations of the analysed anchor increase approximately linearly with the increase of the 1-ß coefficient in both static and seismic conditions. In terms of absolute value, they are more significant in seismic conditions and change direction.

Table 6. Maximum Shotcrete deformation

1-ß	[%]	0	20	40	60	80	100
d static	[m]	0.000439	0.002092	0.004608	0.007152	0.00984	0.01272
d seismic	[m]	0.09845	0.08942	0.08971	0.09021	0.09109	0.0924

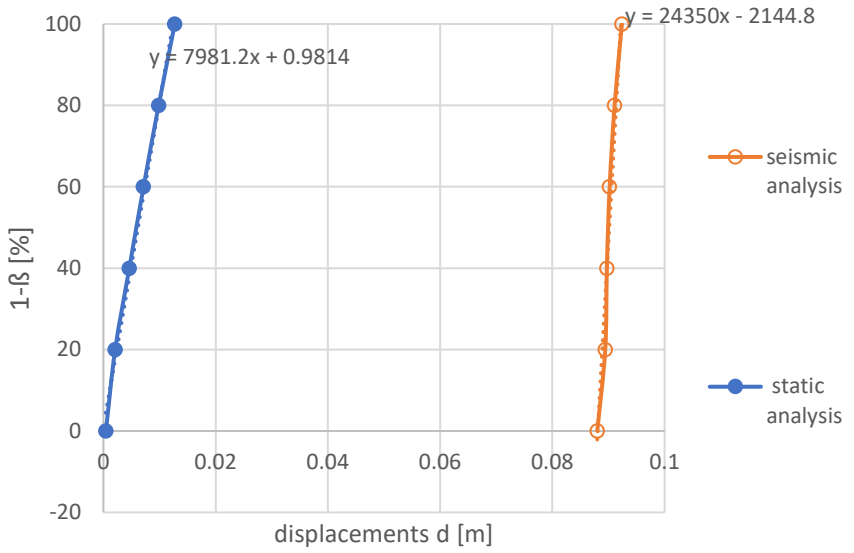

Figure 9. Dependence (1-ß) – d of shotcrete in static and seismic conditions

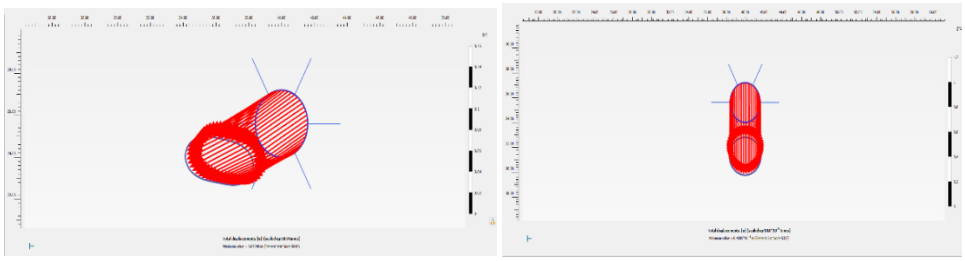

A) Static analysis B) Seismic analysis

Figure 10. Total displacement of shotcrete phase 1-ß= 100%

Based on the results presented in Table 6 and Figures 9 and 10, the shotcrete deformations increase approximately linearly with the increase of the coefficient 1-ß in both static and seismic conditions. In terms of absolute value, they are more significant in seismic conditions and also change direction.

Table 7. The axial force of the anchor

1-ß	[%]	0	20	40	60	80	100
N static [kN/m]	max	-0.00018	-0.1368	-0.2733	-0.4062	-0.5496	-0.6956
	min	-0.00207	-1.157	-2.312	-3.4664	-4.28	-4.805
N seismic [kN/m]	max	-0.1271	-0.06311	0.09757	0.7655	1.502	2.032
	min	-3.798	-3.868	-4.486	-4.926	-5.244	-5.523

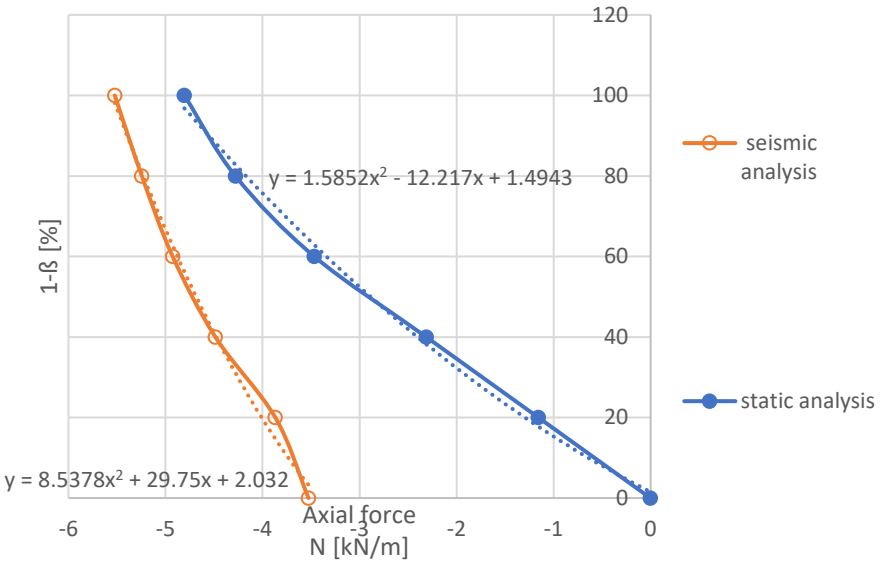

Figure 11. Dependence (1-ß) – N in static and seismic conditions on the anchor

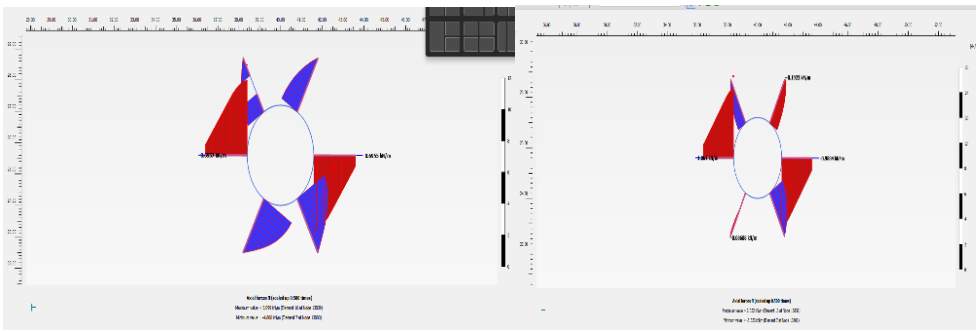

A) Static analysis B) Seismic analysis

Figure 12. The axial force of an anchor phase 1-ß= 100%

Based on the results presented in Table 7 and Figures 11 and 12, it can be concluded that there is an increase in axial force as a function of the increase in the value of 1-ß, which is more significant in static conditions than in seismic conditions.

Table 8. Transverse force in shotcrete

1-ß	[%]	0	20	40	60	80	100
Q static [kN/m]	max	0.05454	7.732	15.43	23.33	34.23	47.69
	min	-0.05448	-7.734	-15.53	-23.38	-34.20	-47.58
Q seismic [kN/m]	max	18.4	18.99	23.35	28.87	34.93	43.20
	min	-16.52	-18.61	-24.03	-30.26	-37.52	-50.42

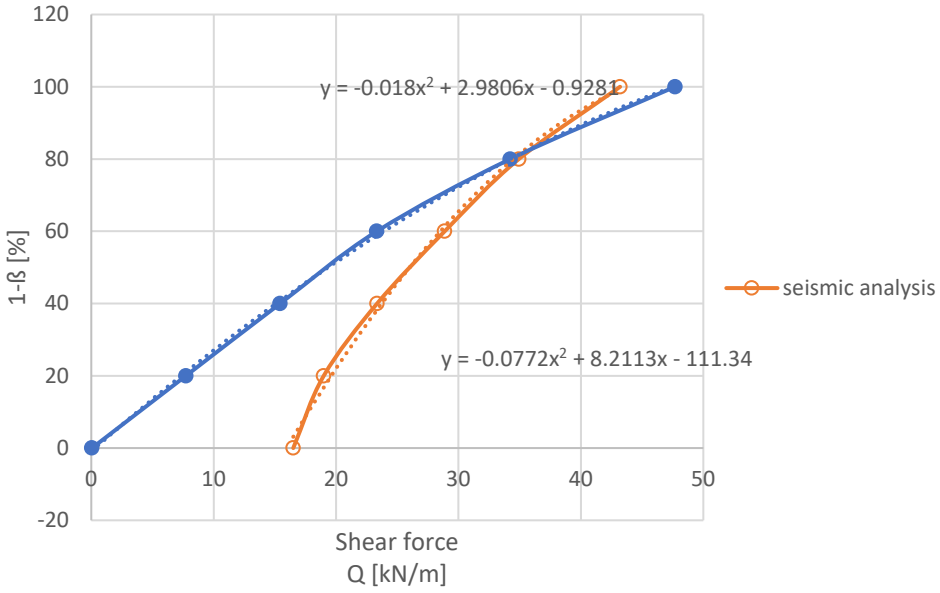

Figure 13. Dependence (1-ß) – Q in static (in blue) and seismic (in orange) conditions on the shotcrete

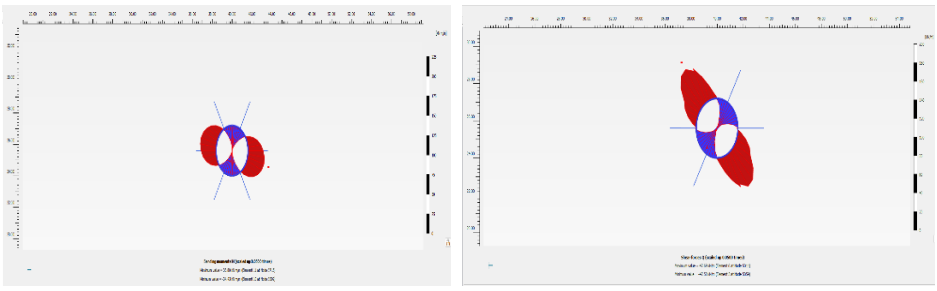

A) Static analysis B) Seismic analysis

Figure 14. Shear force of shotcrete phase 1-ß= 100%

Based on the results presented in Table 8 and Figures 13 and 14, it can be concluded that there is an increase in transverse force as a function of the increase in the value of 1-ß, which is more significant in static conditions than in seismic conditions. For 1-ß=80 %, approximately the same results are obtained in static and seismic conditions.

Table 9. Axial force in shotcrete

1-ß	[%]	0	20	40	60	80	100
N static [kN/m]	max	0.7788	-143.2	-287.3	-432.2	-578.9	-726.9
	min	-1.163	-218.5	-436.6	-654.1	-868.9	-1081.0
N seismic [kN/m]	max	-118.9	-287.2	-443.7	-592.6	-740.4	-887.0
	min	-233.7	-429.9	-637.0	-850.2	-1064.0	-1276.0

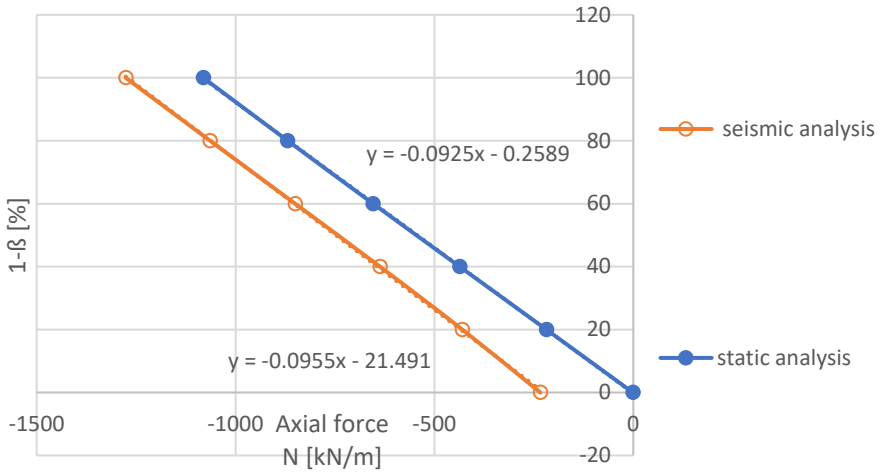

Figure 15. Dependence (1-ß) – N in static and seismic conditions on the shotcrete

A) Static analysis B) Seismic analysis

Figure 16. The axial force of shotcrete phase 1-ß= 100%

Based on the results presented in Table 9 and Figures 15 and 16, it can be concluded that there is an increase in axial force as a function of increasing the value of 1-ß, which is the same in static and seismic conditions. In absolute value, greater axial forces are obtained in seismic conditions.

Table 10. Bending moments in shotcrete

1-ß	[%]	0	20	40	60	80	100
M static [kN m/m]	max	0.02463	6.159	12.30	18.45	24.86	31.77
	min	-0.02541	-6.019	-12.02	-17.96	-23.83	-29.79
M seismic [kN m/m]	max	13.31	14.83	17.94	22.77	28.04	33.80
	min	-13.30	-15.37	-19.16	-23.72	-29.16	-34.43

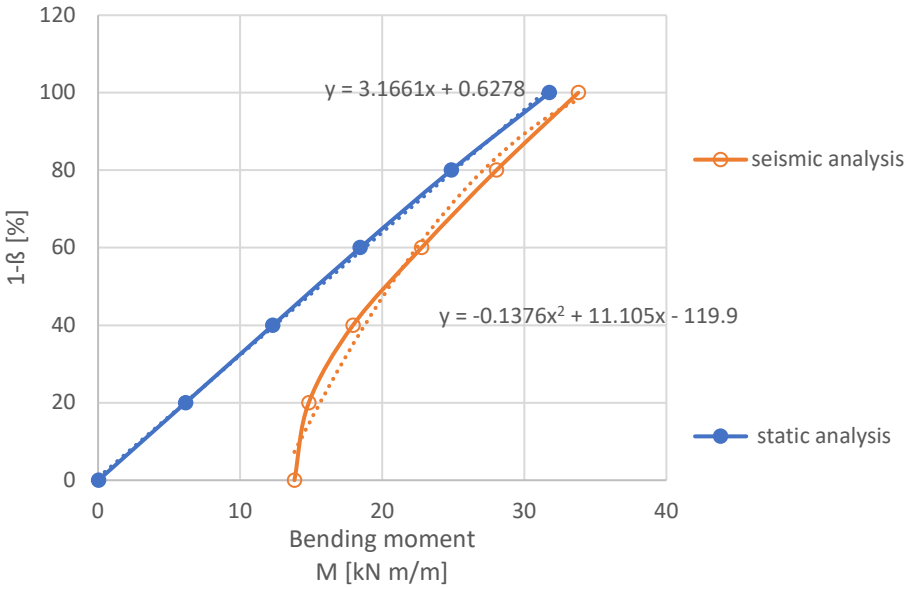

Figure 17. Dependence (1-ß) – M in static and seismic conditions on the shotcrete

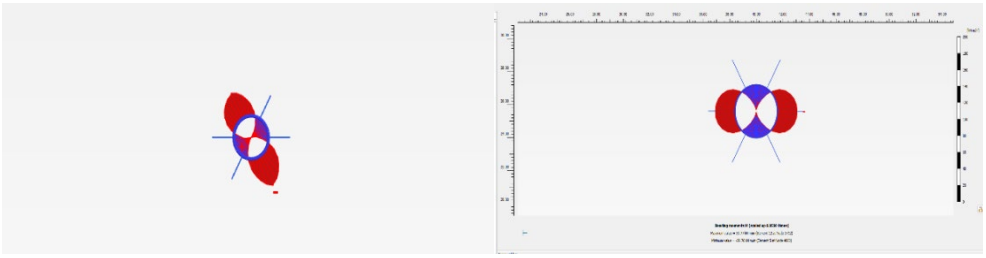

A) Static analysis B) Seismic analysis

Figure 18. Bending moment of shotcrete phase 1-ß= 100%

Based on the results presented in Table 10 and Figures 17 and 18, it can be concluded that there is an increase in bending moments as a function of increasing the value of 1-ß, which is different in static conditions compared to the increase in seismic conditions. However, when 1-ß=100 %, approximate values are reached.

6. CONCLUSION

This paper analyses methods and procedures for tunnel construction through a practical example of constructing an access tunnel to a hydro-technical tunnel from the Mavrovo hydro system. During the exploitation phase, the tunnel suffered certain damages, so its rehabilitation was needed.

A case with support in the excavation phase and primary lining with shotcrete and anchors was analysed. The analysis of the tunnel is made in a software package based on the application of the finite element method and offers the possibility to simulate the phase performance of the tunnel and the simulation of the time required to place the support

through the so-called method 1-β, that is, the percentage enabled realisation of the deformations in excavation.

A parametric analysis was made for different values of the coefficient 1-β, during which the changes in the deformations of the surrounding environment, the deformations of the support elements, and the internal forces of the structural elements were monitored.

The results show that as the 1-β coefficient increases from 0 to 100%, the deformations and internal forces in the shotcrete and anchors grow almost proportionally. The absolute values of the deformations and internal forces of the surrounding environment and the primary support are greater for seismic conditions than for static conditions.

Finally, from the conducted analysis, it can be concluded that through the so-called method 1-β, i.e., the percentage enabled realisation of the deformations in the excavation, can successfully model the time needed to set up the support and obtain relevant parameters for dimensioning the elements of the lining for different load cases in static and seismic conditions and stages of performance.

7. REFERENCES

[1] A. Guilloux, A. Kurdts, V. Bernhardt and H. Wong, “A new stress-strain approach for tunnel face stability“, In *Geotechnical aspects of underground construction in soft ground. Proceedings of the 5th international conference of TC 28 of the ISSMGE*, the Netherlands, 2005, pp. 521-527.

[2] R. Witasse, “Application of the Convergence-Confinement Method in PLAXIS 2D”. Internet: https://blog.virtuosity.com/application-of-the-convergence-confinement-method-in-plaxis-2d, [02.9.2024].

[3] J. K. Pradhan, “Deconfinement in soil cluster inside tunnel in PLAXIS 2D”. Internet: https://www.linkedin.com/posts/jkpradhan_plaxis-geotechnicalengineering-fea-activity-7082235983936581632-aVS2, [02.9.2024].

[4] N. Dumurdjanov, Z. Milutinovic and R. Salic, "Seismotectonic model backing the PSHA and seismic zoning of Republic of Macedonia for National Annex to MKS EN 1998-1: 2012 Eurocode 8," *Journal of Seismology*, 24.2, pp. 319-341, 2020.

[5] Bentley, “PLAXIS 2D-Reference Manual“. Internet: https://bentleysystems.service-now.com/sys_attachment.do?sys_id=7fe3e9171b80d690b5f1da49cc4bcbc4, [02.9.2024].

AUTHORS' BIOGRAPHIES

Zlatko Zafirovski

Zlatko Zafirovski, PhD, associate professor at the Faculty of Civil Engineering in Skopje, was born on October 16th 1979, in Skopje, Republic of North Macedonia. He obtained his PhD in the field of tunnels and railways in 2014. Since 2004, he has been employed at the Faculty of Civil Engineering, University Ss. Cyril and Methodius in Skopje. Since 2019, he has been appointed as Associate Professor. He has been the author of more than 100 scientific and professional papers in his 20 years of engineering and academic career.

Bojan Susinov

Bojan Susinov, PhD, is an assistant professor at the Faculty of Civil Engineering in Skopje. He obtained a bachelor's and master's degree in geotechnical engineering from the same faculty, and he has been the author of more than 100 scientific and professional papers in his 15 years of engineering and academic career.

Sead Abazi

Sead Abazi, PhD, assistent professor at Faculty of Civil Engeneering in Skopje. He obtained a bachelor's and master's degree in geotechnical engineering from the same faculty, and he has been the author of more than 100 scientific and professional papers in his 15 years of engineering and academic career.

Ivona Nedevska Trajkova

Ivona Nedevska Trajkova is a civil engineer and teaching assistant at the Faculty of Civil Engineering in Skopje. Currently, she is a PhD student working in several areas, such as roads and railway engineering, railway maintenance, tunnelling and more.

Riste Ristov

Riste Ristov is a civil engineer and teaching assistant at the Faculty of Civil Engineering in Skopje. Currently, he is a PhD student working in several areas, such as road engineering, road safety, traffic, etc.

Vasko Gacevski

Vasko Gacevski is a civil engineer and teaching assistant at the Faculty of Civil Engineering in Skopje. Currently, he is a PhD student working in several areas, such as construction management, tunnelling, etc.

Mihaela Daniloska

Mihaela Daniloska is a geotechnical engineer who takes pride in being an engineer and gets great satisfaction from knowing that people will benefit from what she has helped to build. Mihaela obtained a bachelor's degree in geotechnical engineering from the Faculty of Civil Engineering, UKIM, and now she is taking her master's degree there while working in the Geotechnical laboratory on the faculty.

Angela Naumceska

Angela Naumceska is a geotechnical engineer who is committed to working with talented professionals in the geotechnical laboratory, conducting various tests on soil samples and interpreting test results. Angela is currently studying for a master's degree in Geotechnical Engineering at the Faculty of Civil Engineering at UKIM, where she previously earned her bachelor's degree in geotechnical engineering.

НУМЕРИЧКО МОДЕЛИРАЊЕ ИСКОПА И ПОДГРАДЕ ТУНЕЛА ПРИМЈЕНОМ МЕТОДЕ РАСТЕРЕЋЕЊА У УСЛОВИМА СТАТИЧКОГ И СЕИЗМИЧКОГ ОПТЕРЕЋЕЊА

Сажетак: У овом раду анализирана је фазна изградња тунела са подградом у статичким и сеизмичким условима. За нумеричко моделирање проблема кориштен је софтверски пакет PLAXIS 2Д. Параметарска анализа ископавања користећи метод растерећења (1-β) спроведена је на стварном тунелу са подградом у фази ископавања и примарном облогом од млазног бетона и анкера. На основу спроведене анализе може се закључити да се тзв. метода 1-β, односно проценат омогућене реализације деформација током ископавања, може успјешно користити за моделирање времена потребног за постављање подграде, као и за добијање релевантних параметара за димензионисање елемената облоге при различитим случајевима оптерећења у статичким и сеизмичким условима, као и у различитим фазама извођења радова.

Кључне ријечи: тунел, подграда тунела, нумеричко моделирање, метода растерећења.

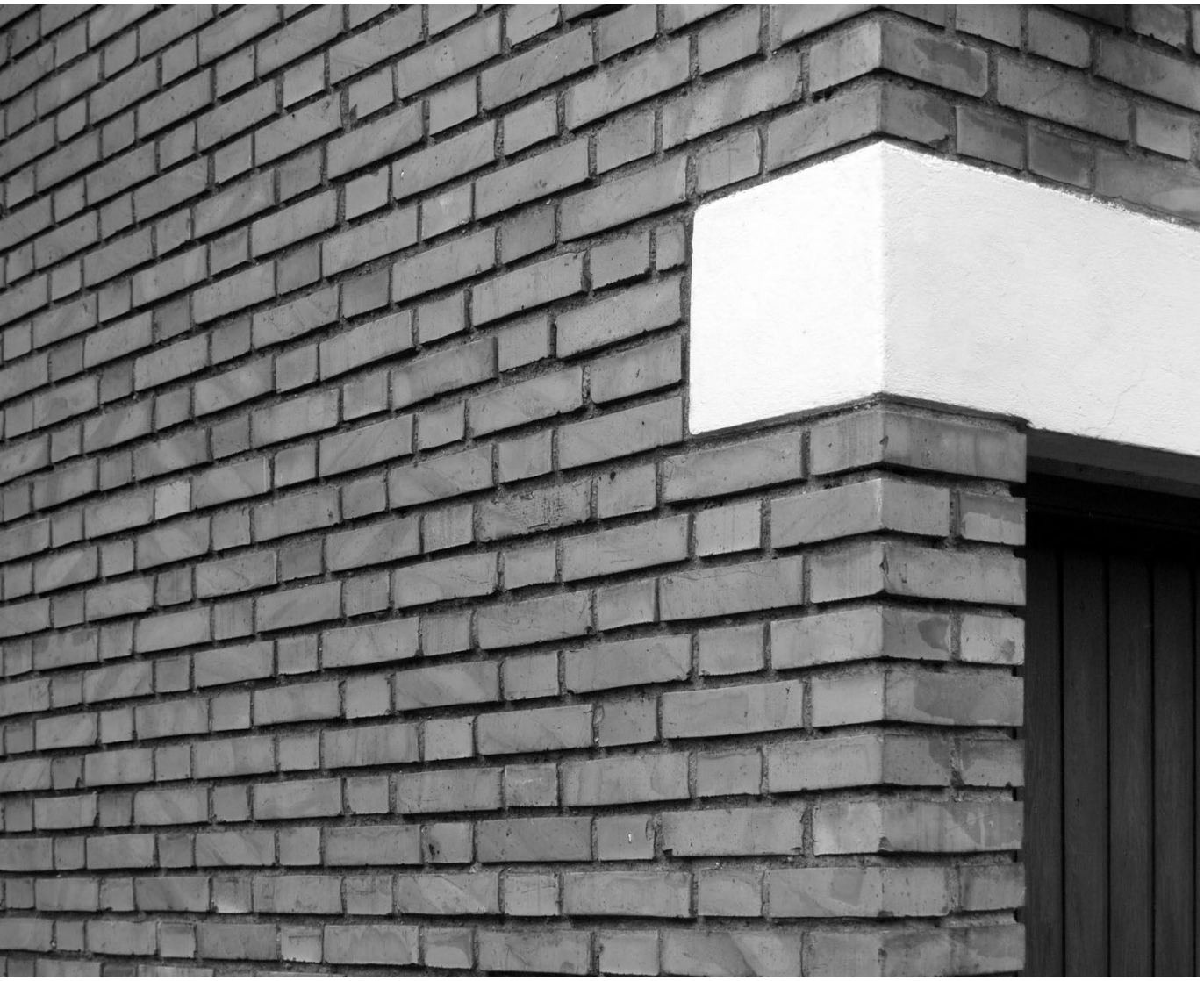

Kingohusene Courtyard Houses, Helsingør/Elsinore, Denmark, 1956-1960, by architect Jørn Utzon. Photographer: Jens Kristian Seier, 2007. Source: https://www.flickr.com/photos/seier/2141693607/in/photostream/ (Wikimedia Commons)

University of Banja Luka I Faculty of Architecture, Civil Engineering and Geodesy
ISSN 2712-0570 I UDC 72

2025
Special Issue
Earthquake Engineering

AGG+ Journal for Architecture, Civil Engineering, Geodesy and Related Scientific Fields
АГГ+ часопис за архитектуру, грађевинарство, геодезију и сродне научне области

050-070 **Categorisation** I Review scientific paper
DOI I 10.61892/AGG202502002C
Paper received I 25/03/2024
Paper accepted I 17/04/2024

Anđelko Cumbo
University of Banjaluka, Faculty of Architecture, Civil Engineering and Geodesy, Bosnia and Herzegovina, andjelko.cumbo@aggf.unibl.org

Gordana Broćeta *
University of Banjaluka, Faculty of Architecture, Civil Engineering and Geodesy, Bosnia and Herzegovina, gordana.broceta@aggf.unibl.org

Marina Latinović Krndija
University of Banjaluka, Faculty of Architecture, Civil Engineering and Geodesy, Bosnia and Herzegovina, marina.latinovic@aggf.unibl.org

Slobodan Šupić
University of Novi Sad, Faculty of Technical Sciences, Serbia, ssupic@uns.ac.rs

Žarko Lazić
University of Banjaluka, Faculty of Architecture, Civil Engineering and Geodesy, Bosnia and Herzegovina, zarko.lazic@aggf.unibl.org

THE EFFECT OF MASONRY INFILL MODEL SELECTION ON THE SEISMIC RESPONSE OF REINFORCED CONCRETE FRAME STRUCTURES

Review scientific paper
DOI 10.61892/AGG202502002C
Paper received | 25/03/2024
Paper accepted | 17/04/2024

* corresponding author

Anđelko Cumbo
University of Banjaluka, Faculty of Architecture, Civil Engineering and Geodesy, Bosnia and Herzegovina, andjelko.cumbo@aggf.unibl.org

Gordana Broćeta *
University of Banjaluka, Faculty of Architecture, Civil Engineering and Geodesy, Bosnia and Herzegovina, gordana.broceta@aggf.unibl.org

Marina Latinović Krndija
University of Banjaluka, Faculty of Architecture, Civil Engineering and Geodesy, Bosnia and Herzegovina, marina.latinovic@aggf.unibl.org

Slobodan Šupić
University of Novi Sad, Faculty of Technical Sciences, Serbia, ssupic@uns.ac.rs

Žarko Lazić
University of Banjaluka, Faculty of Architecture, Civil Engineering and Geodesy, Bosnia and Herzegovina, zarko.lazic@aggf.unibl.org

THE EFFECT OF MASONRY INFILL MODEL SELECTION ON THE SEISMIC RESPONSE OF REINFORCED CONCRETE FRAME STRUCTURES

ABSTRACT

In many countries, reinforced concrete (RC) frames are widely utilized as the primary building structure. The infill is typically composed of traditional masonry (brick elements connected with mortar), commonly without isolation from the frame. It is noted that in engineering practice, seismic force calculations for RC frame buildings are often conducted on models that exclude masonry infill, even when the infill is not isolated from the frame through specific construction elements. In such cases, the walls are considered only as a permanent load. Consequently, the contribution of non-insulated (bonded) masonry infill to changes in bearing capacity, stiffness, and ductility of the RC frame, affecting stresses and horizontal movement during seismic activity, is frequently disregarded. To assess the consequences of prevalent calculation models, four representative types of RC frame models with masonry infill were analysed herein. The study demonstrated that differently conceptualized models of the same building impact dynamic characteristics, including forces and displacements of the main frame structure. The dynamic analysis revealed that inadequate treatment of the frame and non-insulated infill connection in the design phase can lead to dangerous phenomena such as "soft floors," significant torsion, and the effects of short columns going unnoticed. Therefore, this paper underscores the importance of appropriately addressing non-insulated infill in the calculation model in routine design practices. Additionally, it advocates for the issuance of precise instructions for special construction measures that would effectively isolate masonry infill from the frame when such a solution is justified.

Key words: *RC frame buildings, masonry infill, dynamic characteristics, infill stiffness and ductility*

1. INTRODUCTION

In general, when designing buildings in seismically active areas, numerous approximations are typically introduced into analytical models due to many unknowns. This stands in contrast to building design in areas without seismic activity. The question of the correctness (accuracy) of the analytical model in calculation analyses is warranted. To achieve higher "accuracy," it is essential to encompass everything that occurred in the past and evaluate potential events during the building's lifespan. Regulations, standards, professional rules, analytical and experimental research, and engineering knowledge and experience primarily guide us in this endeavour. Simultaneously, the expectation is that building calculations are conducted within a reasonable timeframe, ensuring safety and cost efficiency. Therefore, establishing a high-quality structural conception in the design phase, along with a corresponding calculation model, is crucial.

During calculation analyses, the designer constructs a model representing the actual building structure. Generally assuming the model's adequacy for providing accurate and reliable results, especially with the application of 3D models and modern static and dynamic software packages, often neglects numerous limitations in such analyses. Experienced designers, alongside complex computer calculations, critically review and perform control calculations on simpler models, dividing the structure into logical parts/elements. They also avoid blind adherence to regulations that might be unclear or illogical for a specific case. This approach to computational analyses has proven effective, recognizing that all numerical methods possess advantages and disadvantages, making them inaccurate for all structure types.

The discussion on the "accuracy" of analytical procedures for calculating real construction is justified. Experienced engineers do not rely solely on analytically obtained results but incorporate additional safety measures. The approximation of the structure by mathematical and numerical models, construction methods, execution inaccuracies, material inhomogeneity, etc., confirms that the calculated and actual behaviour of the structure can only approximately align. Building execution occurs in segments, at different time intervals, using heterogeneous and anisotropic materials, whereas calculation models, in practice, consider the building as a whole. Such analyses may not adequately encompass residual stresses, local plasticization, imperfections, crack appearance and propagation, stress redistribution, soil behaviour, and various subsequent phenomena.

In addition to the series of approximations listed above, the simulation of real behaviour becomes more complex when the building is subjected to seismic (dynamic) loading. A rough approximation occurs when seismic load is introduced to buildings. Firstly, the intensity and properties of the future earthquake are unknown, and secondly, seismic forces' intensity is typically derived by reducing the design elastic spectrum specified in regulations. The accuracy of this reduction under specific conditions and the seismic forces' intensity are valid concerns, given that an earthquake is a spatial phenomenon involving the chaotic propagation of seismic waves through the ground, interacting with the building [1].

It is justified to perform seismic impact calculation analyses for completed structures, considering that an earthquake is a load that manifests when the building is in use. However, considering the aforementioned conditions introducing a series of "errors" into the calculations, it cannot be definitively stated that the building will behave as per the calculations or even withstand the predicted earthquake. Therefore, it is reiterated that, for a favourable seismic response, the most crucial aspect is to have a well-conceived building design, incorporating fundamental seismic principles during the design phase. Those basic principles primarily refer to [2]-[4]:

- proper design of the building disposition, in the base and in height (favourable ratio of dimensions, aspiration towards symmetry, increased stiffness towards the bottom of the building, absence of soft floors, proximity of the centre of stiffness and mass on the floors, increased resistance to torsion, no out-of-line dislocation of vertical columns, no short columns in lower floors, etc.);
- proper selection of stiffness, load capacity, and ductility of the vertical structural system, and the use of seismic dividers at discontinuities;
- the use of rigid interfloor structures in their plane, without semi-levels and larger peripheral perforations (preference is given to monolithic RC interfloors in the system with underlays);
- foundation selection in accordance with the characteristics of the soil and structure (for softer soils, preference should be given to foundation slabs and/or rigid grills);
- performing the infill walls in accordance with the calculation model (e.g., isolating the infill from the RC frame if the infill was not included in the analyses).

The structure's stiffness directly affects the magnitude of the horizontal movements of the building in the case of an earthquake. Increasing stiffness limits the second-order adverse effects on the deformed shape of the vertical supporting elements. Limited movements prevent damage to the infill elements, which can realistically occur even in minor earthquakes. The bearing capacity of the structure affects the formation of plastic joints in a strong earthquake. Higher bearing capacity enables the later formation of plastic joints in the elements and allows elements to remain in the linear-elastic area, without excessive damage, in less strong earthquakes. Ductile structures, in strong earthquakes, have proven to be a good choice because, in the process of nonlinear deformation, they absorb seismic energy and prevent brittle fractures and sudden collapse.

It is known that in constructions made of reinforced concrete, satisfactory load-bearing capacity, stiffness, and ductile behaviour can be achieved even in the strongest expected earthquake, especially in regular structures with proper detail shaping and reinforcement. Such monolithic structures, with their multiple static indeterminacy, enable stress redistribution and prevent progressive breakage due to damage to one of its elements/parts. This is of essential importance in preserving the structure's integrity and preventing collapse because the occurrence of damage in the strongest earthquake is assumed in advance. On the one hand, it is not economical to design an ordinary building that would have damage in the main structure and infill elements in weaker earthquakes, while on the other hand, it is not economical to design such a building that would remain completely undamaged in the strongest earthquake.

RC flexible frame structures in seismically active areas must have a limited height (number of above-ground floors) to ensure that horizontal movements remain within satisfactory limits. It is crucial to accurately predict the formation of plastic joints in beams and columns. A viable solution is to initiate the formation of plastic joints first in the beams, then at the base of the columns, with priority given to the columns of the ground floor. Alternatively, it becomes necessary to stiffen the skeleton with reinforced concrete walls. Well-designed, stiffened structural systems of this nature are extensively employed in many countries worldwide, particularly in regions anticipating strong earthquakes.

Masonry infill is primarily utilized for facades and internal space separation in RC frame structures (Figure 1). However, during seismic calculation analyses, the infill is typically omitted from the structural system model and is only considered as an external load per floor. When a building is designed in this manner, it is essential to implement constructive measures to ensure the actual isolation of masonry infill from the main RC structure.

Specific measures must be taken to prevent walls from tipping out of their plane. If the masonry infill is connected to the RC structure, it will inevitably influence the dynamic characteristics of the structure. Simultaneously, the response of a structure with bonded (non-insulated) infill may be more or less favourable compared to a pure skeleton. The possibility of an unfavourable response must be considered and adequately analysed during the design phase to ensure the building's safety against excessive damage or collapse in a timely manner.

Figure 1. RC frame structures with masonry infill: a) unanchored walls; b) walls anchored with vertical cerclages; c) walls anchored with horizontal and vertical cerclages. Case studies from Banja Luka, Bosnia and Herzegovina. Photography by authors, 2024.

It is known from practice in our region that infill walls of RC frames are traditionally made with classic masonry blocks connected with mortar, without insulating the infill from the frame (Figure 2a). It is not a rare case that reinforcement anchors are placed in each or every other horizontal mortar joint, which are drilled into the columns. Through this connection, overturning out of the plane is ensured (Figure 2b). Another procedure to prevent overturning is to fasten the walls to the RC frames by means of horizontal and/or vertical cerclages, especially for high floors and/or larger spans (Figure 2c). However, it is not rare in recent practice, even in tall buildings construction, that during the masonry process there is no additional rigid binding of the infill, that is, no anchoring of the infill walls for the basic RC skeleton structure.

Figure 2. Execution of frame infill: a) classic masonry; b) anchoring; c) with horizontal cerclage. Case studies from Banja Luka, Bosnia and Herzegovina. Photography by authors, 2024.

The load capacity, stiffness, and ductility of the non-insulated infill will certainly affect the behaviour of the RC frame. These influences are not taken into account or are not adequately considered in everyday engineering calculations. The question of the correctness of such calculation procedures arises because they do not correspond to the

actual state of frame buildings and affect their behaviour in earthquakes. There is a need to consider analyses with non-insulated masonry infill in addition to the calculation analysis of the RC frame structure without included infill. Modern software can relatively quickly analyse several different structure models, and such an approach should be prescribed and standardized in an adequate form, facilitating the application of such calculation analyses in everyday design practice.

1.1. FRAME AND MASONRY INFILL MODELLING

Regarding the infill characteristics, it should be noted that classic walls are made of masonry elements (blocks) and mortar as a binding material. These are heterogeneous elements/materials with anisotropic properties, i.e., there is a big difference in the behaviour of the walls under pressure, tension, and shear. While the walls, on one hand, can accept significant compressive stresses, on the other hand, their tensile load capacity is negligible, and they have a modest shear load capacity. However, shear resistance largely depends on vertical compressive stresses, and without gravity loading, such stresses are almost non-existent, so the shear capacity of infill walls is relatively low.

As noted, rigidly bonded infill with RC columns can disrupt the expected behaviour of a pure frame structure. Reducing the horizontal displacement of the frame is a favourable contribution of the infill, but the rigid infill, even with large cracks and failure, can damage the columns in the contact zones (Figure 3), because the frames under horizontal load exert great pressure on the infill through their deformation. Such frame stresses cause the effects of compressed diagonals and short (shear) columns. In addition, the different purpose on different floors affects the amount of the infill, and thus its effects. It is often the case that infill is omitted on the ground floor (due to business activity), and that infill is significantly represented in the upper floors (due to residential use). This can cause a soft ground floor effect, which is particularly dangerous. Also, the amount of the infill can be different in specific facades in the building. Street facades are often more open than the rest, which significantly causes asymmetry of the building (increasing the eccentricity of the centres of stiffness and mass) and the appearance of unwanted strong torsion under seismic load.

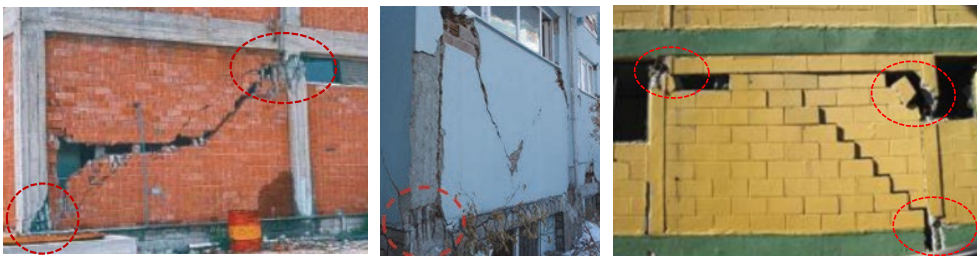

Figure 3. Cracks and crushing of infill and columns in an earthquake as a consequence of mutual action: a) Adana-Ceyhan earthquake 1998 [1]; b) Van earthquake 2011 [1]; c) Chile earthquake 2010 [12].

1.2. OVERVIEW OF CURRENT METHODS

Recent earthquakes in various locations (Petrinja, Croatia, in 2020 [5], Zagreb, Croatia, in 2020 [6], Aegean Sea, Izmir, Turkey, in 2020 [7], Turkey and Syria in 2023 [8], Morocco in 2023) demonstrated significant damage to different building types, especially to brick buildings and masonry infill in RC buildings. Past earthquakes over the last 15 years (L'Aquila – Italy in 2009 [9], Lorca – Spain in 2011 [10], Central Italy in 2016 [11], Albania in 2019 [12]) have also shown that masonry infill in RC frames is highly susceptible to damage. Studies on the earthquake impact on buildings in the 2015 Nepal earthquake revealed that masonry

infill notably increases building stiffness [13]. The contribution of masonry infill to the horizontal bearing capacity of RC frame buildings, using sophisticated computational models, was investigated in [14]. The change in the oscillation period of the building structure caused by non-insulated masonry infill, and thus the change in the calculated seismic forces, was discussed in [15]-[17]. Also, in [18]-[21], different behaviour of rigid masonry infill in flexible frames was investigated. In [22], a broader overview of tests on walls for buckling outside the main plane is given, and the interaction of in-plane and out-of-plane forces is discussed in [23]-[25], and the complex behaviour of RC frames in such conditions is indicated. The conducted tests concluded that frame deformation could lead to the detachment of the masonry infill, potentially causing walls to fall out of their plane.

Omitting non-insulated infill in the design phase calculations can lead to unpredictable behaviour in buildings during earthquakes, particularly in those with irregularly arranged infill walls. Such irregularities cause a number of unfavourable effects (torsion, soft floors, short columns, etc.). These problems were pointed out in [26], [27]. In [28], it was pointed out that the induced torsion easily leads to the out-of-plane buckling of the infill walls. In [29], the problem of a soft floor, which appears due to different requirements for space utilization, was discussed, with the conclusion that this phenomenon must be avoided. The problem of the soft floor was also pointed out in [30]. Also, the dangers of short columns due to strong parapet walls appear, which can be a significant problem, as pointed out in [31], and in [32], it was shown that such infill must be isolated (separated) from the RC frame.

With the ongoing evolution of computational models, combined with growing experience and insights into the impact of infill walls on RC frames, a considerable variety of models have been developed, incorporating masonry infill in their analyses. At the same time, the modelling of RC frames with masonry infill can, in general, be divided into two groups: macro-modelling and micro-modelling. Macromodels are intended for the global calculation analysis of the RC framework structure, where the infill is incorporated in an acceptable form, such as an equivalent compressed diagonal. Micromodels are designed to vary a number of parameters, which include the masonry infill and the boundary conditions of the connection with the RC frame. The goal of such micromodels is to capture as realistically as possible the local yielding of the connection between the infill and the frame. It's important to note that there is still no universally accepted consensus on a single approach to these analyses.

The concept of the equivalent diagonal, by which the masonry infill is introduced into the calculation models, dates back to the 60s of the last century, and over time this concept has been perfected (Figure 4) [33]. However, the equivalent diagonal model cannot capture the change in stress along the column, caused by the infill as a panel with a continuous connection to the column [34], [35]. For this reason, cases of different orientation and number of diagonals were analysed (Figure 5), which reduce the lack of continuous connection between the infill and the frame [36]. Also, some authors dealt with defining the stiffness of the diagonals, that is, the force-displacement relationship. In [37], the width of the diagonal was taken as a percentage of its length, and in [38], [39], a more complex method for calculating the diagonal's width is adopted, taking into account factors such as the contact length between the frame and the infill and the relative stiffness ratio between them.

Also, there are proposals for adequate inclusion of infill bearing capacity and the capacity of different types of failure in RC frames for horizontal force action. In [40], it was recommended to include more types of infill failure in the analyses, and in [41], a nonlinear force-displacement connection was proposed, while a trilinear connection was considered

in [42], [43]. Also, the hysteresis behaviour of the material was considered, but in this case, there are a number of problems in dynamic nonlinear analyses. One of the most frequently applied models is given in [44], [45], while in [46], an improved model is shown, along with experimental tests, which includes the cyclic behaviour of the equivalent diagonal.

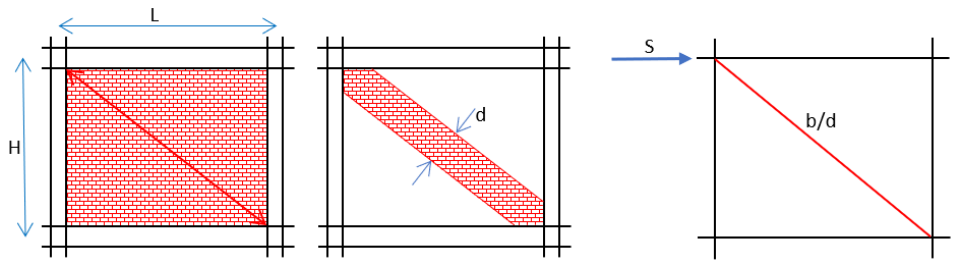

Figure 4. Diagonal action of masonry infill - equivalent pressed diagonal. Diagrams by authors.

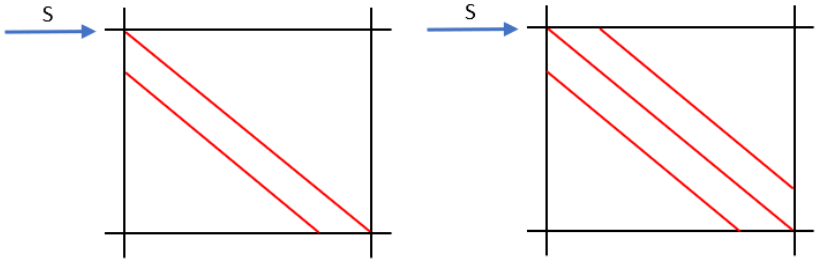

Figure 5. The models with a different number of equivalent pressed diagonals. Diagrams by authors.

The fact is that there is an interaction of horizontal forces in the plane and outside the plane of the frame, yet this presents a complex challenge for accurate modelling. This issue necessitates further research and validation to develop adequate modelling approaches. Increasing the bearing capacity of the masonry infill in the form of the application of reinforced, instead of ordinary walls [47], [48], or using a textile/wire mesh in the mortar [49]-[51], can be one of the solutions to this problem. Also, the formation of horizontal special sliding surfaces is a procedure that increases the deformability of the infill, while not disturbing the influences in RC frames [52]-[55]. By completely isolating infill walls from RC elements using special inserts, the RC frames can function in a way that allows the infill to be disregarded, because in such a case its activation occurs only after significant deformations of the RC elements. Placing soft material in the joints between the infill and the RC elements is imposed as a more simple solution [56], [57], with the fact that the safety of the infill against falling out of the plane should be ensured. In [58], [59], steel anchors were used for the connection of the infill and RC elements, an examination of such connections was conducted, and appropriate recommendations were given.

It has been established that there's a need to persist in developing and refining solutions for insulating infill, and also to validate these solutions through experimental testing. Although the majority of regulations allow the use of isolated infill, these procedures are still not clearly and widely elaborated, so in practice improvisations can often be seen. The INODIS infill frame isolation system (Figure 6) is based on specially designed details supported by experimental tests and numerical analyses [60], [61]. In the non-linear analyses, the software package SAP2000 and the characteristics of the joints after plasticization was used, in accordance with [62]. In the INODIS models, link elements were introduced to simulate the non-linear behaviour of the equivalent diagonal, and the initial

stiffness and stiffness with cracks were determined according to [63]. With such models, different infill configurations were analysed, using the approach from [64], [65].

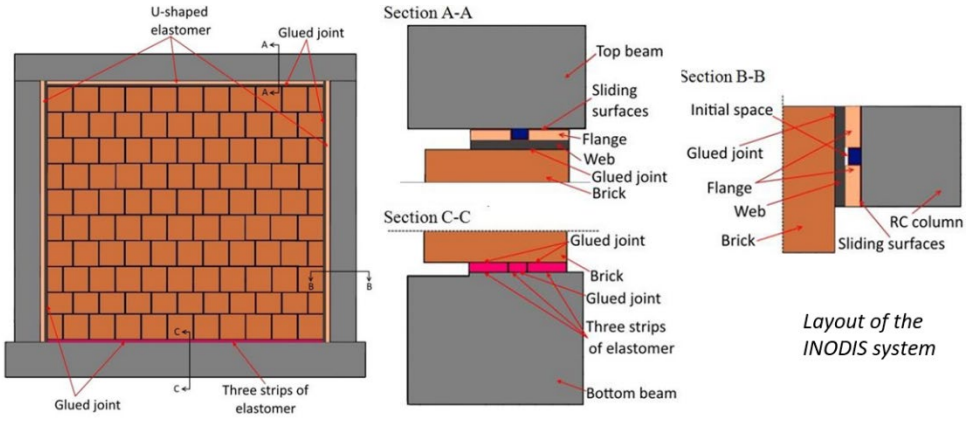

*Figure 6. Infill insulation model in the **INODIS** system [61].*

2. SUGGESTIONS OF POSSIBLE INFILL MODELS

The typical patterns of damage and failure for masonry infill within a RC frame's plane usually manifest in one or a combination of the following three ways:

- horizontal shearing (sliding) of the wall along the mortar joint,
- crushing the wall in the corners due to exceeding the bearing capacity in the pressed diagonal direction,
- cracking the wall as a result of exceeding the tensile load capacity perpendicular to the pressed diagonal.

The expected behaviour of the RC frame with masonry infill, when subjected to lateral forces, in the case of the strongest design earthquake, is non-linear in nature, that is, in a short time it transitions from linear to non-linear behaviour. In this paper, four different cases of frame building with masonry infill are included in the analysis (Figure 7):

a) masonry infill continuously bonded with frame – model Ma,
b) masonry infill isolated from the frame, i.e., frame without infill – model Mb,
c) masonry infill modelled in the form of equivalent elastic diagonals that bear only pressure – model Mc,
d) masonry infill modelled in the form of equivalent diagonals with non-linear behaviour, that only bear pressure up to a certain limit – model Md.

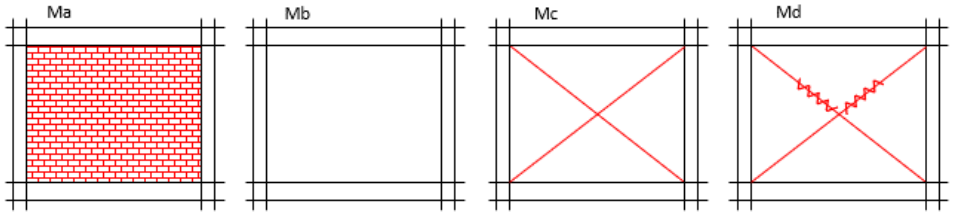

Figure 7. Calculation models of RC frames with masonry infill – Ma, Mb, Mc and Md. Diagrams by authors.

For all cases considered in the analysis, the assumption made was that there is no masonry infill on the ground floor, reflecting a typical design in modern urban multi-story buildings

in these areas (Figure 8). These buildings typically have commercial spaces on the ground floor, which are often subject to changes in usage. As a result, these areas usually lack rigid partitions and facade walls. Conversely, the upper floors, designated for residential use, tend to have a higher density of walls, particularly due to the growing demand for smaller apartments.

Figure 8. Typical buildings in Banja Luka (the ground floor for commercial spaces, and the upper floors for residential use). Photography by authors, 2024.

The discussion presented herein aims to highlight the varying responses of RC frames depending on the type of masonry infill model, illustrated through examples of actual buildings. The numerical modelling was conducted using the *Tower8 software* (*Radimpex*, *Belgrade*), which is well-suited for the calculation of multi-story buildings, including brick buildings.

Cracking of concrete and infill walls in seismic analyses, in all models, was introduced through the realistically expected reduction in stiffness, in accordance with the usual recommendations. In the Md model, non-linear connections of equivalent diagonals/rods with the frame are additionally introduced. The non-linearity of the connections is taken in the form of a bilinear diagram (Figure 9) for pressed rods because, in all cases, the rods are prevented from receiving tension.

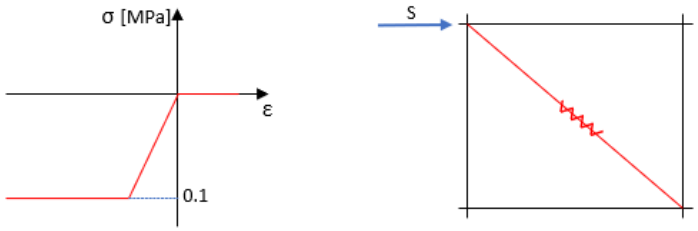

Figure 9. Bilinear elastoplastic working diagram for equivalent diagonals in the Md model. Diagrams by authors.

2.1. SEISMIC ANALYSIS OF ESTABLISHED MODELS

To align with the objective of assessing the impact of masonry infill on the seismic response of the RC frame structures, different numerical models (Ma, Mb, Mc and Md) with different

infill-frame connection modelling were illustrated (Figure 7). As an example, the residual building's frame structure was considered, with the ground floor dimensions being 15.0 x 33.0 m, the upper floors' dimensions being 18.0 x 36.0 m, with a total of P_0+P+4 floors, and an overall height of 2 x 4.0 + 4 x 3.2 = 20.8 m. The basement is a rigid structure with extensive RC walls, so the seismic analysis is performed only for the above – ground part H = 16.8 m. Spatial modelling of the structure was performed (Figure 10a), and the relevant section frames were taken for detailed analysis for all models (Ma, Mb, Mc and Md), where the results are better presented (Figures 10b, 11a and 11b). Seismic analysis was performed according to EC8 (Lateral forces method), for ground acceleration a_{gR} /g=0.25, soil category B and importance factor II (γ=1).

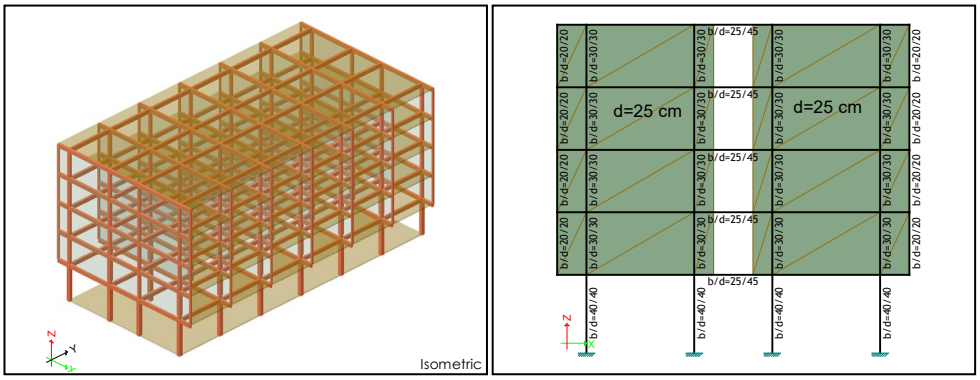

Figure 10. a) Calculation 3D model of the building structure; b) Section frame for model Ma. Diagrams by authors (Radimpex Tower 8).

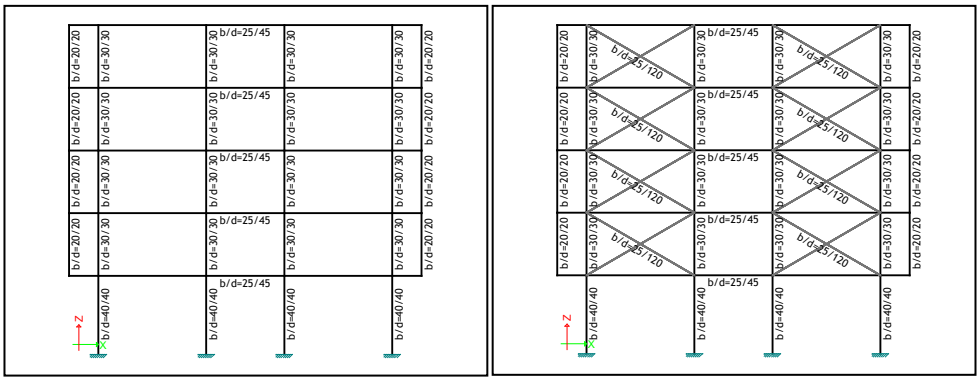

Figure 11. a) Section frame for model Mb; b) Section frame for models Mc and Md. Diagrams by authors, (Radimpex Tower 8).

The dimensions of the columns on the upper floors are w/d=30/30 cm, and on the ground floor are w/d=40/40 cm, to increase the stiffness of the lower floor where the largest stresses are expected. All beams have a cross-section w/d=25/45 cm, while the infill walls have a thickness of d=25 cm (medium class brick). The dimensions of the equivalent diagonal cross-section were taken in accordance with the previously mentioned recommendations, i.e. the width of the diagonal was taken as the value of the wall thickness (b=d_w=25 cm), while the height was taken as 25% of the mean value of the length of the diagonal and the height of the frame (d=0.25·0.5·(h_w+l_d)=0.25·0.5·(320+640)=120 cm). The diagonals are placed only in case of the walls without openings, where they can be fully

activated, that is, only in the two main spans of the frame (Figure 11). Diagonals exclude tension forces.

The initial values of the mechanical characteristics of concrete and infill (uncracked state) were adopted in accordance with the mentioned usual recommendations (Table 1). In the seismic analysis, those values were reduced for the expected cracked state (Table 2).

Table 1. *Table of Materials*

No	Material name	E [kN/m^2]	μ	γ [kN/m^3]	E_m [kN/m^2]	μ_m
1	Brick – medium	3.790e+4	0.2	16.0	2.275e+6	0.2
2	C 25/30	3.100e+7	0.2	25.0	3.100e+7	0.2

Table 2. *Advanced Options of Seismic Analysis*

Masses grouped in the selected ceilings levels	
Beams – reduction of bending stiffness:	0.750
Walls – reduction of bending stiffness:	0.001
Walls – axial stiffness reduction:	0.500
Columns – bending stiffness reduction:	0.750

The gravitational load is identical for all models, so the mass distribution by levels (floors) and the total mass, for all models, is the same (ΣM_{ass}=212 t). The oscillation periods for models Ma, Mb, Mc and Md are 0.532 s, 1.050 s, 0.943 s and 0.943 s, respectively. The behaviour factors were calculated for the *DCM ductility class* in accordance with the structural systems and their regularity. For model Ma, behaviour factor is $q = 0.8 \cdot q_o \cdot k_w = 0.8 \cdot 3 \cdot 1.3 \cdot 1.0 = 3.12$, and for remaining models (Mb, Mc and Md) behaviour factor is $q = q_o \cdot k_w = 3 \cdot 1.3 \cdot 1.0 = 3.90$. The distribution of seismic forces by levels (floors) and the total seismic force ΣS, differ for each model. Thus, for models Ma, Mb, Mc and Md, the values for ΣS are 399 kN, 190 kN, 180 kN and 180 kN, respectively.

Project spectra are given for models Ma and Mb (Figure 12). Models Mc and Md show small deviations from model Mb, so a separate presentation is omitted.

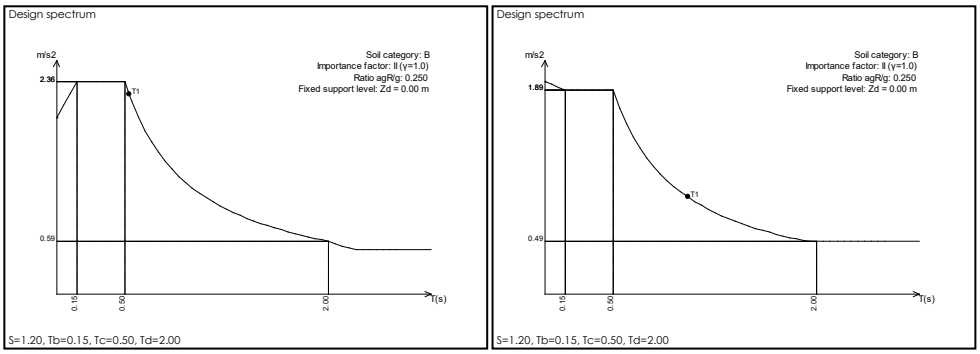

Figure 12. Design spectra: a) for model Ma (T_1=0.532 s, ΣS=399 kN); b) for model Mb (T_1=1.050 s, S=190 kN). Diagrams by authors (Radimpex Tower 8).

For display of characteristic calculation results, diagrams of horizontal displacements X_d and columns bending moments M_3, induced by the horizontal seismic force, are presented (Figures 13-16).

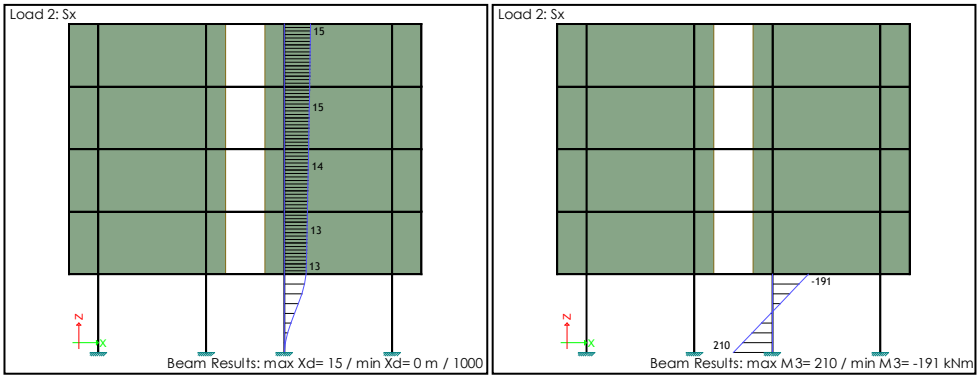

Figure 13. Model Ma impacts: a) horizontal displacement; b) column bending moments. Diagrams by authors, (Radimpex Tower 8).

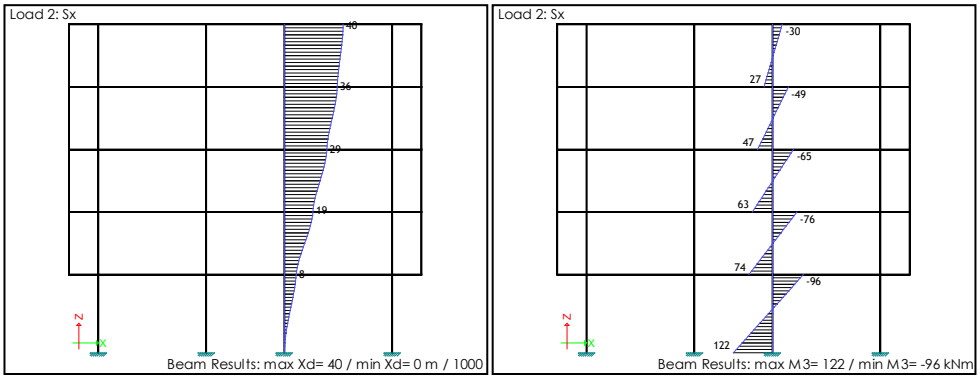

Figure 14. Model Mb impacts: a) horizontal displacement; b) column bending moments. Diagrams by authors, (Radimpex Tower 8).

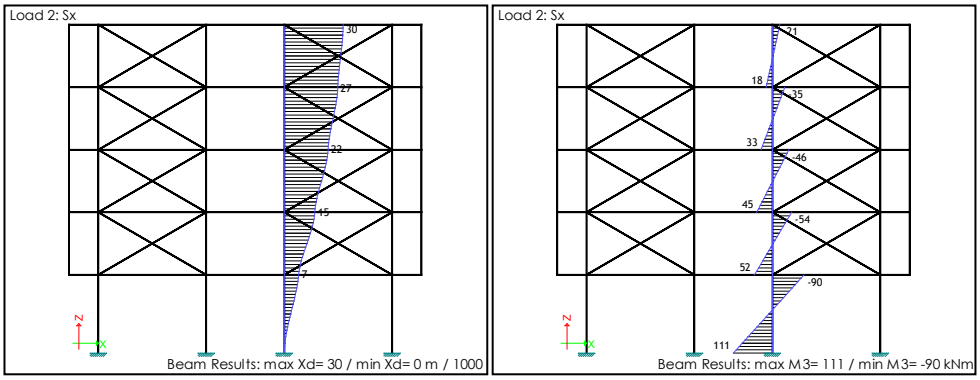

Figure 15. Model Mc impacts: a) horizontal displacement; b) column bending moments. Diagrams by authors, (Radimpex Tower 8).

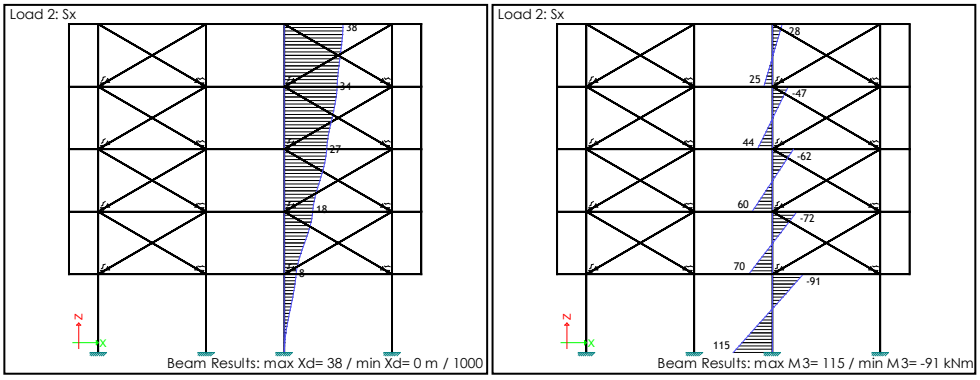

Figure 16. Model Md impacts: a) horizontal displacement; b) column bending moments. Diagrams by authors, (Radimpex Tower 8).

2.2. DISCUSSION OF ANALYSIS RESULTS

From the comparison of the results for the frame without infill and the frame with bonded (non-insulated) infill, a significant drop in the basic oscillation period (by almost 2 times) can be observed, from T=1.050 s for the frame without infill to T=0.532 s for the frame with traditionally bonded infill. On the other hand, the reduction of the period in the case of the frame with equivalent diagonals, compared to the frame without infill is much smaller. The frame with equivalent diagonals has a basic period T=0.943 s, which represents a reduction of only 9%, compared to the frame without infill.

When the oscillation periods on the response spectrum curve are observed (Figure 12), a clear difference can be seen between the frame with bonded infill (model Ma) and the frame without infill (model Mb), showing a significant underestimation of the seismic load level if the infill is not taken into consideration during the calculation. The frame with bonded infill (model Ma) activates a total horizontal force of S=399 kN, whereas the frame without infill activates a force of S=190 kN (model Mb), which is an increase of more than two times. In the frame with bonded infill, the bending moment in the ground floor column is M=210 kNm (model Ma, Figure 13b), while in the frame without infill, that moment is M=122 kNm (model Mb, Figure 14b), which is an increase of approximately 1.7 times. A frame with bonded infill requires a significant increase in reinforcement in the ground floor columns compared to the other frames.

The relative horizontal displacement of the infilled frame floors indicates very small differences, where the absolute floor displacements do not differ a lot from the ground floor displacement (model Ma). This indicates the emergence of a soft ground floor because the horizontal movement of the frame mostly takes place on the ground floor (model Ma, Figure 13a). It is known that the effect of the soft ground floor, due to irregularity, requires the introduction of a smaller behaviour factor, which additionally increases the calculated seismic forces. As expected, due to the increase in stiffness caused by the masonry infill, the displacement of the floors of the frame with bonded infill is significantly less than in the case of the other frames. The maximum horizontal displacement of the frame with bonded infill is X_d=15 mm, while the displacement for isolated infill is X_d=40 mm, which is a decrease of 2.7 times. Also, in the case of frames with bonded infill, the absolute displacements on the ground floor are the largest (X_d=13 mm), compared to all other models (X_d=7.5 mm).

The horizontal floor movement of the frame without infill, due to the uniform stiffness of the floors, indicates its almost linear increase along the height of the building (model Mb,

Figure 14a). As expected, the movement of the floors of the frame without infill indicates that there is no occurrence of a soft ground floor. Also, for the frame without infill, the absolute displacement at the top of the building is greater than the displacement for all other models. The frame with equivalent diagonals is somewhat stiffer than the frame without infill, and the displacements are somewhat smaller (model Mc, Figure 15a). With this frame, the maximum absolute movement at the top of the object is 30 mm, while with the frame without infill, this movement is 40 mm, which is a reduction of 25%. The frame with diagonals, which has a limited ability to receive compressive stress (model Md, Figure 16a), has larger displacements than the frame with standard elastic diagonals, which is expected. The maximum displacement of the frame with the plasticization of the diagonals is 38 mm, which is close to the value of the frame without infill, which is 40 mm.

3. CONCLUSIONS AND RECOMMENDATIONS

In this paper, various instances of masonry infill within calculation models are analysed in accordance with the realistic design and execution of RC frame buildings in Banja Luka and the wider region. Such types of buildings usually have an open ground floor, for business purposes, and floors filled with masonry walls, for residential purposes. The research was conducted to examine the influence of different masonry infill models on the seismic response of an RC frame with an open ground floor. Appropriate conclusions and recommendations were formulated.

The research was conducted on four different models (Ma, Mb, Mc and Md). The basic model consists of a frame without infill (isolated infill) – Mb, and all other models in different ways include masonry infill (continuously bonded, so-called traditional infill – Ma, infill in the form of equivalent elastic diagonals that bear only pressure – Mc and infill in in the form of equivalent diagonals with non-linear behaviour that bear only pressure up to a certain limit – Md). The behaviours between the models were compared, the most interesting being the comparison of the frame with isolated infill (Ma) with the other frames.

The results show that the bonded (non-isolated) infill significantly reduces the natural periods of the frame, thereby increasing the level of seismic load acting on the structure. In addition, the bonded infill produces a soft ground floor effect, which reduces the behaviour factor and increases the intensity of seismic forces. This is not the case with a frame with no infill, or even with a frame filled with equivalent diagonals. The force-displacement curves confirm the low deformation capacity of the frame with traditional infill compared to the frame without an infill and the frames with diagonals. The negative effects of traditional infill on the behaviour of the frame are best illustrated by the large jump in the relative inter-floor displacement, which occurs on the ground floor. In contrast, RC frames with equivalent diagonals behave similarly to unfilled frames, having slightly lower relative inter-story displacements and a gradual increase in absolute displacements along the height of the frame.

Seismic analysis showed very bad effects of traditional infill on the overall behaviour of the building with an open ground floor. The rigid connection of the infill with the frame leads to a significant change in the stiffness of the entire building, which results in a reduction in displacements and the appearance of a soft ground floor (in the case of a building with an open ground floor) and the appearance of significant torsion (in the case of a corner building open to the street). The results show that the building with traditional infill has significantly smaller absolute displacements as well as relative inter-floor displacements, compared to other configurations. However, the movement along the height of the building confirms the

occurrence of a soft ground floor that happens due to large movements at the ground floor level, although the relative inter-floor displacements are small. These negative effects can be removed by applying infill insulation, which results in a slight change in displacement and relative inter-floor displacement. The occurrence of a soft ground floor with a frame without infill is not present because the insulation of the masonry infill eliminates the change in stiffness between floors, which comes from the infill. This is confirmed by calculation analyses of the frame without infill and frames with diagonals, that is, the model of the frame without infill can realistically represent the situation of a building with isolated infill.

Based on the presented results, it can be concluded that the traditional infill, continuously attached to the frame columns, significantly changes the behaviour of RC buildings, which is necessary to take into account during the design process. However, modelling masonry infill is a rather complex and difficult task for everyday practice, especially when that numerical model needs to consider the interaction of out-of-plane and in-plane wall influences, which is necessary. In that case, the calculation of RC frame structure with traditional infill is practically impossible. Therefore, the concept of the design of RC buildings with masonry infill must be improved so as to offer engineers a reliable and stable solution based on constructive measures and not on detailed numerical models. The benefit of the isolation procedure is reflected in the delayed activation of the masonry infill and thus the significant increase in deformation capacity, as well as the removal of in-plane and out-of-plane influence interaction, which significantly improves the behaviour of the RC building with infill. The additional contribution of infill insulation is seen in case of any change in the basic structure or infill during the building construction or use because such changes do not have a significant effect on the basic RC frame. In addition, the numerical model in the form of an RC frame, which takes into account the isolated masonry infill only as a load, is simple to use in everyday practice.

The insulation of the masonry infill should be done correctly because its unprofessional separation of from the RC frame can lead to the infill falling perpendicularly to the wall plane. This is especially dangerous for the upper floors of tall buildings because the movements of those floors are significant. Recently, it has been noticeable that in domestic practice this is not taken into account, i.e. there is infill with classic masonry without special insulation, but also without additional connections to the frame in the form of cerclage or anchors. This is the worst possible form because during an earthquake the frames are not saved from the impact of the rigid infill, and the walls are not secured from falling out of the frame. It is necessary to urgently innovate construction rules and procedurally oblige contractors to comply with those rules. This would prevent the possibility of excessive damage to the RC frame and/or walls falling out, thereby endangering human lives and buildings as a result of the earthquake.

4. REFERENCES

[1] G. Broćeta, A. Cumbo, S. Cvijić Amulić, M. Latinović Krndija, E. Zlatanović, S. Šupić, "Seismic waves analysis," *Book of Proceedings, International Scientific Forum – Geotechnical Aspects of Civil Engineering and Earthquake Engineering*, Vrnjačka Banja, Serbia, pp. 289-298, 2023.

[2] A. Cumbo, "Evaluation of seismic resistance of existing buildings – experience from Banja Luka," *Conference proceedings, Ninth international conference: Assessment, maintenance and rehabilitation of structures and settlements*, Zlatibor, Serbia, pp. 569-578, 2015. (in Serbian).

[3] A. Cumbo, “The reinforcement and upgrading of existing buildings complex in Sarajevo,” *Conference proceedings, Sixth international conference: Earthquake engineering and engineering seismology*, Kraljevo, Serbia, pp. 457-464, 2018. (in Serbian).

[4] A. Cumbo, “Structure state assessment of the public health institute building in Banja Luka,” *Conference proceedings, Eleveenth international conference: Assessment, maintenance and rehabilitation of structures and settlements*, Zlatibor, Serbia, pp. 271-282, 2019. (in Serbian).

[5] J. Radnić, N. Grgić, A. Buzov, I. Banović, M. Smilović Zulim, G. Baloević, M. Sunara, “Mw 6.4 Petrinja earthquake in Croatia: Main earthquake parameters, impact on buildings and recommendation for their structural strengthening,” *Građevinar,* vol. 73, no. 11, pp. 1109-1128, 2021, doi: 10.14256/JCE.3243.2021.

[6] M. Šavor Novak, M. Uroš, J. Atalić, M. Herak, M. Demšić, M. Baniček, D. Lazarević, N. Bijelić, M. Crnogorac, M. Todorić, “Zagreb earthquake of 22 March 2020 – preliminary report on seismologic aspects and damage to buildings,” *Građevinar*, vol. 72, no. 10, pp. 843-867, 2020, doi: 10.14256/JCE.2966.2020.

[7] H.C. Mertol, G. Tunc, T. Akis, “A site survey of damaged RC buildings in İzmir after the Aegean sea earthquake on October 30,” *Građevinar,* vol. 75, no. 5, pp. 451-470, 2023, doi: 10.14256/JCE.3343.2021.

[8] A. Arbinja. D. Janković, R. Vukomanović G. Broćeta, A. Cumbo, “Razorni zemljotresi u Turskoj i Siriji – uzroci i posljedice,” *SAG+, Sav. grad. – Časopis za arh., građ. i geod.*, vol. 13, pp. 20-27, 2023. (in Serbian).

[9] F. Braga, V. Manfredi, A. Masi, A. Salvatori, M. Vona, “Performance of non-structural elements in RC buildings during the L’Aquila, 2009 earthquake,” *Bull. of Earth. Eng.*, vol. 9, no. 1, pp. 307-324, 2011, doi: 10.1007/s10518-010-9205-7.

[10] L. Hermanns, A. Fraile, E. Alarcón, R. Álvarez, “Performance of buildings with masonry infill walls during the 2011 Lorca earthquake,” *Bull. of Earth. Eng.*, vol. 12, no. 5, pp. 1977-1997, 2014, doi: 10.1007/s10518-013-9499-3.

[11] A. Masi, L. Chiauzzi, G. Santarsiero, V. Manfredi, S. Biondi, E. Spacone, C. Del Gaudio, P. Ricci, G. Manfredi, G.M. Verderame, “Seismic response of RC buildings during the M w 6.0 August 24, 2016 Central Italy earthquake, The Amatrice case study,” *Bull. of Earth. Eng.*, vol. 17, no. 10, pp. 5631-5654, 2017.

[12] S. Nikolić-Brzev, M. Marinković, I. Milicević, N. Blagojević, “Posledice zemljotresa u Albaniji od 26.11.2019. na objekte i infrastrukturu,” (Consequences of the November 26, 2019 Albania earthquake on the buildings and infrastructure), *Serbian Association for earthquake engineering (SUZI-SAEE)*, Belgrade, Serbia, p. 80 p, 2020. (in Serbian).

[13] H. Varum, A. Furtado, H. Rodrigues, J. Dias-Oliveira, N. Vila-Pouca, A. Arêde, “Seismic performance of the infill masonry walls and ambient vibration tests after the Ghorka 2015, Nepal earthquake,” *Bull. of Earth. Eng.*, vol. 15, no. 3, pp. 1185-1212, 2017, doi: 10.1007/s10518-016-9999-z.

[14] S. Yousefianmoghadam, M. Song, M.E. Mohammadi, B. Packard, A. Stavridis, B. Moaveni, R.L. Wood, “Nonlinear dynamic tests of a reinforced concrete frame building at different damage levels,” *Earth. Eng. and Struct. Dyn.*, vol. 49, no. 9, pp. 924-945, 2020, doi: 10.1002/eqe.3271.

[15] P. Ricci, G.M. Verderame, G. Manfredi, “Analytical investigation of elastic period of infilled RC MRF buildings,” *Eng. Struc.*, vol. 33, no. 2, pp. 308-319, 2011, doi: 10.1016/j.engstruct.2010.10.009.

[16] P.G. Asteris, C.C. Repapis, A.K. Tsaris, F. Di Trapani, L. Cavaleri, “Parameters affecting the fundamental period of infilled RC frame structures,” *Earth. and Struct.*, vol. 9, no. 5, pp. 999-1028, 2015, doi: 10.12989/eas.2015.9.5.999.

[17] D. Perrone, E. Brunesi, A. Filiatrault, R. Nascimbene, "Probabilistic estimation of floor response spectra in masonry infilled reinforced concrete building portfolio," *Eng. Struct.*, vol. 202, 109842, 2020, doi: 10.1016/j.engstruct.2019.109842.
[18] G. Al-Chaar, M. Issa, S. Sweeney, "Behavior of masonry-infilled nonductile reinforced concrete frames," *Jour. of Struct. Eng.*, vol. 128, no. 8, pp. 1055-1063, 2002, doi: 10.1061/(ASCE)0733-9445(2002)128:8(1055).
[19] A. Stavridis, P.B. Shing, "Finite-element modeling of nonlinear behavior of masonry-infilled RC frames," *Jour. of Struct. Eng.*, vol. 136, no. 3, pp. 285-296, 2010, doi: 10.1061/(ASCE)ST.1943-541X.116.
[20] C. Zhai, J. Kong, X. Wang, Z. Chen, "Experimental and finite element analytical investigation of seismic behavior of full-scale masonry infilled RC frames," *Jour. of Earth. Eng.*, vol. 20, no. 7, pp. 1171-1198, 2016, doi: 10.1080/13632469.2016.1138171.
[21] S. Hak, P. Morandi, G. Magenes, "Prediction of inter-storey drifts for regular RC structures with masonry infills based on bare frame modelling," *Bull. of Earth.Eng.*, vol. 16, pp. 397–425, 2017, doi: 10.1007/s10518-017-0210-y.
[22] A. Furtado, H. Rodrigues, A. Arêde, H. Varum, "Out-of-plane behavior of masonry infilled RC frames based on the experimental tests available: A systematic review," *Const. and Build. Mat.*, vol. 168, pp. 831-848, 2018, doi: 10.1016/j.conbuildmat.2018.02.129.
[23] A. Furtado, H. Rodrigues, A. Arêde, H. Varum, "Assessment of the mainshock-aftershock collapse vulnerability of RC structures considering the infills in-plane and out-of-plane behaviour," *Proc. Eng.*, vol. 199, pp. 619-624, 2017, doi: 10.1016/j.proeng.2017.09.107.
[24] M.T. De Risi, M. Di Domenico, P. Ricci, G.M. Verderame, G. Manfredi, "Experimental investigation on the influence of the aspect ratio on the in-plane/out-of-plane interaction for masonry infills in RC frames," *Eng. Struct.*, vol. 189, pp. 523-540, 2019, doi: 10.1016/j.engstruct.2019.03.111.
[25] C. Butenweg, M. Marinković, R. Salatić, "Experimental results of reinforced concrete frames with masonry infills under combined quasi-static inplane and out-of-plane seismic loading," *Bull. of Earth. Eng.*, vol. 17, no. 6, pp. 3397-3422, 2019, doi: 10.1007/s10518-019-00602-7.
[26] K. Kostinakis, A. Athanatopoulou, "Effects of in-plan irregularities caused by masonry infills on the seismic behavior of R/C buildings," *Soil Dyn. and Earth. Eng.*, vol. 129, 2020, doi: 10.1016/j.soildyn.2019.03.012.
[27] M. Ferraioli, A. Lavino, "Irregularity Effects of Masonry Infills on Nonlinear Seismic Behaviour of RC Buildings," *Math. Prob. in Eng.*, vol. 59, pp. 105737, 2020, doi: 10.1155/2020/4086320.
[28] O. Onat, A.A. Correia, P.B. Lourenço, A. Koçak, "Assessment of the combined in-plane and out-of-plane behavior of brick infill walls within reinforced concrete frames under seismic loading," *Earth. Eng. and Struct. Dyn.*, vol. 47, no. 14, pp. 2821-2839, 2018, doi: 10.1002/eqe.3111.
[29] T.K. Padhy, A.M. Prasad, D. Menon, D.P. Robin, "Seismic Performance Assessment of Open Ground Storey Buildings," *Proceedings, 15th World Conference on Earthquake Engineering*, Lisbon, 2012.
[30] A. Pokhrel, D. Gautam, H. Chaulagain, "Effect of variation on infill masonry walls in the seismic performance of soft story RC building," *Austr. Jour. of Struct. Eng.*, vol. 20, no. 1, pp. 1-9, 2019, doi: 10.1080/13287982.2018.1546449.
[31] Y.J. Chiou, J.C. Tzeng, Y.W. Liou, "Experimental and analytical study of masonry infilled frames," *Journal of Structural Engineering*, vol. 125, no. 10, pp. 1109-1117, 1999, doi: 10.1061/(ASCE)0733-9445(1999)125:10(1109).

[32] C.V.R. Murty, S. Brzev, H. Faison, A. Irfanoglu, C.D. Comartin, " At risk: The seismic performance of reinforced concrete frame buildings with masonry infill walls. A tutorial developed by a committee of the World Housing Encyclopedia, a project of the Earthquake Engineering Research Institute and the International Association for Earthquake Engineering," *Earth. Eng. Res. Inst*., Oakland, California, 2006. Accessed: Jan 12, 2024. [Online]. Available: https://www.world-housing.net/wp-content/uploads/2011/05/RCFrame_Tutorial_English_Murty.pdf

[33] L. Liberatore, F. Mollaioli, "Influence of masonry infill modelling on the seismic response of reinforced concrete frames," *Civil-Comp Proceedings*, vol. 108, pp. 1-17, 2015.

[34] F.J. Crisafulli, "Seismic behaviour of reinforced concrete structures with masonry infills," Ph.D. dissertation, Depart. of Civ. Eng., University of Canterbury, Christchurch, New Zealand, 1997.

[35] P.G. Asteris, "Finite element micro-modelling of infilled frames," *Elect. Jour. of Struct. Engi.*, vol. 8, pp. 1-11, 2008, doi: 10.56748/ejse.894.

[36] R. Žarnić, M. Tomaževič, "An Experimentally Obtained Method for Evaluation of the Behaviour of Masonry Infilled R/C Frames," *Proceedings of the 9th World Conference on Earthquake Engineering*, Tokyo, Japan, Vol. VI, pp. 163-168, 1988.

[37] B.S. Smith, "Lateral stiffness of infilled frames," *Jour. of the Struct. Div.*, vol. 88, no. 6, pp. 183-226, 1962.

[38] G. Al-Chaar, "Evaluating strength and stiffness of unreinforced masonry infill structures (No. ERDC/CERL-TR-02-1)," *Engineer research and development center champaignil construction engineering research lab*, 2002.

[39] C.Z. Chrysostomou, P.G. Asteris, "On the in-plane properties and capacities of infilled frames," *Eng. Struct.*, vol. 41, pp. 385-402, 2012, doi: 10.1016/j.engstruct.2012.03.057.

[40] B. Stafford-Smith, H. Coull, "Infilled-Frame Structures," *Tall Building Structures: Analysis and Design, John Wiley and Sons*, Inc., New York, pp. 168-183, 1991.

[41] T.B. Panagiotakos, M.N. Fardis, "Seismic response of infilledrc frames structures". *11th World Conference on Earthquake Engineering*, paper 225, pp. 23-28, 1996.

[42] M. Dolšek, P. Fajfar, "The effect of masonry infills on the seismic response of a fourstorey reinforced concrete frame – a deterministic assessment," *Eng. Struct.*, vol. 30, no. 7, pp. 1991–2001, 2008, doi: 10.1016/j.engstruct.2008.01.001.

[43] P.B. Shing, A. Stavridis, "Analysis of seismic response of masonry-infilled RC frames through collapse," *ACI Symposium Publication, vol. 297.*, pp. 1–20, 2014.

[44] R.E. Klingner, V.V. Bertero, "Infilled frames in earthquake resistant construction," Report No. EERC 76-32, University of California, Berkely, 1976.

[45] F.J. Crisafulli, A.J. Carr, "Proposed macro-model for the analysis of infilled frame structures," *Bull. NZ Soc. Earth. Eng*, vol. 40, no. 2, pp. 69–77, 2007, doi: 10.5459/bnzsee.40.2.69-77.

[46] L. Cavaleri, M. Fossetti, M. Papia, "Infilled frames: developments in the evaluation of cyclic behaviour under lateral loads," *Struct. Eng. and Mech.*, vol. 21, no. 4, pp. 469-494, 2005, doi: 10.12989/sem.2005.21.4.469.

[47] G.M. Calvi, D. Bolognini, "Seismic response of reinforced concrete frames infilled with weakly reinforced masonry panels," *Jour. of Earth. Eng.*, vol. 5, no. 2, pp. 153-185, 2001, doi: 10.1080/13632460109350390.

[48] A. Furtado, H. Rodrigues, A. Arêde, H. Varum, "Experimental tests on strengthening strategies for masonry infill walls: A literature review," *Const. and Build. Mat.*, vol. 263, pp. 120520, 2020, doi: 10.1016/j.conbuildmat.2020.120520.

[49] F. Da Porto, G. Guidi, N. Verlato, C. Modena, "Effectiveness of plasters and textile reinforced mortars for strengthening clay masonry infill walls subjected to

combined in-plane/out-ofplane actions/Wirksamkeit von Putz und textilbewehrtem Mörtel bei der Verstärkung von Ausfachungswänden aus Ziegelmauerwerk, die kombinierter Scheiben-und Plattenbeanspruchung ausgesetzt sind," *Mauerwerk*, vol. 19, no. 5, pp. 334-354, 2015, doi: 10.1002/dama.201500673.

[50] F. Akhoundi, G. Vasconcelos, P. Lourenço, L.M. Silva, F. Cunha, R. Fangueiro, "In-plane behavior of cavity masonry infills and strengthening with textile reinforced mortar," *Eng. Struct.*, vol. 156, pp. 145-160, 2018, doi: 10.1016/j.engstruct.2017.11.002.

[51] D.A. Pohoryles, D.A. Bournas, "Seismic retrofit of infilled RC frames with textile reinforced mortars: State-of-the-art review and analytical modelling," *Compos. Part B: Eng.*, vol. 183, pp. 107702, 2020, doi: 10.1016/j.compositesb.2019.107702.

[52] M. Preti, N. Bettini, G. Plizzari, "Infill walls with sliding joints to limit infill-frame seismic interaction: large-scale experimental test," *Jour. of Earth. Eng.*, vol. 16, no. 1, pp. 125-141, 2012, doi: 10.1080/13632469.2011.579815.

[53] M. Preti, L. Migliorati, E. Giuriani, "Experimental testing of engineered masonry infill walls for post-earthquake structural damage control," *Bull. of Earth. Eng.*, vol. 13, no. 7, pp. 2029-2049, 2015, doi: 10.1007/s10518-014-9701-2.

[54] N. Verlato, G. Guidi, F. Da Porto, C. Modena, "Innovative systems for masonry infill walls based on the use of deformable joints: combined inplane/out-of-plane tests," in *Brick and Block Masonry*, CRC Press, 2016, pp. 1359-1366.

[55] P. Morandi, R.R. Milanesi, G. Magenes, "Innovative solution for seismic-resistant masonry infills with sliding joints: in-plane experimental performance," *Eng. Struct.*, vol. 176, pp. 719-733, 2018, doi: 10.1016/j.engstruct.2018.09.018.

[56] Q. Peng, X. Zhou, C. Yang, "Influence of connection and constructional details on masonryinfilled RC frames under cyclic loading," *Soil Dyn. and Earth. Eng.*, vol. 108, pp. 96-110, 2018, doi: 10.1016/j.soildyn.2018.02.009.

[57] A.V. Tsantilis, T.C. Triantafillou, "Innovative seismic isolation of masonry infills using cellular materials at the interface with the surrounding RC frames," *Eng. Struct.*, vol. 155, pp. 279-297, 2018, doi: 10.1016/j.engstruct.2017.11.025.

[58] J.S. Kuang, Z. Wang, "Cyclic load tests of rc frame with column-isolated masonry infills," In *Second European Conference on Earthquake Engineering and Seismology*, Istanbul, pp. 25-29, 2014.

[59] L. Facconi, F. Minelli, "Retrofitting RC infills by a glass fiber mesh reinforced overlay and steel dowels: experimental and numerical study," *Const. and Build. Mat.*, vol. 231, 117133, 2020, doi: 10.1016/j.conbuildmat.2019.117133.

[60] M. Marinković, C. Butenweg, "Innovative decoupling system for the seismic protection of masonry infill walls in reinforced concrete frames," *Eng. Struct.*, vol. 197, 109435, 2019, doi: 10.1016/j.engstruct.2019.109435.

[61] M. Marinković, S. Flores Calvinisti, C. Butenweg, "Numerical analysis of reinforced concrete frame buildings with, decoupled infill walls," *Build. Mat. and Struct.,* vol. 63, no. 4, pp. 13-48, 2020, doi: 10.5937/GRMK2004013M.

[62] FEMA 356, "Prestandard and Commentary for the Seismic Rehabilitation of Buildings," *Fed. Emerg. Manag. Ag.*, Washington, D.C., U.S.A., 2000.

[63] N. M. Noh, L. Liberatore, F. Mollaioli, S.Tesfamariam, "Modelling of masonry infilled RC frames subjected to cyclic loads: State of the art review and modelling with OpenSees," *Eng. Struct.*, vol. 150, pp. 599-621, 2017, doi: 10.1016/j.engstruct.2017.07.002.

[64] L. Liberatore, F. Noto, F. Mollaioli, P. Franchin, "In-plane response of masonry infill walls: Comprehensive experimentally-based equivalent strut model for deterministic and probabilistic analysis," *Eng. Struct.*, vol. 167, pp. 533-548, 2018, doi: 10.1016/j.engstruct.2018.04.057.

[65] M. M. Abdelaziz, M. S. Gomaa, H. El- Ghazaly, “Seismic evaluation of reinforced concrete structures infilled with masonry infill walls,” *A. Jour. of Civ. Eng.*, vol. 20, pp. 961–981, 2019, doi: 10.1007/s42107-019-00158-6.

Acknowledgement

The research has been conducted within the project "Scientific and experimental research and improvement of educational process in the field of civil engineering, geodesy and disaster risk management and fire safety”, developed at the Department of Civil Engineering and Geodesy, Faculty of Technical Sciences, University of Novi Sad, Serbia.

AUTHOR'S BIOGRAPHIES

Anđelko Cumbo

Prof. dr Anđelko Cumbo has been working as an assistant professor at the Faculty of Architecture, Civil Engineering, and Geodesy of the University of Banja Luka. In his research work, he focuses on the development of computational modelling for the analysis of complex composite structures, as well as analyses and modelling of structures under strong earthquakes. This includes the behaviour and strengthening of retrofitted and older structures.

Gordana Broćeta

Prof. dr Gordana Broćeta has been working as an associate professor at the Faculty of Architecture, Civil Engineering, and Geodesy at the University of Banja Luka. The focuses of her scientific research are influential factors on various aspects of the durability of concrete structures, assessment of concrete structures, and building materials.

Marina Latinović Krndija

Marina Latinović Krndija has been working as a teaching assistant at the Faculty of Architecture, Civil Engineering, and Geodesy at the University of Banja Luka. She is currently working on a doctoral dissertation at the Faculty of Civil Engineering, University of Belgrade, in the field of numerical and experimental vibration analysis of pedestrian bridges.

Slobodan Šupić

Prof. dr Slobodan Šupić is an Assistant Professor at the Faculty of Technical Sciences, University of Novi Sad. His research of interest is related to: building materials, technology of concrete, contemporary composites based on waste and recycled materials, assessment and repair of structures, fire safety.

Žarko Lazić

Žarko Lazić worked as a teaching assistant at the Faculty of Architecture, Civil Engineering, and Geodesy at the University of Banja Luka. He is currently working on a doctoral dissertation at the Faculty of Civil Engineering, University of Belgrade, in the field of bond transfer length between concrete and strands in pretensioned concrete structures.

УТИЦАЈ ИЗБОРА ТИПА МОДЕЛА ЗИДАНЕ ИСПУНЕ НА СЕИЗМИЧКИ ОДГОВОР АРМИРАНОБЕТОНСКИХ ОКВИРНИХ ЗГРАДА

Сажетак: Армиранобетонски (АБ) оквири су, у многим земљама, широко заступљени као главна конструкција зграда. При томе се испуна оквира најчешће изводи традиционалним зидањем (опекарски елементи повезани малтером) без раздвајања од оквира. Познато је да се у инжењерској пракси прорачунске анализе АБ оквирних зграда на сеизмичке силе уобичајено раде на моделима без укључивања зидане испуне, чак и у случајевима када посебним конструктивним мјерама испуна није изолована од оквира, при чему се зидови узимају само као стално оптерећење. Тиме је потпуно занемарен допринос неизоловане зидане испуне на промјену носивости, крутости и дуктилности АБ оквира, односно на промјену напрезања и хоризонталног помјерања конструкције приликом дејства сеизмичких сила. У циљу сагледавања посљедица овако, за праксу уобичајено, постављеног прорачунског модела, у раду су анализирана четири карактеристична типа модела АБ оквира са зиданом испуном. Показало се да различито постављени модели исте зграде мијењају динамичке карактеристике, односно силе и помјерања главне оквирне конструкције. Наиме, приказаном динамичком анализом, показује се да због неадекватног третирања везе оквира и неизоловане испуне, у фази пројектовања, на жалост, неријетко, "остају непримјећене" врло опасне појаве попут "меке етаже", значајне торзије и сл. Стога се у раду наглашава важност да се у свакодневној инжењерској пракси неизолована испуна третира у прорачунском моделу на едекватан начин. Такође, у раду се апелује на потребу да се донесу прецизна упутства за посебне конструктивне мјере, којим би се потпуно изоловала зидана испуна од оквира, када је такво рјешење оправдано.

Кључне ријечи: АБ оквирне зграде, зидана испуна, динамичке карактеристике, крутост и дуктилност испуне

St. James's Church (Mali Vrh) consequences Petrinja earthquake. Photographer: Janezdrilc. Source: https://commons.wikimedia.org/wiki/File:St._James%27s_Church_(Mali_Vrh)_09.jpg (Wikimedia Commons)

University of Banja Luka I Faculty of Architecture, Civil Engineering and Geodesy
ISSN 2712-0570 I UDC 72

2025
Special Issue
Earthquake Engineering

AGG+ Journal for Architecture, Civil Engineering, Geodesy and Related Scientific Fields
АГГ+ часопис за архитектуру, грађевинарство, геодезију и сродне научне области

074-087 **Categorisation** I Review scientific paper
DOI I 10.61892/AGG202502033K
Paper received I 26/09/2024
Paper accepted I 28/02/2025

Branko Kordić *
Croatian Geological Survey, Croatia, bkordic@hgi-cgs.hr

Stéphane Baize
French Nuclear Safety and Radiation Protection Authority, France, stephane.baize@asnr.fr

Josipa Maslač Soldo
Croatian Geological Survey, Croatia, jmaslac@hgi-cgs.hr

ENVIRONMENTAL IMPACT ASSESSMENT AND SEISMIC HAZARD ANALYSIS: PETRINJA 2020 EXPERIENCE

Review scientific paper
DOI 10.61892/AGG202502033K
Paper received | 26/09/2024
Paper accepted | 28/02/2025

* corresponding author

Branko Kordić *
Croatian Geological Survey, Croatia, bkordic@hgi-cgs.hr

Stéphane Baize
French Nuclear Safety and Radiation Protection Authority, France, stephane.baize@asnr.fr

Josipa Maslač Soldo
Croatian Geological Survey, Croatia, jmaslac@hgi-cgs.hr

ENVIRONMENTAL IMPACT ASSESSMENT AND SEISMIC HAZARD ANALYSIS: PETRINJA 2020 EXPERIENCE

ABSTRACT

On December 29, 2020, a shallow magnitude 6.2 earthquake struck northern Croatia near Petrinja. This earthquake was preceded by a strong foreshock with a magnitude of 5. In response to the Petrinja earthquake, a team of European geologists and engineers from Croatia, Slovenia, France, Italy, and Greece was promptly mobilized to conduct a thorough assessment of the environmental impact of the earthquake. Their observations in the Petrinja area revealed surface deformation, tectonic breaks along the earthquake source at the surface, liquefaction features in the fluvial plains of the Kupa, Glina, and Sava rivers, and slope failures caused by strong motion. However, with the analysis of geodetic data, the team concluded that the field measurements largely underestimated the total coseismic deformation at the surface: a large part has been distributed and diffused off the main fault. Liquefaction extended over nearly 600 km^2 around the epicenter, with the typology of liquefaction features including sand blows, lateral spreading phenomenon spreads along the road and river embankments, and sand ejecta of different grain sizes and matrices. After a series of investigations along the 2020 earthquake causative fault, we documented several paleo-ruptures during the Holocene and evidenced a cumulative strike-slip fault displacement all along the Petrinja Pokupsko Fault (PPF), including a few of those segments which did not rupture in 2020. Based on the Croatian experience of the last three years, we stress that further detailed studies, including neotectonics, paleoseismological and geophysical investigations, could bring new relevant information on the seismic activity and seismic hazards in the regional fault zone, the southern continuation of the PPF, along the related fault zone that stretches towards Kostajnica.

Keywords: *earthquake, investigation, field survey, seismic hazard.*

1. INTRODUCTION

The ML 6.2 Petrinja earthquake that occurred on 29 December 2020 is one of the largest continental earthquakes in central Europe since the ML 6.5 earthquake in Central Italy in 2016 and the ML 6.4 Durres earthquake in Albania on 26 November 2019, both in the Central Mediterranean area. The characteristics of this earthquake closely resemble those of the 1969 earthquake in Banja Luka, which had a mainshock of magnitude 6.4, preceded by a strong foreshock with a magnitude of 6.0. The series of earthquakes that occurred in the Petrinja area in 2020, as well as the earthquake near Zagreb nine months earlier, resulted in the loss of human lives and significant damage to infrastructure and buildings. The material damage is enormous and will take years to repair.

This 2020 earthquake cannot be claimed as a “surprise”: the historic Croatian earthquake occurred on 8 October 1909 very close to Petrinja (20 km to the northwest), and it is known as the Pokupsko or Kupa Valley earthquake [1,2]. Both earthquakes present focal mechanisms consistent with the activation of an NW-SE right-lateral fault, which belongs to the fault system that runs along the southwestern margin of the Pannonian basin. After the 2020 Petrinja event, HGI (Croatian Geological Survey), in collaboration with a European team of geologists and engineers from France, Italy, Slovenia, and Greece, conducted a detailed survey of the environmental effects on the surface after the Mw 6.4 earthquake near Petrinja in December 2020. Despite field challenges (rain, snow, COVID-19, minefields), more than 700 observation points were collected on an area of 625 km^2 [3] and then analyzed in the office and laboratories. Field research was conducted using an existing geological map at a scale of 1:100,000, a 1:5,000 topographic map, historical aerial photogrammetric data provided by the Croatian State Geodetic Administration, and InSAR interferograms derived from Sentinel-1 satellite observations. An Unmanned Aerial System (UAS) was used during the fieldwork to document surface evidence. Airborne Laser Scanning (ALS) measurements were also conducted to generate high-resolution Digital Terrain Models (DTMs). These DTMs provided a foundation for on-site research and further investigation within a Geographic Information System (GIS) environment. An office spatial analysis was then conducted for a specific location in preparation for upcoming paleoseismological research. Following this analysis, the identified sites underwent further examination through the implementation of Ground Penetrating Radar (GPR) and Electrical Resistivity Tomography (ERT) geophysical profiles.

The Petrinja earthquake took place nine months after a magnitude 5.5 earthquake hit the City of Zagreb on March 22, 2020—Zagreb's strongest instrumentally recorded seismic event since Andrija Mohorovičić established the first seismograph in 1908. In contrast with the 2020 Petrinja earthquake, this event shows reverse kinematics along an ENE-WSW blind fault [4]. Seismic activity in the Zagreb region is well-documented, indicating high seismic hazard [5]. The earthquake caused extensive damage to residential buildings, especially those built in the first half of the 20th century [4]. Unfortunately, in addition to material damage, the earthquakes that occurred in 2020 in the areas of Zagreb and Petrinja also claimed human lives and had lasting consequences on people's lives, which was further worsened by the quarantine due to COVID-19 [6]. In contrast with the 2020 Petrinja earthquake, this event shows reverse kinematics along an ENE-WSW blind fault [5].

Basili [7] used at least partly the available information on those historical and instrumental earthquakes, as well as geological data, to define the main crustal earthquake sources of the region (Figure 1). Besides the ENE-WSW striking, south-dipping and left-reverse source

beneath Zagreb, a 75 km-long NW-SE dextral source crosses almost the entire north-central territory of Croatia and terminates at Kostajnica. In the south, a series of NW-SE dextral sources are aligned, running beneath Banja Luka and Sarajevo.

This depiction of sources aims to represent the seismic hazard associated with major geologic features, supported by first-order evidence, for a calculation at the continental scale. However, it is a drastic simplification of the tectonic "reality". For instance, it does not match either the actual segmentation of the PPF or its real dip, as shown by the recent studies performed by the EU-Group [8,9]. To properly describe the earthquake sources, especially in order to further evaluate the hazards at the site-specific level, we claim that a proper analysis and interpretation of active faults and related effects is of primary importance. Because there is evidence that the NW-SE faults running across Croatia (under study) have a continuation in the northern part of Bosnia and Herzegovina, we emphasize that cooperation between the so-called EU group and the scientists from Bosnia and Herzegovina is paramount.

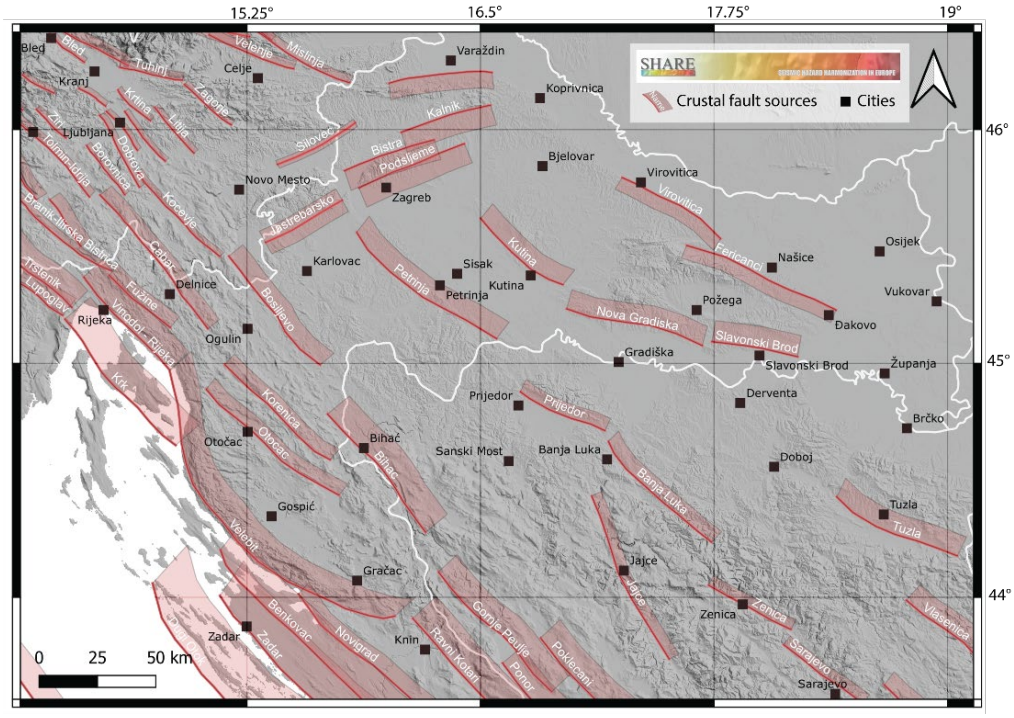

Figure 1. Map of seismic sources from SHARE European Earthquake Catalogue; shaded relief map produced from Copernicus 25 m Digital Elevation Model; WGS84 coordinate system

2. METHODOLOGY

Significant crustal earthquakes with a magnitude greater than six often lead to noticeable immediate effects, such as surface faulting, uplift, and subsidence, which are directly associated with the seismic rupture occurring deep underground. These effects are reliable indicators of the earthquake's location, magnitude, and movement. Secondary effects, including ground failure and liquefaction, are influenced by the extent and pattern of the earthquake ground motion, along with specific geological and geomorphic conditions. The primary and secondary coseismic effects noticed during a major modern earthquake like

the Petrinja one, which had directly threatened the structural integrity of buildings and infrastructure in 2020, are expected to reproduce during future earthquakes of similar characteristics. In hazard assessment, modelers need to understand whether larger events could be possible, and hazard calculation requires an estimation of the recurrence of such events. The classical approach to do so is to extend the recordings of modern events to ancient times, as far as they were generated within the same seismotectonic and stress contexts.

Acquiring geodetic velocity fields is recommended to complete the understanding of the regional seismotectonic and fault behaviour. This can be done through GNSS data sets or interseismic analysis of InSAR data. Thanks to this, we can estimate potential rigid or semi-rigid blocks, zones of deformation accommodation (typically fault zones), and relative motions (rate of displacement per year).

2.1. SEISMOTECTONIC AND GEOLOGICAL BACKGROUND

Central Croatia is a seismically active region with a dense population and several active fault systems, many of which have yet to be fully characterized in terms of their seismic activity. The PPF is currently the only fault that has been partially studied and documented, mainly due to its identification as the main source of the 2020 Petrinja Earthquake [7]. Regionally, this fault is situated at the boundary between the southwestern margin of the Pannonian Basin system and the Internal Dinarides [10]. The complex Cenozoic tectonics in this region are related to the slow convergence of the Adriatic microplate and the Eurasian plate [11, 12], initiated by the obduction of ophiolites on the eastern margin of the Adriatic microplate. Throughout the Oligocene–Miocene, the Adriatic microplate shifted northward, while the European plate retreated eastward, resulting in the lateral extrusion of the Eastern Alps and Tisza tectonic blocks [13]. These pivotal tectonic events have been the primary drivers of the current structural configuration, which has undergone various changes in tectonic regimes during the evolution of the Pannonian Basin System [14]. Miocene extension enabled the Pannonian Basin system to open through the formation of NW-SE-oriented normal faults, which were later inverted during the Pliocene-Quaternary compressional phase.

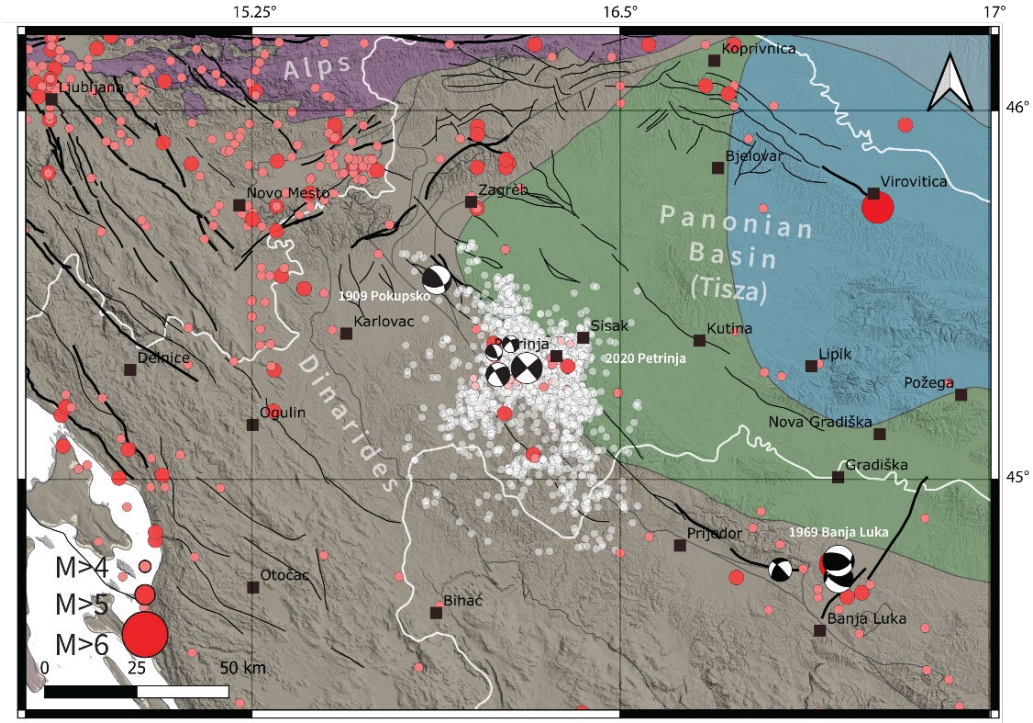

Figure 2. An overview of seismicity with the highlighted Petrinja earthquake series [1,15] combined with a European database of epicenters larger than M>4 on a 25 m hillshade colored according to the main tectonic units- Alps, Dinarides and Pannonian Basin; depicting active and potentially active faults (modified after [8]); WGS84 coordinate system

The present compressional/transpressional phase of the Croatian part of the Pannonian Basin is confirmed by geodetic measurements [9, 16] and a multitude of earthquake focal mechanisms, which are consistent with dextral kinematics of the NW-SE PPF. The seismic events of the Petrinja series [15] confirm the kinematics of the NW-SE striking dextral PPF. The southern segment of the PPF system extends towards the East Bosnian–Durmitor thrust in Bosnia and Herzegovina, while the northern segment continues through the Vukomeričke gorice, where the historic Pokupsko earthquake of 1909 (M > 5.8) was recorded [2]. This event provided crucial insights into the Moho layer and was instrumental in reconstructing the seismic kinematics, demonstrating the dextral-transpressive activation of the northern segment.

The northern part of Vukomeričke Gorice is less pronounced geomorphologically and is covered by younger Pliocene and Quaternary deposits, whereas the main part of the system is characterized by the uplift of Hrastovica Hills, constituted of Neogene deposits: this is along this latter section that the 2020 surface rupture occurred [17,18]. The tectonic uplift of Hrastovica is confirmed by borehole data and seismic profile analysis [8]. The post-earthquake survey has shown that the majority of the ruptures are located within Badenian (Middle Miocene) limestones and Pleistocene and Holocene unconsolidated sediments. Further paleoseismological research focuses specifically on these youngest sediments, where the most recent potential deformations caused by paleoseismic events are likely to be preserved.

2.2. GEODETIC ANALYSIS OF THE PETRINJA EARTHQUAKE USING GNSS AND INSAR DATA

The importance of geodesy has grown with advancements in technology and spatial data collection methods. After the 2020 Petrinja earthquake, we acquired unique geodetic datasets through field investigation. The deformation pattern of such events is often challenging to capture using terrestrial geodesy due to the constraints of monitoring resources. Following this event, we could take advantage of the data from a dense near-field network of numerous geodetic benchmarks. However, a multidisciplinary approach is required to calculate position corrections based on the geodynamics of the research area. This allowed for the accurate evaluation of the slip distribution causing the earthquake [9].

Before the Petrinja earthquake sequence, benchmarks were established for cadastral and engineering purposes (2003–2020). They were remeasured just after the sequence (8 January 2021–13 March 2021) using a GNSS receiver and Croatian Positioning System (CROPOS), an online service for precise positioning. The geodetic benchmark kinematic measurements are accurate at the centimetre level, while the deformation values are at the level of a few decimeters. The largest displacement values resulting from the seismic activity were observed near the Petrinja centre, with a magnitude of 75 cm in the ESE direction. Sisak experienced planar displacements of approximately 7 cm to the east, while in Glina, the displacements were noted at around 6 cm in the NW direction. Notably, the most significant NW displacements, measuring 65 cm, were recorded in Strašnik, near the epicentre. This rich dataset allowed for the reconstruction of a dense displacement field related to the sequence and was therefore used to assess better the displacement field recorded after the event on 29 December 2020 and inform about the slip distribution on the earthquake source [8,9].

Rapid re-measurement of preexisting civilian networks provides unique coseismic constraints in the near field, particularly useful where InSAR may experience decorrelation [9]. The Sentinel-1 constellation captured surface deformation thanks to pre-earthquake (18 December 2020) and post-earthquake (4 January 2021) SAR images. The GNSS and Sentinel-1 SAR images show that the movements related to the 2020 earthquake are consistent with a right-lateral motion along the NW–SE striking PPF zone, covering approximately 10-15 km. The initial analysis of the line-of-sight displacement from the earthquake's InSAR signal clearly indicated that surface rupture may have occurred, which partly guided our field survey.

The coseismic InSAR signal is somewhat obscured in the anticipated area of the ground breaks. The low coherence observed in the near-field fault area could be attributed to the presence of vegetation, water, soft-sediment deformation, or even liquefaction. However, the detection of post-seismic deformation was possible to document, relying on the analysis of a set of ascending and descending InSAR time series data from December 30, 2020, to January 28, 2021. The observed ground deformation patterns, both during (coseismic) and after (post-seismic) the seismic event, align with a significant right-lateral and NW–SE oriented surface fault trace, fitting to the surface breaks checked in the field [8].

Figure 3:Geodetic benchmark post-seismic observation with GNSS receiver. Photo by authors.

2.3. INSIGHTS FROM THE PALEOSEISMOLOGICAL STUDIES ON THE 2020 PETRINJA EARTHQUAKE"

Paleoseismology is a robust methodology for studying past earthquake activity at a specific fault or region (see [19] for a comprehensive overview). It provides valuable information to the understanding of the active tectonics still at work and yields critical data to hazard modelers. Paleoseismology performed directly on the fault is a primary source of information because it directly provides data on the earthquake source. The common bias of this approach is the poor completeness of stratigraphic information (and then we can miss events), which can be compensated for in extensive and well-dated sedimentary records like lakes [20]. However, these methods are not always available close to a fault, and they tend to provide inadequate constraints on the spatial parameters (i.e. lacustrine layers record near-field and far-field earthquakes). When the coseismic effects are found in the stratigraphy of recent deposits and soils on a fault, this represents evidence for the occurrence of an earthquake in the past along this structure. This evidence can then be characterized in terms of age, location and size. The repetition of large surface-rupturing earthquakes on the same fault leaves a cumulative, permanent signature in the landscape that defines an active fault. Therefore, even though they may not have produced earthquakes in modern times, the active faults are visible and mappable at the surface through the morphological signature of past earthquakes, and a level of hazard can be associated. This signature is specific and recognizable in the morphology and contains information on their behaviour: deciphering this information documents the seismic hazard

of a region. For instance, a careful geomorphological analysis of the PPF allowed the identification of right-lateral offsets of river channels and terraces that cross perpendicularly to the fault, corresponding to the cumulative effect of similar right-lateral faulting events in the past millennia [21].

The Petrinja earthquake effects gave us important information potentially helpful to decipher the fault behaviour from geological, geomorphological and paleoseismological information: the significant proportion of off-fault deformation determined with spaceborne and terrestrial geodetic observations leads us to a crucial methodological statement. Thus, to be complete, we must account for deformation accommodated over a wide zone (at the several hundred meters scale) when analyzing geomorphological and paleoseismological information. The first trenches dug between 2021 and 2023 confirmed this off-fault distribution of deformation [22]. This means that, in the future, in order to get a more complete assessment, we should, for instance, trench parallel and branching segments or consider long piercing lines crossing the fault zone in geomorphological analyses.

The NW-SE PPF is today the best-known active fault due to the occurrence of the 2020 earthquake. Several months later, a series of new actions were engaged, particularly concerning earthquake geology and the tectonic morphology of that fault bearing the 2020 surface ruptures. However, very little is known about the other NW-SE potential active faults that stretch north and south to Slovenia and Bosnia and Herzegovina, their relationships with NE-SW contractional faults, such as the one that caused the March 2020 earthquake below Zagreb, the capital city of Croatia. Considering the similarities between all these areas in terms of fault characteristics and local geology, the warning expressed in the previous paragraph on the methodological aspect is applicable to Bosnia and Herzegovina. Our suggestion is, in parallel to the studies in Croatia, to reconstruct the seismic history of the NW-SE PPF by mapping and defining its long-term seismic history. A similar project is engaged in Bosnia and Herzegovina on the faults running beneath/close to Banja Luka and Sarajevo.

Paleoseismological studies provide specific parameters that are essential for the evaluation of seismic hazards. Among these parameters, the slip rate of a fault is particularly significant and can be assessed using trench information and geomorphological analysis. Analyzing the stratigraphic signals present in trenches is crucial for establishing a timeline of surface-rupturing earthquakes, especially when the sediments affected and unaffected by faulting contain datable material. Under favorable conditions, it is possible to estimate the displacement that occurs during faulting events, which is closely related to the magnitude of those events. To further our understanding, we have engaged in or are preparing to engage in the following actions in Croatia:

- A comprehensive geomorphological study of the fault zone was conducted using a high-resolution LiDAR-based Digital Terrain Model (DTM) with a one-meter resolution. This analysis focuses on the area affected by the 2020 earthquake (see Figure 4). It has been possible to identify and locate the potential active fault segments surrounding the 2020 Petrinja earthquake surface rupture [21]. The fault pattern appears distributed over hundreds of meters to kilometers around the Hrastovica Hills front and is coupled with an active fold to the north. We could identify relevant sites that show a long-term displacement (on the order of tens of meters) of morphological features. Sampling campaigns have been conducted to date alluvial terraces using cosmogenic isotopes and

radiocarbon (14C). This process has allowed us to establish slip rate values for each parallel fault segment. After a precise fault mapping based on geomorphology, surface geophysics is usually performed before trenching. This has been done in the past two years following the 2020 earthquake, with a series of GPR, ERT, and seismic surveys have been done to locate the further paleoseismological trenches [22,23] successfully. We can also envisage using GPR (or ERT), these geophysical techniques, to map piercing lines buried linear features that cross fault zones because the main component of faulting is to estimate the lateral component of displacement and then calculate their displacement and rate of displacement if they can be dated. The deformation zone width is large, so one strategy to overcome this limiting factor could be to trace a channel edge (for instance) and try to map it across the fault zone. Such an approach in Bosnia and Herzegovina will probably require the acquisition of a spatial dataset for high-resolution DTM.

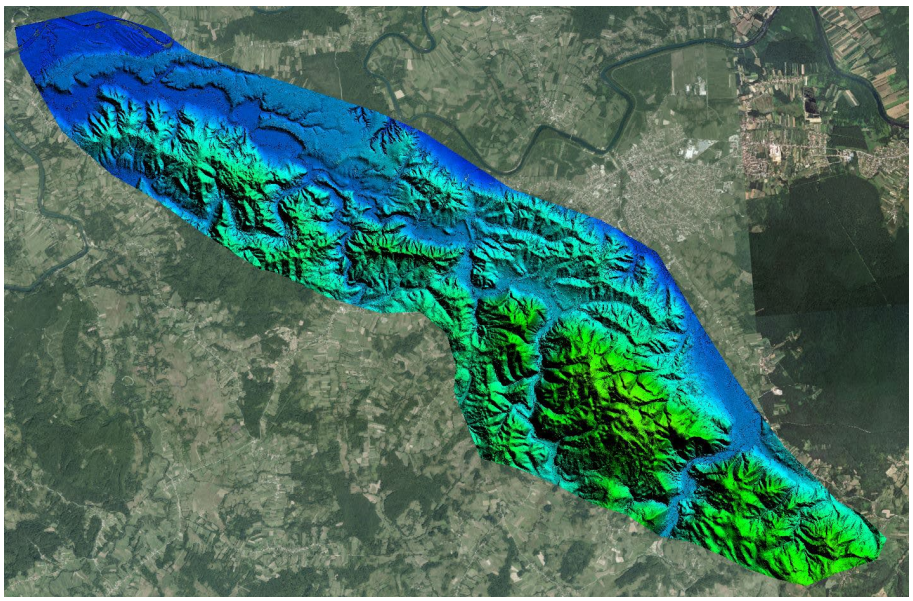

Figure 4: Orthophoto overlayed with high-resolution lidar-based DTM of the research area

- Paleoseismological trenching studies were initiated for the first time in Croatia to investigate the structure of the PPF and recognize its past activity. The first trench walls revealed the style of deformation at shallow depth, composed of faulting and warping in a wide zone that occurs persistently in coincidence with the morphologic fault scarp and 2020 ruptures at the surface. The permanent signature in the trenches' exposures suggests cumulative coseismic deformation, with a series of events during the Holocene and possibly with Roman-age and historical ones. However, we still need to work on the datasets of four trench sites to formulate a coherent calendar of events.

Figure 5: The first-ever trench excavated in Croatia, in Hrastovica, along the PPF that ruptured during the 2020 Petrinja earthquake. The central section shows white material (fine sands) corresponding to uplifted Pliocene-Miocene within the Holocene soils and sediments during successive coseismic offsets. Photo by authors.

Figure 6: Detail of a trench wall dug across the northernmost section of the 2020 Petrinja surface rupture in Medurace. The section shows that a series of fault strands displaces the whitish to yellowish sands at the bottom (probably Pliocene to Miocene in age), together with overlying pebbles and silts (probably Pleistocene to Holocene) during successive faulting events. The height of the wall is ~2 meters. Photo by authors.

3. CONCLUSION

The 2020 Petrinja earthquake is one of the most significant inland earthquakes of this decade. Although it is tragic, a unique opportunity has been created to survey and document new datasets and information about the earthquake and its manifestation on the earth's surface. Following the earthquake, the staff of the Croatian Geological Institute formed field groups. Soon after, teams from other EU institutions arrived at the site. This extensive and rapid mobilization of field earth scientists enabled regional field geologists and specialists in the geological impact of earthquakes to collaborate. We conducted a detailed examination of the primary surface evidence in the field, thoroughly documented our findings, and collected evidence that is often compromised due to the involvement of other services.

Geodetic benchmarks established for trigonometric and control networks play a crucial role in providing valuable information about fault sources and complementing satellite methods. This method is relatively cost-effective compared to the resources needed to maintain permanent stations. Therefore, it's essential to prioritize their installation, maintenance, and proper documentation.

Surface evidence is related to the main event, as the aftershocks were not intense enough to cause superficial deformations. Based on field observations, processing and analysis of earthquake environmental effects, we have characterized the fault as NW-SE oriented right-lateral strike-slip. Future research will investigate structures to the north and south. In addition, paleoseismological research and geophysical field surveys will be conducted at the sites (markers).

A paleoseismological investigation needs significant experience to be efficient and to provide relevant information, which could be shared by our team during future cooperation with regional scientists. The collected datasets and pieces of information will be organized into a unique database, which will be permanently stored for current and future generations of researchers.

4. REFERENCES

[1] D. Herak and M. Herak, “The Kupa Valley (Croatia) Earthquake of 8 October 1909—100 Years Later,” Seismological Research Letters, vol. 81, no. 1, pp. 30–36, 2010, doi: https://doi.org/10.1785/gssrl.81.1.30.

[2] A. Mohorovičić, “Earthquake of 8 October 1909, translation to English,” Geofizika, vol. 9, pp. 3–55, 1992.

[3] D. Pollak et al., “The preliminary inventory of coseismic ground failures related to December 2020 – January 2021 Petrinja earthquake series,” Geologia Croatica, vol. 74, no. 2, pp. 189-208, 2021. [Online]. Available: https://doi.org/10.4154/gc.2021.08.

[4] S. Markušić et al., “The Zagreb (Croatia) M5.5 Earthquake on 22 March 2020,” Geosciences, vol. 10, no. 7, p. 252, 2020. [Online]. Available: https://doi.org/10.3390/geosciences10070252.

[5] M. Herak, D. Herak, and N. Orlić, “Properties of the Zagreb 22 March 2020 earthquake sequence – analyses of the full year of aftershock recording,” vol. 38, no. 2, 2021, doi: https://doi.org/10.15233/gfz.2021.38.6.

[6] M. Šavor Novak et al., “Zagreb earthquake of 22 March 2020 – preliminary report on seismologic aspects and damage to buildings,” GRAĐEVINAR, vol. 72, no. 10, pp. 843-867, 2020, doi: https://doi.org/10.14256/JCE.2966.2020.
[7] R. Basili et al., “European Database of Seismogenic Faults (EDSF), compiled in the framework of the Project SHARE,” 2013. [Online]. Available: http://diss.rm.ingv.it/share-edsf/.
[8] S. Baize et al., “Environmental effects and seismogenic source characterization of the December 2020 earthquake sequence near Petrinja, Croatia,” Geophysical Journal International, vol. 230, no. 2, pp. 1394–1418, 2022. [Online]. Available: https://doi.org/10.1093/gji/ggac123
[9] M. Henriquet et al., “Rapid remeasure of dense civilian networks as a game-changer tool for surface deformation monitoring: The case study of the Mw 6.4 2020 Petrinja earthquake, Croatia,” Geophysical Research Letters, vol. 49, e2022GL100166, 2022. [Online]. Available: doi: https://doi.org/10.1029/2022GL100166.
[10] S. M. Schmid et al., “Tectonic units of the Alpine collision zone between Eastern Alps and western Turkey,” Gondwana Research, vol. 7, pp. 308-374, 2020.
[11] I. Vlahović et al., “Evolution of the Adriatic Carbonate Platform: Paleogeography, main events and depositional dynamics,” Palaeogeography, Palaeoclimatology, Palaeoecology, vol. 220, pp. 333–360, 2005. doi: https://10.1016/j.palaeo.2004.12.017
[12] S. M. Schmid et al., “The Alpine-Carpathian-Dinaridic orogenic system: correlation and evolution of tectonic units,” Swiss Journal of Geosciences, vol. 101, pp. 139-183, 2008. doi: https://10.1007/s00015-008-1247-3
[13] K. Ustaszewski, S. M. Schmid, B. Fügenschuh, M. Tischler, E. Kissling, and W. Spakman, “A map-view restoration of the Alpine-Carpathian-Dinaridic system for the Early Miocene,” *Swiss Journal of Geosciences*, vol. 101, pp. 273–294, 2008. doi: https://10.1007/s00015-008-1283-z
[14] D. Pavelić and M. Kovačić, “Sedimentology and stratigraphy of the Neogene rift-type North Croatian Basin (Pannonian Basin System, Croatia): A review,” *Marine and Petroleum Geology*, vol. 91, pp. 455–469, 2018. doi: https://10.1016/j.marpetgeo.2017.11.011
[15] M. Herak and D. Herak, “Properties of the Petrinja (Croatia) earthquake sequence of 2020–2021—Results of seismological research for the first six months of activity,” *Tectonophysics*, vol. 858, 2023. doi: https://10.1016/j.tecto.2023.229646
[16] J. Weber, M. Vrabec, P. Pavlovčič-Prešeren, T. Dixon, Y. Jiang, and B. Stopar, “GPS-derived motion of the Adriatic microplate from Istria Peninsula and Po Plain sites, and geodynamic implications,” *Tectonophysics*, vol. 483, nos. 3-4, pp. 214–222, 2010. https://doi.org/10.1016/j.tecto.2009.09.001
[17] M. Pikija, “Osnovna geološka karta SFRJ 1:100 000, list Sisak,” Inst. za geol. istraž., Zagreb, Inst. za geol., Sarajevo, Sav. geol. zavod, Beograd, 1987.
[18] K. Šikić, O. Basch, and A. Šimunić, “Basic Geological Map of Yugoslavia 1:100000, Sheet Zagreb L33-80,” Federal Geological Institute Beograd, Belgrade, 1978.
[19] J. P. McCalpin, *Paleoseismology*, 2nd ed., Academic Press, Amsterdam-London, 2009.
[20] P. Sabatier, J. Moernaut, S. Bertrand, M. Van Daele, K. Kremer, E. Chaumillon, and F. Arnaud, “A review of event deposits in lake sediments,” *QUATERNARY*, vol. 5, no. 3, 2022. doi: https://doi.org/10.3390/quat5030034
[21] M. Henriquet et al., “ Kinematics and morphotectonics of the Petrinja Fault (Croatia): unraveling the 2020 M 6.4 EarthquakeActive Fault mapping and

kinematics of the Petrinja-Pokupsko fault (Croatia), source of the 2020 M 6.4 Petrinja earthquake: insights from morphotectonic analysis and Quaternary dating," in preparation submitted to Tektonika.

[22] J. Maslač et al., "First Paleoseismological Study In Croatia: Preliminary Results After The 2020 Earthquake On The Petrinja-Pokupsko Fault," in *7. hrvatski geološki kongres s međunarodnim sudjelovanjem: knjiga sažetaka*, Fio Firi and Karmen (eds.), Croatian Geological Institute, Zagreb, pp. 112–113, 2023.

[23] P. Jamšek Rupnik et al., "Update on the geophysical surveys of the Petrinja-Pokupsko Fault: lecture at the Webinar Croatia - Advancement of research on 2020 Petrinja earthquake and related topics," 18th Sept. 2024

AUTHORS' BIOGRAPHIES

Branko Kordić

Dr. Branko Kordić is a Research Associate at the Croatian Geological Survey (HGI-CGS). His work specializes in satellite geodesy, hydrography, remote sensing, and geodynamics, utilizing modern geodetic techniques for the collection of spatial data. He utilizes methods such as LiDAR, InSAR, GNSS, and UAS, which are crucial for gathering and analyzing information about the surface effects of earthquakes. Currently, he is working on research that focuses on assessing the seismic impacts of recent earthquakes through advanced geodetic methods.

Stéphane Baize

Stéphane Baize is a senior geologist specializing in earthquake geology (geomorphology and trenching), Quaternary geology and seismic hazard assessment. He is affiliated with the Nuclear Safety Agency in France, where he works in the Seismic Hazard Division. His professional activities and scientific interests focus on studying active faults, paleoseismology, and surface rupture surveys to contribute to seismic hazard studies. He has been involved in various research projects in France and around the world, including in the Balkans and Italy, South America and New Zealand, among others.

Josipa Maslač Soldo

Josipa Maslač Soldo is a young scientist, a research assistant at the Croatian Geological Institute, and a PhD student at the Faculty of Mining, Geology, and Petroleum Engineering at the University of Zagreb. Her research focuses on active faults in central Croatia and coseismic phenomena. She applies expertise in tectonic geomorphology and seismotectonics, as well as applied geophysics, to investigate active fault segments, thereby contributing to the geological understanding necessary for a more effective assessment of seismic hazards.

ПРОЦЈЕНА УТИЦАЈА НА ЖИВОТНУ СРЕДИНУ И АНАЛИЗА СЕИЗМИЧКОГ ХАЗАРДА: ИСКУСТВО ИЗ ПЕТРИЊЕ (2020.)

Сажетак: Дана 29. децембра 2020. године, сјеверну Хрватску у близини Петриње погодио је плитак земљотрес магнитуде 6,2. Овом земљотресу претходио је снажан потрес магнитуде 5. Убрзо након тога, тим европских геолога и инжењера из Хрватске, Словеније, Француске, Италије и Грчке био је мобилисан ради спровођења свеобухватне процјене утицаја земљотреса на животну средину. Њихова запажања у подручју Петриње открила су површинске деформације, тектонске пукотине при површини дуж сеизмичког жаришта, појаве ликвефакције у алувијалним равницама ријека Купе, Глине и Саве, као и урушавања косина изазвана јаким помјерањем. Ипак, анализом геодетских података тим је закључио да теренска мјерења знатно потцјењују укупну косеизмичку деформацију на површини: велики дио деформације био је распрострањен и расут изван главног расједа. Ликвефакција се проширила на готово 600 km² око епицентра, а забиљежене појаве укључују пјешчане ерупције, латерална ширења дуж путева и ријечних насипа, те избацивање пијеска различитих величина и састава. Након низа истраживања дуж расједа који је проузроковао земљотрес 2020. године, документовано је више палеорасједа током Холоцена и утврђено је кумулативно хоризонтално помјерање дуж цијелог расједа Петриња–Покупско, укључујући и сегменте који се нису помјерили 2020. године. На основу хрватског искуства из протекле три године, наглашавамо потребу за даљим детаљним истраживањима, укључујући неотектонска, палеосеизмолошка и геофизичка испитивања, која би могла пружити нова значајна сазнања о сеизмичкој активности и сеизмичким хазардима у зони регионалног расједа, односно јужном наставку расједа Петриња–Покупско, дуж повезане расједне зоне која се протеже према Костајници.

Кључне ријечи: *земљотрес, истраживање, теренска мјерења, сеизмички хазарди*

Tectonic plates under Japan. Author: Pimvantend. Source: https://commons.wikimedia.org/wiki/File:Bosotriplejunction.svg (Wikimedia Commons)

University of Banja Luka I Faculty of Architecture, Civil Engineering and Geodesy
ISSN 2712-0570 I UDC 72

2025
Special Issue

Earthquake Engineering

AGG+ Journal for Architecture, Civil Engineering, Geodesy and Related Scientific Fields
АГГ+ часопис за архитектуру, грађевинарство, геодезију и сродне научне области

090-107 **Categorisation** I Review scientific paper
DOI I 10.61892/AGG202502011J
Paper received I 04/03/2024
Paper accepted I 12/03/2025

Vladan Janković
University of Banja Luka, Faculty of Architecture, Civil Engineering and Geodesy, Bosnia and Herzegovina, vladan.jankovic@student.aggf.unibl.org

Tanja Đukanović
University of Banja Luka, Faculty of Architecture, Civil Engineering and Geodesy, Bosnia and Herzegovina, tanja.djukanovic@aggf.unibl.org

Sanja Tucikešić
University of Banja Luka, Faculty of Architecture, Civil Engineering and Geodesy, Bosnia and Herzegovina, sanja.tucikesic@aggf.unibl.org

MODELING TECTONIC MOVEMENTS USING THE KALMAN FILTER ON GNSS COORDINATE TIME SERIES

Review scientific paper
DOI 10.61892/AGG202502011J
Paper received I 04/03/2024
Paper accepted I 12/03/2025

* corresponding author

Vladan Janković

University of Banja Luka, Faculty of Architecture, Civil Engineering and Geodesy, Bosnia and Herzegovina, vladan.jankovic@student.aggf.unibl.org

Tanja Đukanović *

University of Banja Luka, Faculty of Architecture, Civil Engineering and Geodesy, Bosnia and Herzegovina, tanja.djukanovic@aggf.unibl.org

Sanja Tucikešić

University of Banja Luka, Faculty of Architecture, Civil Engineering and Geodesy, Bosnia and Herzegovina, sanja.tucikesic@aggf.unibl.org

MODELING TECTONIC MOVEMENTS USING THE KALMAN FILTER ON GNSS COORDINATE TIME SERIES

ABSTRACT

The paper is dedicated to the modeling of tectonic movements based on GNSS coordinate time series, which were analyzed using the Kalman filter. The research area includes the territory of Japan, which is one of the most seismically active regions on Earth. The devastating Tohoku earthquake of 2011 was the result of subduction between the Pacific and North American plates. Different offsets were observed by analyzing the time series of GNSS coordinates. The intensity of the offset caused by the Tohoku earthquake is proportional to the distance of the observed station from the epicentre of the earthquake. The horizontal and vertical movements of Honshu Island are not homogeneous, which results from the fact that the GNSS stations are located on different tectonic plates.

Keywords: *Tectonic movements, seismology, GNSS coordinate time series, Kalman filter.*

1. INTRODUCTION

Earthquakes are one of the most dangerous natural disasters, claiming a large number of human lives every year around the world [1]. The first step toward earthquake prediction is to accurately observe what happens during an earthquake to use the information obtained for geophysical models. Geodynamic research is based on the monitoring of GNSS (Global Navigation Satellite Systems) coordinate time series, from which information is obtained about the movements and velocities of GNSS stations over time. Based on GNSS measurements, the three-dimensional positions of the stations can be estimated with a precision ranging from several millimetres to several centimetres. If station observations are conducted over a long period, conclusions can be drawn about the processes occurring before, during and after the earthquake. It often happens that the movement starts days or weeks before the earthquake itself. Additionally, after strong earthquakes, slight movements can be observed for months, leading to continued deformation of the affected area and often to a return to its original state. If the network of GNSS stations is densely distributed in the vicinity of an earthquake, data on the spread and course of the earthquake can be obtained from dense temporal resolution measurements [1].

The first regional continuous GNSS networks for geodynamics have been developed since 1990. A small regional continuous GNSS network for geodynamics with a spacing of about 1,000 km was established in Japan in 1991. Such networks were developed primarily to measure deformations related to tectonic processes. The Geospatial Information Authority of Japan (GSI) operates GNSS CORSs that cover the Japanese archipelago with over 1,300 stations at an average interval of about 20 km for crustal deformation monitoring and GNSS surveys in Japan [2].

The paper focuses on the modelling of tectonic movements based on GNSS measurement technology. The result of continuous GNSS measurements is represented by a time series of GNSS coordinates over which the Kalman filter was applied.

Kalman filtering is an algorithm that uses a series of measurements observed over time, including statistical noise and other inaccuracies, and makes estimates of unknown variables [3]. It is a recursive method used to estimate the random state of a dynamic system in a way that minimizes the mean square prediction error. The recursive method refers to solving the problem by breaking it down into smaller instances of the same problem, which are then solved in the same way. The algorithm enables optimal evaluation of time-varying parameters of a dynamic system. The Kalman filter is particularly suitable for processing satellite measurements because the station coordinates and their velocities, phase uncertainties, atmospheric influences or clock conditions can be viewed as parameters that change as a function of time. The extended Kalman filter is a nonlinear version of the Kalman filter that linearizes the estimation of the current mean and covariance and is used in the theory of nonlinear state estimation of navigation systems and GPS (Global Positioning System).

It is necessary to point out that the implementation of the Kalman filter is most effective for linear systems and that its use is limited in cases where the system is not strictly linear. In such cases, variations of the Kalman filter, such as the Extended Kalman Filter (EKF) and the Unscented Kalman Filter (UKF), can be applied.

The Extended Kalman Filter (EKF) is a generalization of the Kalman filter that is well-suited for most nonlinear systems. In the EKF, the state of the nonlinear system is approximated

by its linearization, using the first term of the partial derivatives of the Taylor series around the current estimated mean value of the state and covariance. For the linear approximation to converge properly, the system should not be extremely nonlinear, and the initial state and variance values should be accurate. If the system is linear, the EKF would give the same results as the standard Kalman filter [4].

The UKF represents a newer version of the Kalman filter for nonlinear systems in which the so-called "unscented" transformation overcomes the shortcomings of the EKF linearization, where the state covariance expansion is assumed to be linear [4], [5]. In UKF, the unknown state probability distribution is approximated by a discretized version using several sampled state values called “sigma points”. The probability distribution of the newly estimated state is obtained from the sigma point propagation directly through the nonlinear model.

The Kalman filter represents a precise method by which the velocities of GNSS stations can be derived from epochal geodetic measurements [6]. By applying the Kalman filter, during the analysis of the time series of the positions of the GNSS stations, deformations of the Earth's crust can be estimated.

A time series is used to monitor some statistical phenomenon and represents an ordered series of measurements, which were realized in different epochs, usually in equal time intervals. Although they provide three-dimensional displacements, the vertical component is less precise than the horizontal one. By extracting geophysical signals from a time series of GNSS coordinates, clear insights into Earth deformation patterns are obtained. In combination with seismological data, time series of GNSS coordinates are used to develop algorithms for earthquake modelling. Seismological data includes data from seismographs, which measure earthquake waves as they pass through the Earth. GNSS data provide information about long-term ground motions, such as slow deformation before and after an earthquake, while seismological data provide fast information about the waves moving through the Earth during an earthquake. The correlation between the dynamics of the recorded seismic waves and the time series of GNSS data leads to an understanding of which parts of the ground deformations are associated with certain types of waves (P-waves, S-waves, etc.) [20], [21].

High-frequency GNSS data can be used to model the rupture process during strong earthquakes, providing useful information on the correlation between GNSS and seismic data [22].

To understand the dynamics that cause deformations, interseismic models of surface deformation and seismic hazard analyses are most important [7], [4], [9], [8].

Time series models represent different stochastic processes. A stochastic process is a function of the outcome of a statistical experiment and time. Accordingly, the time series represents one realization of the stochastic process [10]. In the analysis of time series, this mutual dependence is used to form a time series model, after which it is used to make a forecast of future observations based on past observations [10].

2. MATERIALS AND METHODS

2.1. THE STUDY AREA

The area of study includes the territory of Japan, which is one of the most seismically active regions on Earth. Japan is an island country in East Asia, comprising 6,852 islands, the largest of which are Hokkaido, Honshu, Shikoku and Kyushu. The Japanese islands are part of a geologically very unstable region known as the Pacific Ring of Fire. This area is characterized by a large number of seismic and volcanic activities. Most earthquakes are the result of tectonic movements, which lead to the interaction of the Pacific, Philippine, North American and Eurasian plates (Figure 1). The most famous volcano is Fuji, which is also the highest peak in Japan, with a height of 3776 m. Some of the many earthquakes are highly destructive, such as the Tohoku earthquake in 2011. Therefore, the Japanese have invested significant effort and funding into geodynamic research, leading to the establishment of a network of 1,200 GPS stations in 2000.

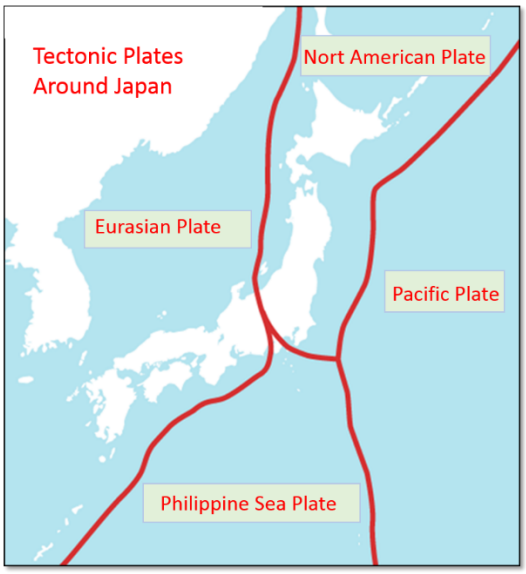

Figure 1. *Layout of tectonic plates in the research area* [11]

2.1. INPUT DATA

The Nevada Geodetic Laboratory (NGL) conducts research in the field of satellite geodesy to study scientific problems of both regional and global significance [12]. The Global Positioning System is used to study tectonic and geothermal activity. The main research objective of this laboratory is the Earth's deformation in different time trends and different areas. These deformations are mostly caused by the movement of tectonic plates. Seismic activities occur at the boundary zones of the plates. It is precisely by quantifying the deformation at the boundary zones of the plates that we want to understand as much as possible the complex force of interaction that leads to seismic processes [12].

The GPS station network data, which is updated weekly, daily, and even at five-minute intervals, can be accessed via the NGL web service. NGL publishes metadata, station lists, coordinate position charts, and data tables. In addition to station locations, time series data are available in various formats: tenv3, tenv, xyz, kenv, trop, and QA files. Furthermore,

information about equipment changes or earthquakes in the vicinity of each station, as published by the USGS (United States Geological Survey), is available for each station.

NGL collects raw GPS data from more than 17,000 stations around the world and then processes it. The region of Japan is densely covered by a network of GPS stations with time series lasting about 14 years. The final NGL products can be used for various research, such as tectonic plate motion or the improvement of the global reference frame for studying global sea level change [12].

To model tectonic movements, the time series of four GPS stations shown in Figure 2 were analyzed. All stations are located on the Japanese island of Honshu.

Figure 2. Station positions (source: author)

The reference frame for all stations is IGS14 (International GNSS Service 2014), which, for most practical tasks, is equivalent to the international terrestrial reference frame ITRF14 (International Terrestrial Reference Frame 2014). The coordinates of the stations are shown in Table 1. The observation period ranges from the beginning of 2009 to August 2023.

Table 1. *Coordinates of stations*

Point mark	J549	J191	I053	J645
Latitude	38.425˚	39.206˚	34.751˚	35.621˚
Longitude	141.213˚	139.908˚	138.990˚	134.677˚
Height	49.081 m	47.294 m	52.721 m	70. 208 m

2.2. MATHEMATICAL MODEL OF GNSS COORDINATE TIME SERIES

The mathematical model of GNSS coordinate time series can be represented as the sum of deterministic (functional) and stochastic parts (noise). The deterministic part refers to long-term trends and seasonal changes, while the stochastic part remains after removing the deterministic model from the data [7].

The following form represents a complete linear model for a GNSS coordinate time series related to a single position component [13]:

$$y(t_i) = a + bt_i + c\sin(2\pi t_i) + d\cos(2\pi t_i) + e\sin(4\pi t_i) + f\cos(4\pi t_i) + \sum_{j=1}^{n_j} g_j H\left(t_i - T_{gj}\right) + \varepsilon(t_i) \quad (1)$$

where t_i represents the daily solutions of the GNSS coordinate time series, t_i denotes the series of n elements, where $i = 1, \dots, n$, a is the position of the station, and b is the linear velocity of the station. The coefficients c and d in the model describe the annual motion, while e and f describe the semi-annual motion. The following terms in the model describe the sudden occurrences caused by equipment or seismic events for any number of deviations n_g of size g and epoch t_{g_j}, using the Heaviside function (a single jump function used in signal processing to represent the signal that changes state). In addition, t_{eq} is the time of the earthquake (represents the time of the main shock), c represents the coseismic displacement after the earthquake (modeled with a logarithmic or exponential function), A is the amplitude of the simplified Omori's law, τ is the time delay of the occurrence of post-seismic deformation after the main shock. The remaining term in the model t_{e_i} denotes measurement errors, i.e. any remaining changes attributable to other random or systematic instabilities.

The Heaviside function corresponds to shifts in the time series, which are most often the result of seismic events or changes in instruments, software, or reference frames. The linear expression is analogous to the position and rate of change of the GNSS antenna, while the harmonic components are included to model annual, seasonal and high-frequency dependent phenomena present in the time series [7].

2.3. GNSS TIME SERIES ANALYSIS METHODS

GNSS networks for geodynamic research are based on permanent stations that continuously collect data. The obtained positions that make up the time series are originally expressed in geocentric coordinates (X, Y, Z). To make the concept of moving a specific location more intuitive, geocentric coordinates are transformed into topocentric ones, and thus, three components (N, E, U) are obtained, which represent north, east, and elevation. Based on the analysis of the time series, we arrive at the movement speed vector as well as the anomalies that could have occurred in the period covered by the time series.

Topocentric GNSS time series are burdened with errors originating from various sources. Therefore, the precision of the ephemeris, correction of the satellite oscillator, parameters of the Earth's rotation, tropospheric and ionospheric influence, station stability, multiple reflections, etc., decisively influence the quality of the calculated time series. The existence of observations with errors, loss of observations due to obstacles, noises originating from other signals, and others make necessary a preliminary descriptive analysis of the measured time series. By analyzing the raw series, outliers, gross errors, and especially the noise level can be detected [14].

Given the differences in terms of horizontal components and vertical components, as well as the linear and nonlinear behaviour of a time series and the like, there is no single method

for analyzing each time series. Therefore, different time series analysis procedures have been developed, which are shown in Figure 3.

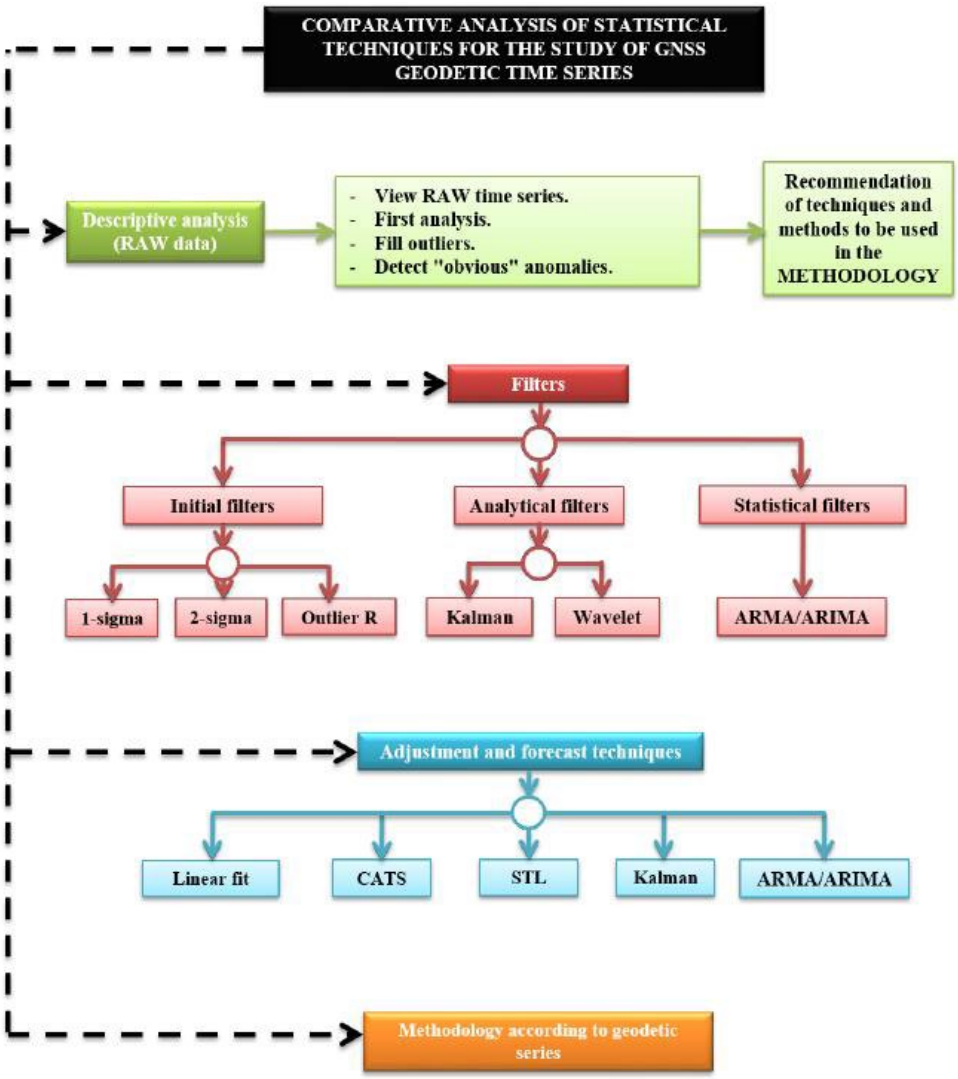

Figure 3. *Methods of analysis of GNSS time series* [14]

The essence of the initial filtering applied to the GNSS series is reflected in the elimination of data that deviate greatly from the rest of the series in terms of values. 1-sigma and 2-sigma filters eliminate data depending on the distance of the series points from the linear regression line. However, in the case of nonlinear series, this process takes place along linear sections within the series.

In the paper, the Kalman filter was applied to GNSS coordinate time series.

The estimation process of the Kalman filter can be divided into continuous and discrete, where they can be represented by the following equations that describe the dynamic system and the measurement system [15]:

$$\dot{X} = F(t).X(t) + G(t).w(t), \text{ dynamic system} \quad (2)$$

$$\tilde{Z} = H(t).X(t) + v(t), \text{ measurement system} \quad (3)$$

$$X_k = \Phi_{k-1}X_{k-1} + \Gamma_{k-1}\omega_{k-1}, \text{ dynamic system} \quad (4)$$

$$\tilde{Z}_k = H_k \cdot X_k + v_k, \text{ measurement system} \quad (5)$$

where $F(t)$ dynamic matrix, $X(t)$ system state vector, $G(t)$ disturbance configuration matrix, $w(t)$ disturbance function (system noise), $\tilde{Z}$ observation vector, $H(t)$ observation configuration matrix, $v(t)$ measurement noise, Φ transition matrix, Γ configuration matrix of system disturbance. Equations under (4) refer to continuous time, while under (5) refer to discrete time, where both X_k and $\tilde{Z}_k$ contain position components (N, E, U).

3. RESULTS OF NUMERICAL RESEARCH

3.1. APPLICATION OF SARI SOFTWARE FOR ANALYSIS OF TIME SERIES

The time series of GNSS coordinates contain signals caused by the deformation of the Earth but also by systematic errors at different moments, from daily to seasonal and annual variations [4]. With the help of the SARI software (French: Señales y Análisis de Ruido Interactivo), it is possible to visualize GNSS position time series, remove outliers and discontinuities, fit the model and save the results. There are additional options that enable the extraction of adequate information from the time series, including spectral analysis with the Lomb-Scargle periodogram and wavelet transform, signal filtering using the Kalman filter, and estimating the time correlation of the stochastic residual noise. The program is oriented toward daily/weekly time series of GPS positions in NEU format, but it is possible to analyze other data series as well.

First of all, it is necessary to download the data from the NGL website and prepare it in the appropriate format. After loading the data, it is necessary to set the time resolution of the series, as well as the linear dimensions. It is then possible to visualize the time series by components in the form of points, points and lines, or only lines, as can be seen in Figure 4.

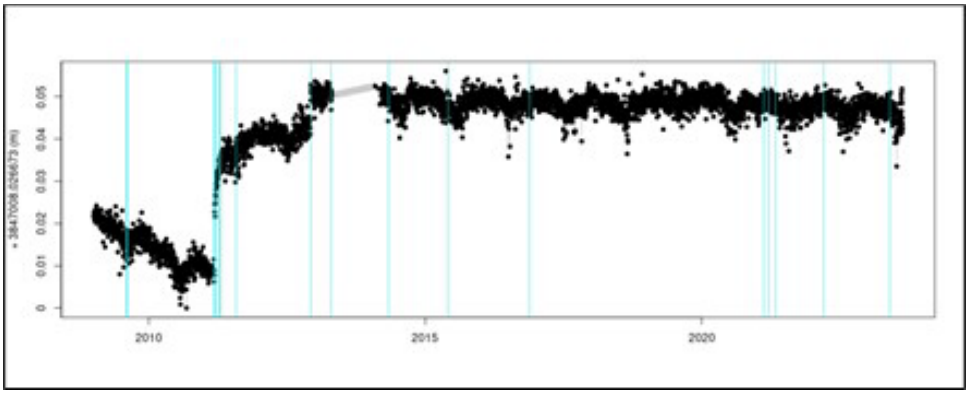

Figure 4. *The northern component of the time series from the station I053 (source: author)*

Vertical cyan lines represent offsets downloaded from the Nevada Geodetic Laboratory web service. The displayed offsets are a consequence of seismic activity, as well as changes in equipment at the stations themselves. After visualizing the time series, we get information about the number of points, that is, observations in the series, the length of the series, its range, the sampling period and the completeness of the series. The above time series data for station I053 are presented in Table 2.

Table 2. *Time series data for the station I053*

Time series data	Values
Number of points	4978
Series length	14.6256 years
Series range	2009.0048 - 2023.6304
Series sampling	0.0027 years
Series completeness	91.9 %

After that, it is necessary to fit the model using the least squares method. In this procedure, linear and sinusoidal functions were used. A linear function is used to model the trend of a time series, while a sinusoidal function is used to model periodic variations that occur due to different seasonal changes. The period of the sinus function itself can be estimated based on the Lomb-Scargle periodogram, where the amplitudes are shown as a function of the period of the year (Figure 5). In the figure, we can see a pronounced amplitude between the five-year and one-year periods, and therefore, in the modeling of the northern component, it is necessary to include a sine function.

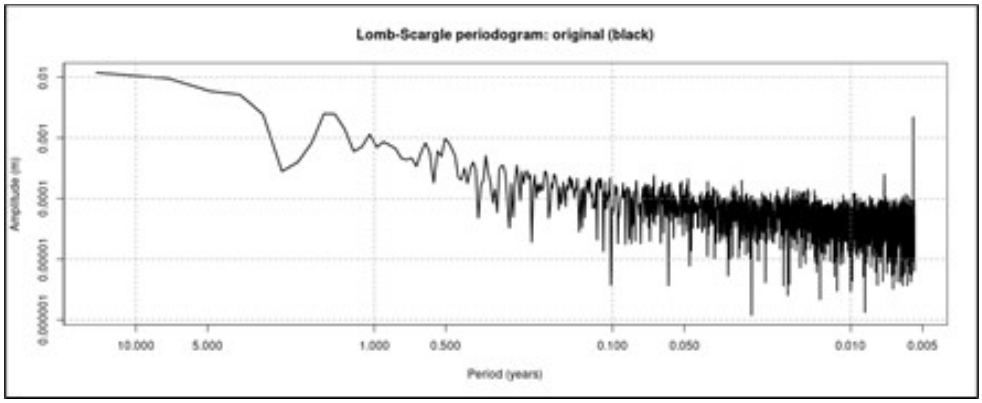

Figure 5. *Periodogram of the northern component of the time series I053 (source: author)*

After modelling using the least squares method, the Kalman filter is applied to model the time series as accurately as possible and estimate the velocity of the station with the greatest possible precision. When using the Kalman filter, it is necessary to define the measurement noise and the a priori state of all parameters that are evaluated. The quality of the Kalman filter depends precisely on the assumed a priori values, which are derived from the time series data. If modeling was performed using the least squares method, estimates of certain parameters would serve as a priori values of the state parameters of the Kalman filter system. After running the filter, the result shown in Figure 6 is obtained. Figure 6 shows the actual modelling of the data using the Kalman filter, that is, the time series of the northern component data with the modelled data overlaid to show how well the Kalman filter fits the observed data.

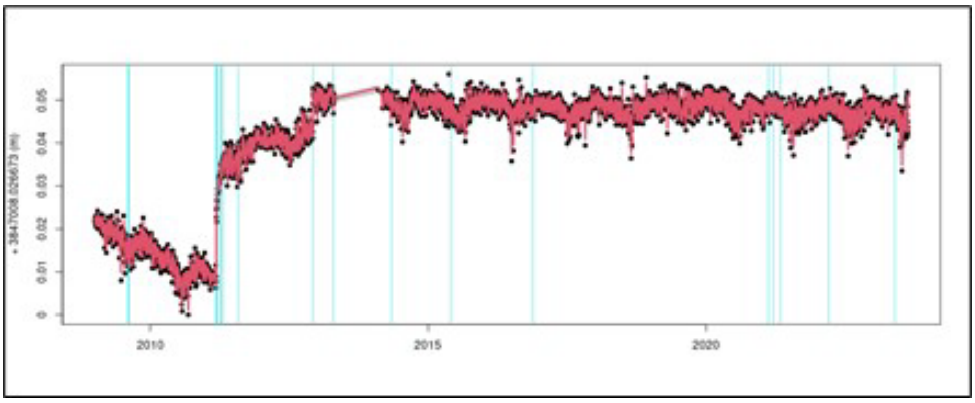

Figure 6. *Modelling of the northern component of station I053 using the Kalman filter (source: author)*

Also, it is useful to show the residuals of the performed modeling (Figure 7), as well as the histogram of the residuals (Figure 8). Based on them, it can be seen whether the residuals follow a normal distribution, that is, whether the modeling was performed adequately.

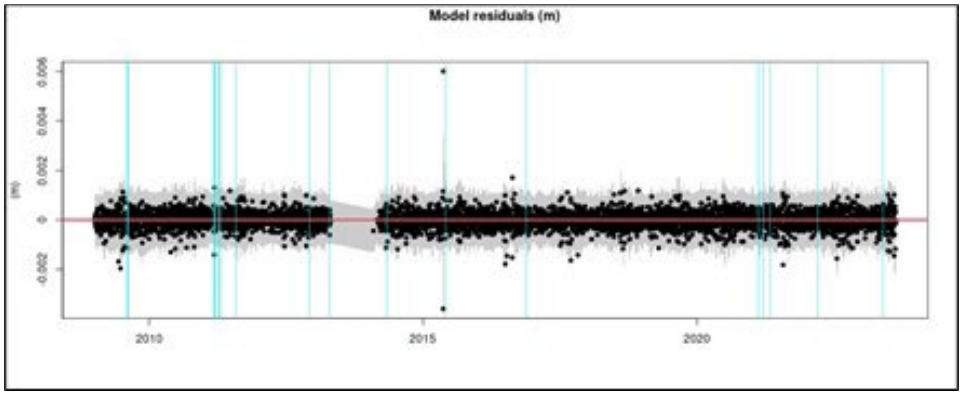

Figure 7. *Residual model for the northern component of the station I053 (source: author)*

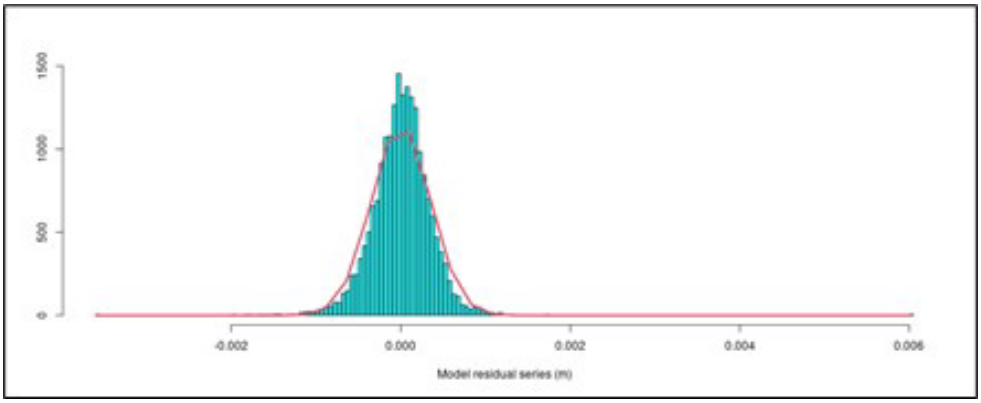

Figure 8. *Histogram of residuals of the northern component of the station I053 (source: author)*

Using the described procedure, a time series analysis was performed with the four mentioned GNSS stations. The obtained values of horizontal and vertical velocities are presented in Table 3. The table shows the estimated annual displacement values for GNSS stations in three dimensions: north (N), east (E) and vertical (Up). These values are expressed in millimetres per year (mm/year). For example, for station J549, the displacement in the north is -111.41 mm/year, in the east 317.13 mm/year, and vertically 12.49 mm/year. This indicates that the station has moved south and east and has risen.

Table 3. *Estimated speed values of GNSS stations*

Stations	Station position velocities		
	N [mm/year]	E [mm/year]	Up [mm/year]
J549	-111.41	317.13	12.49
J191	-70.74	165.61	-1.84
I053	1.49	4.26	1.57
J645	-5.94	33.12	-4.65

The intensity of the resultant vector of displacement of GNSS stations is shown in Table 4, the graphic display of horizontal velocities is shown in Figure 9, and the vertical velocities are presented in Figure 10.

Table 4 presents the intensity of the resultant displacement vector for the same GNSS stations, also expressed in millimetres per year. The intensity of the resultant vector provides an overall measure of the station's displacement regardless of direction, by combining both horizontal and vertical components.

Table 4. *The intensity of the resultant displacement vector*

Stations	The intensity of the resultant displacement vector [mm/year]
J549	336.13
J191	180.08
I053	4.51
J645	33.65

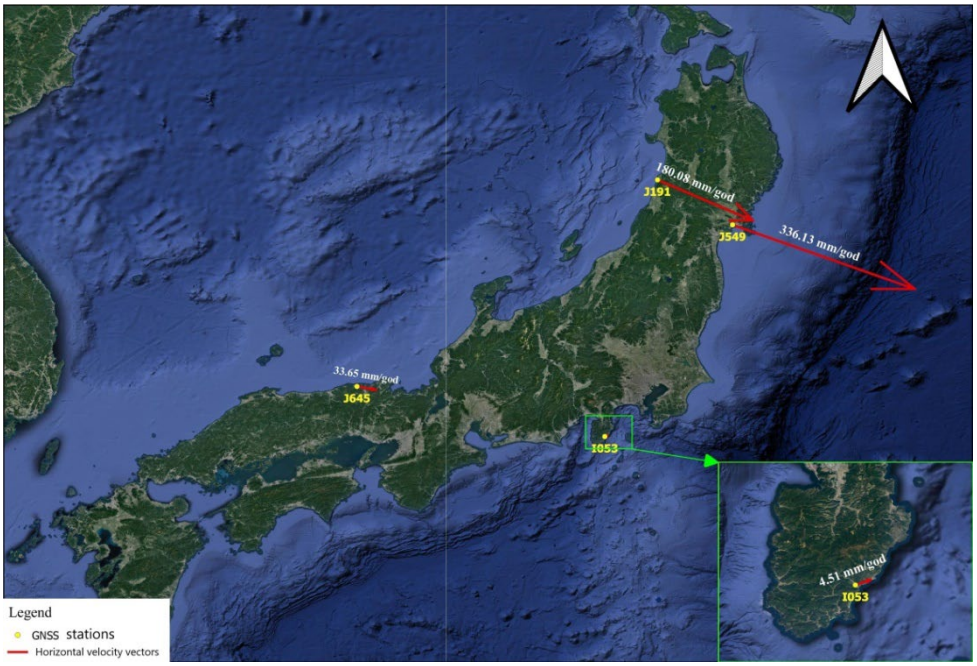

Figure 9. *Horizontal velocities of GNSS stations (source: author)*

Figure 10. *Vertical velocities of GNSS stations (source: author)*

Figure 9 shows the horizontal velocities of the GPS stations. The arrows show the direction and velocity of horizontal movement in millimetres per year (mm/year). Each marked point on the map represents a GPS station, and the speeds are indicated next to the arrows. In northern Japan, the velocity of movement is 180.08 mm/year in the southeast direction. The large red arrows on the map highlight the higher movement speeds in northeastern Japan and its eastern coastal region. The figure also shows the location in the southern part, marked as IO53, with a movement velocity of 4.51 mm/year.

Figure 10 shows the vertical velocities of the GPS stations and indicates the vertical movement of the ground, where the values are given in millimetres per year. Positive values (e.g. 12.49 mm/year) indicate soil elevation, while negative values (e.g. -4.65 mm/year) indicate soil subsidence. In northeastern Japan, the GNSS station, which is marked as 3549, recorded the highest ground uplift of 12.49 mm/year. In contrast, station 3645 in central Japan shows ground subsidence of -4.65 mm/year.

3.2. ANALYSIS OF THE RESULTS OBTAINED

Based on the obtained results, an analysis of horizontal and vertical velocities was performed, as well as the most noticeable offset, which is noticeable in the all-time series and occurred as a result of the devastating Tohoku earthquake on March 11, 2011.

The earthquake occurred near the northeastern coast of the island of Honshu, at a depth of about 25 km, with a magnitude of 9.1 Mw [16]. The earthquake resulted from a shallow subduction fault at the boundary between the Pacific and North American plates. In this area, the Pacific Plate is moving approximately westward relative to the North American Plate at a speed of 83 mm/year and is subducting under the mainland of Japan in the Japan Trench. Earthquake rupture modelling showed that the fault moved as much as 50-60 m

[16]. The Tohoku earthquake was preceded by a series of earthquakes two days before the main shock, starting on March 9 with a magnitude 7.4 Mw earthquake. Also, since 1973, nine earthquakes of magnitude over 7 Mw have been recorded in this area [16]. The distance values are shown in Table 5.

Table 5. *Distance of GNSS stations from the epicentre of the Tohoku earthquake*

Stations	Distance [km]
J549	102.1
J191	236.5
I053	496.7
J645	745.4

Observing the time series of GNSS stations, it can be seen that the largest offsets are represented in the time series of GNSS station J549, which is the closest to the epicentre of the earthquake. During the period of the earthquake, displacements in the northern component of approximately 1.3 m were recorded, while in the eastern component, the intensity of the displacement was as much as 4.5 m. Also, an offset with a value of almost 0.5 m was observed in the vertical component. In the time series of station J191, the offsets are also significant but still smaller compared to station J549. Based on the assumed expectations, the offsets at GNSS stations I053 and J645 are much smaller than those at the previous two stations, where there were almost no significant movements in the vertical components.

By analyzing the horizontal velocities of the observed stations, it can be seen that the resultant vectors of stations J549 and J191 are higher in intensity compared to the other two stations. Also, the directions of these vectors approximately coincide and indicate the movements of the North American part of the tectonic plate towards the southeast. The horizontal velocity of station J645 is rather less intense compared to the previous two velocities, while the direction of the vector also indicates movement in the southeast direction. The largest differences were observed during the analysis of the resultant vectors of horizontal displacement at station I053. The intensity of the vector indicates significantly smaller movements in this area, while the direction also differs compared to the previous three stations. Looking at Figure 12, it can be assumed that these differences arose from the fact that the GNSS station is located on Izu Island, which belongs to the Philippine tectonic plate. In addition, it can be observed that station J645 is located on the Eurasian plate, which, in addition to the distance from the epicentre of the Tohoku earthquake, is probably another reason for the slower horizontal movement compared to stations J549 and J191 located on the North American tectonic plate.

Differences in intensity and direction can also be observed in vertical velocities. By observing the vertical velocities, a lowering of the west coast of the island of Honshu, where GNSS stations J191 and J645 are located, was observed, while stations J549 and I053 indicate an uplift of the east coast of this island. The obtained results are in agreement with the detected subduction of the Pacific Plate under the mainland of Japan, which was precisely the cause of the Tohoku earthquake.

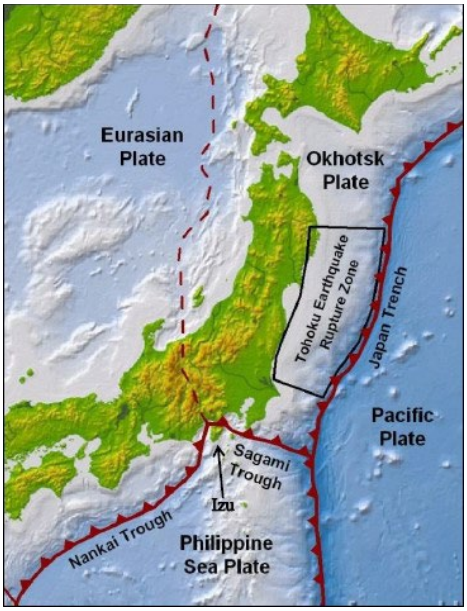

Figure 11. *The position of the Izu peninsula in the arrangement of tectonic plates [14]*

In addition to the above, in most components of the analyzed time series of GNSS stations in the post-seismic phase, movements similar to those before the earthquake were observed. Also, in certain components of the time series, a movement was observed that returns the stations to their pre-earthquake condition, for example, in the case of the vertical component of station J549.

4. CONCLUSION

GNSS technology is a powerful tool for monitoring and quantifying deformations on the surface of the Earth's crust. The progress of the aforementioned technology, i.e. the development of other global navigation satellite systems in addition to GPS, has made it possible to monitor deformations on a global level. Based on continuous GNSS measurements, three-dimensional station coordinates are estimated daily over a long period.

In the paper, an analysis of the time series of GNSS coordinates, which are publicly available on the Nevada Geodetic Laboratory website, was performed. During the analysis, the time series that contained daily estimates of coordinates were used. The Kalman filter was used to estimate the velocities of the observed GNSS stations, based on which tectonic movements were modeled in the area of Japan.

Japan is located at the junction of several important tectonic plates: the Pacific, Philippine, North Pacific, and Amur plates. The movements of these plates cause seismic activity, volcanism, and tectonic deformations in the Earth. The horizontal velocities of the GPS stations, the arrows showing the directions and the movement velocities, indicate how different parts of Japan are moving due to tectonic forces. The larger arrows in northeastern Japan may indicate an area where the Pacific Plate is subducting beneath the North Pacific Plate, which is responsible for intense tectonic activity. The different speeds and directions of movement indicate the complexity of the interactions between the different plates. The

northern part of Japan shows significant movements, which is consistent with the region where the Pacific Plate is subducting, while the central and southern parts of Japan exhibit less movement.

These differences in horizontal and vertical velocities may be the result of different geological and tectonic processes in the region. Japan is known for its complex tectonic situation, where multiple plates meet and move, causing varying rates of ground motion. Areas with higher vertical velocities may be particularly susceptible to seismic activity, such as earthquakes and volcanic eruptions. This information is important for understanding tectonic activity, earthquake risk, and long-term monitoring of relief change in Japan.

The Tohoku earthquake, which occurred on March 11, 2011, was one of the strongest earthquakes on record, with a magnitude of 9.0. This earthquake caused massive ground movements and changed the geological structure of a large part of Japan. The ground movements, both horizontal and vertical, which are shown in this paper, can be directly related to the long-term effects of that earthquake. During the Tohoku earthquake, horizontal ground movements were extremely significant. Some parts of Japan's east coast moved up to 2.4 meters eastward. GPS stations display different horizontal drift rates. These changes are a continuation of post-seismic processes, where the ground under stress during the earthquake recover and adapt to new tectonic conditions.

The large horizontal velocity shown in northeast Japan may be part of the recovery process after the large movement during the earthquake. During the Tohoku earthquake, there were significant vertical movements in addition to horizontal movements. Some parts of Japan fell as much as 1 meter, increasing the risk of a tsunami, while other parts rose. After the earthquake, the vertical movements currently underway may be related to post-earthquake ground adjustment processes.

A link between tectonic movements and seismic activity can be established. It is assumed that in the future, a lot of effort will be invested in understanding seismic processes, as well as phenomena that indicate the possible occurrence of earthquakes. In proportion to the development of technology and scientific achievements, progress can be expected in improving the reliability of early warning systems for earthquakes, which would undoubtedly reduce the number of victims of this natural disaster.

5. REFERENCES

[1] D. Angermann, R. Pail, F. Seitz, and U. Hugentobler, *Mission Earth: Geodynamics and Climate Change Observed Through Satellite Geodesy*. Springer, 2022.

[2] “GEONET | GSI HOME PAGE.” https://www.gsi.go.jp/ENGLISH/geonet_english.html (accessed March 17, 2025).

[3] F. Daum, “Extended Kalman Filters,” 2014, pp. 1–3. doi: 10.1007/978-1-4471-5102-9_62-2.

[4] A. Santamaría-Gómez, “SARI: interactive GNSS position time series analysis software,” *GPS Solut.*, vol. 23, no. 2, p. 52, 2019.

[5] S. J. Julier and J. K. Uhlmann, “Unscented filtering and nonlinear estimation,” *Proc. IEEE*, vol. 92, no. 3, pp. 401–422, 2004.

[6] C. T. Çelik, “Crustal deformation monitoring by the Kalman filter method,” University of Nottingham, 1998.

[7] S. S. Tucikešić, “Modelovanje tektonskih pomjeranja i kvantifikacije deformacija zemljine kore korišćenjem GNSS tehnologije,” Univerzitet u Beogradu-Građevinski fakultet, 2020.
[8] “WGCEP | Working Group on California Earthquake Probabilities.” https://wgcep.org/ (accessed November 06, 2023).
[9] J. Jackson and P. Molnar, “Active faulting and block rotations in the western Transverse Ranges, California,” *J. Geophys. Res. Solid Earth*, vol. 95, no. B13, pp. 22073–22087, 1990.
[10] Z. J. Kovačić, *Analiza vremenskih serija*. Ekonomski fakultet, 1998. [Online]. Available: https://books.google.ba/books?id=Qq_BAAAACAAJ
[11] “The Next Big One: Government Map Forecasts Likely Future Japanese Earthquakes | Nippon.com.” https://www.nippon.com/en/features/h00234/ (accessed November 06, 2023).
[12] “Nevada Geodetic Laboratory - Home.” http://geodesy.unr.edu/ (accessed November 06, 2023).
[13] R. Nikolaidis, Observation of geodetic and seismic deformation with the Global Positioning System. University of California, San Diego, 2002.
[14] P. Barba, B. Rosado, J. Ramirez-Zelaya, and M. Berrocoso, “Comparative analysis of statistical and analytical techniques for the study of GNSS geodetic time series,” *Eng. Proc.*, vol. 5, no. 1, p. 21, 2021.
[15] B. Gourine, A. Niati, A. Benyahia, and M. Brahimi, “Analysis of GPS coordinates time series by Kalman filter,” *FIG Work. Week 2015 From Wisdom Ages to Challenges Mod. World*, pp. 17–21, 2015.
[16] G. P. Hayes *et al.*, “Tectonic summaries of magnitude 7 and greater earthquakes from 2000 to 2015,” 2017.
[17] T. Apel, C. Williams, and P. Grossi, “The M9. 0 Tohoku, Japan Earthquake: Short-Term Changes in Seismic Risk,” *Risk Manag. Solut. Inc. Spec. Rep.*, 2012.

AUTHORS' BIOGRAPHIES

Vladan Janković

Vladan Janković was born in Banja Luka on August 5, 1999. He obtained the title of Bachelor of Science in Geodesy in 2022. During his undergraduate studies, he was a recipient of the "Dr. Milan Jelić" Fund scholarship and received the award as the best graduate student in Geodesy. In May 2023, he began an internship at the Republic Administration for Geodetic and Property-Legal Affairs.

Tanja Đukanović

Tanja Đukanović was born on February 22, 1994, in Nevesinje. She completed her bachelor's studies in Geodesy in 2017 at the Faculty of Architecture, Civil Engineering and Geodesy, University of Banja Luka. She obtained her Master's degree from the same faculty in 2021. She is currently a PhD student at the Faculty of Civil Engineering, University of Belgrade. Since 2019, she has been employed at the Faculty of Architecture, Civil Engineering and Geodesy, where she works as a teaching assistant in a group of course units within the scientific field of geodetic surveying.

Sanja Tucikešić

She was born in Banja Luka on May 13 1981. She graduated in 2008 from the Faculty of Civil Engineering at the University of Belgrade. She obtained her PhD from the Faculty of Civil Engineering of the University of Belgrade in 2020. In her scientific research, she deals with the analysis and modeling of tectonic movements and Earth's crust deformations using GNSS technology, as well as with the calibration and quality control of geodetic instruments and the laboratory testing of scales used in geodesy, civil engineering, and other related fields, including volumetric scales. She is employed at the Faculty of Architecture, Civil Engineering and Geodesy as an assistant professor.

МОДЕЛОВАЊЕ ТЕКТОНСКИХ ПОМЈЕРАЊА ПРИМЈЕНОМ КАЛМАН ФИЛТЕРА НА ВРЕМЕНСКЕ СЕРИЈЕ GNSS КООРДИНАТА

Сажетак: Рад се односи на моделовање тектонских помјерања на основу временских серија GNSS координата које су анализиране примјеном Калман филтера. Подручје истраживања обухвата територију Јапана која представља једно од сеизмички најактивнијих подручја на Земљи. Резултат субдукције Пацифичке и Сјеверноамеричке плоче је разорни земљотрес Тохоку 2011. године. Посматрањем анализираних временских серија GNSS координата уочени су различити офсети. Интензитет офсета који је изазван земљотресом Тохоку је сразмјеран растојању посматране станице од епицентра земљотреса. Хоризонтална и вертикална помјерања острва Хоншу нису хомогена, што проистиче из чињенице да се GNSS станице налазе на различитим тектонским плочама.

Кључне ријечи: *тектонска помјерања, сеизмологија, временске серије GNSS координата, Калман филтерзоне*.

Map of earthquake magnitude in Bosnia and Herzegovina. Source:

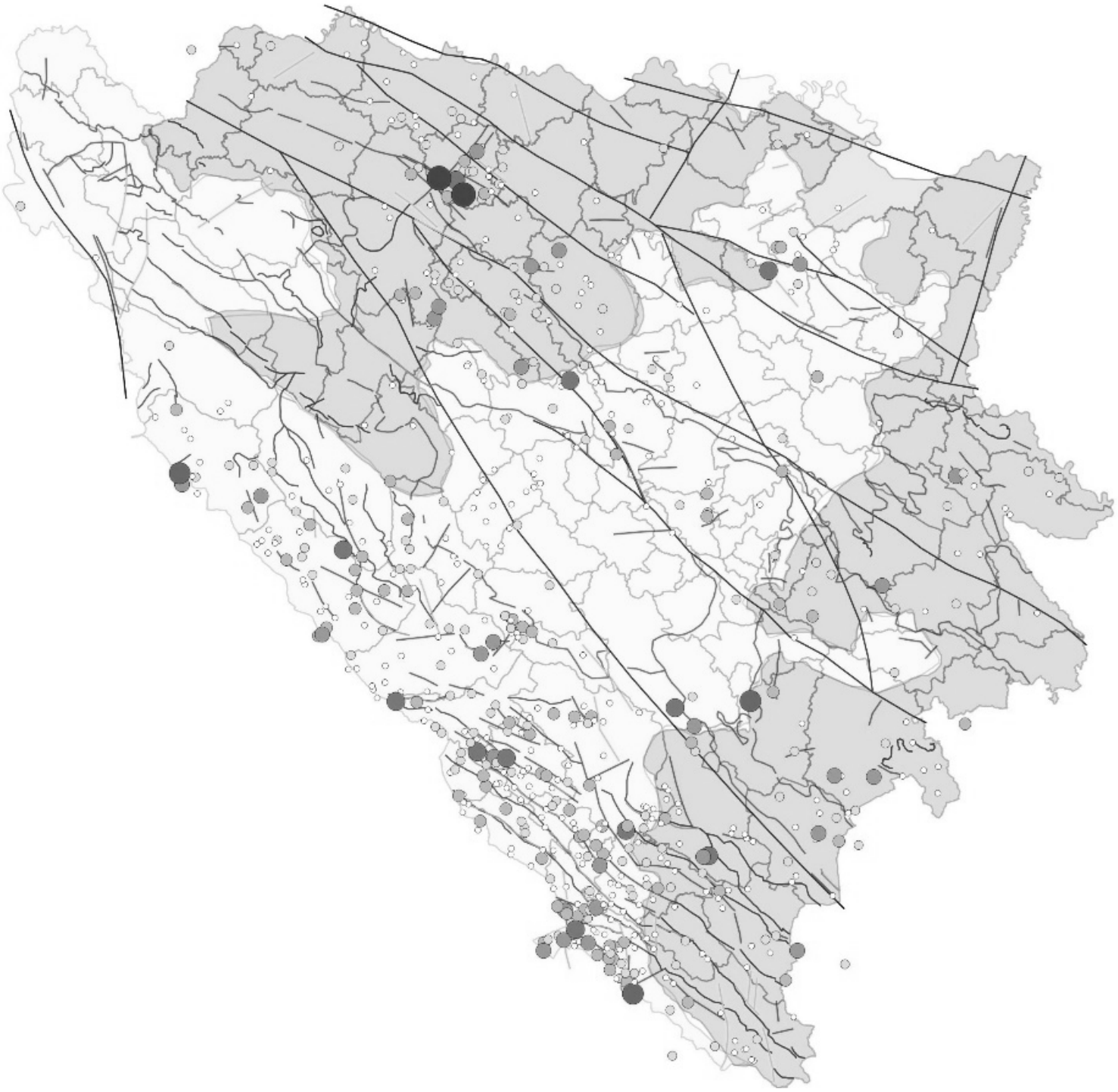

University of Banja Luka I Faculty of Architecture, Civil Engineering and Geodesy
ISSN 2712-0570 I UDC 72

2025
Special Issue

Earthquake Engineering

AGG+ Journal for Architecture, Civil Engineering, Geodesy and Related Scientific Fields
АГГ+ часопис за архитектуру, грађевинарство, геодезију и сродне научне области

110-122

Categorisation I Review scientific paper
DOI I 10.61892/AGG202502010DJ
Paper received I 01/03/2024
Paper accepted I 28/05/2024

Tanja Đukanović
University of Banja Luka, Faculty of Architecture, Civil Engineering and Geodesy, Bosnia and Herzegovina, tanja.djukanovic@aggf.unibl.org

Sanja Tucikešić *
University of Banja Luka, Faculty of Architecture, Civil Engineering and Geodesy, Bosnia and Herzegovina, sanja.tucikesic@aggf.unibl.org

Snježana Cvijić Amulić
Republic Hydrometeorological Service of the Republic of Srpska, Bosnia and Herzegovina, s.cvijic-amulic@rhmzrs.com

TECTONIC GEODESY AS A SUPPLEMENT DATA IN SEISMOLOGY

Review scientific paper
DOI 10.61892/AGG202502010DJ
Paper received I 01/03/2024
Paper accepted I 28/05/2024

* corresponding author

Tanja Đukanović
University of Banja Luka, Faculty of Architecture, Civil Engineering and Geodesy, Bosnia and Herzegovina, tanja.djukanovic@aggf.unibl.org

Sanja Tucikešić *
University of Banja Luka, Faculty of Architecture, Civil Engineering and Geodesy, Bosnia and Herzegovina, sanja.tucikesic@aggf.unibl.org

Snježana Cvijić Amulić
Republic Hydrometeorological Service of the Republic of Srpska, Bosnia and Herzegovina, s.cvijic-amulic@rhmzrs.com

TECTONIC GEODESY AS A SUPPLEMENT DATA IN SEISMOLOGY

ABSTRACT

Geodesy and its high precision are important instruments for the study of active tectonics and the presentation of the movement of solid parts of the earth. Deformations caused by earthquakes represent essential information for defining seismogenic zones. Precise measurements must be made on the wall of the fault itself or the system of connected active faults to measure the rate of deformation of the earth's crust between, during, and after earthquakes. In Bosnia and Herzegovina, the spatial density of GNSS stations used in modern geodynamic studies is low. The permanent GNSS station "SRJV" in Sarajevo is the only permanent GNSS station in the region. It is part of the EUREF Permanente GNSS network and, in that segment, has up-to-date available time series from GNSS coordinates.

Keywords: *GNSS station SRJV, seismogenic faults, seismogenic zones*

1. INTRODUCTION

Earthquakes that periodically threaten certain parts of the earth's surface represent seismic movements of the solid earth caused by tectonic activities. Most destructive earthquakes occur in the contact zones of large tectonic plates. These regions contain zones of the highest seismic hazard and, therefore, the risk of strong and destructive earthquakes. The most seismic active region in the world is Taiwan, where plate convergence occurs when the ground moves at a velocity greater than 83 mm/year, and it belongs to the Pacific „Ring of Fire“, where the most powerful earthquakes have ever been registered.

High seismic activity registered in these parts not only exhibits a constant potential danger to human lives and material goods but also threatens the whole of human activity and its normal development in these areas. Today, it is an indisputable fact that at certain time intervals within the same zone, earthquakes reoccur. Thus, these areas are defined as seismically active. However, earthquakes can also trigger other hazards, such as landslides, tsunamis, volcanic activity and others.

Geodetic observations in seismology are challenging and important for understanding plate boundary processes. Surface geodetic deformation data can help to find a new slip distribution capable of producing surface displacements. Tectonic geodesy is an important prong of geodesy and geophysics and has broad applications in geoscience. Tectonic geodesy is an interdisciplinary field that studies the tectonic activity of the crust and its fundamental kinematics using geodetic observation techniques, such as the Global Navigation Satellite Systems (GNSS). GNSS technology is used to compute long-term velocities, coseismic motions, and postseismic motions separate from the total motion. Real-time measurements from GNSS networks located around the world provide a characterization of ground motions that are directly related to seismic phenomena. The analysis of crustal deformations plays an important role in studies related to the whole seismic cycle. The seismic cycle refers to the notion of observing an earthquake before, during, and after its occurrence. An important part of the seismic cycle in many subduction zones is Slow Slip Events (SSE), which release some portion of accumulated strain and perhaps trigger large earthquakes by loading nearby segments of the fault.

The Mediterranean, which belongs to a group of seismically active regions, including Bosnia and Herzegovina, was exposed to catastrophic earthquakes. Bosnia and Herzegovina, in terms of geographical position, are located in south-eastern Europe on the Balkan Peninsula.

2. LOCAL TECTONICS AND URBAN PLANNING

Today, besides the usual geotechnical and seismic zonation techniques considered when developing or restoring an urban region, the local active tectonics must be taken into account [1]. Reliable estimates of the seismic hazard start with the identification and evaluation of earthquake sources by reviewing geologic evidence, tectonic evidence, historical seismicity, and instrumental seismicity [2].

The first stage of the study aims to locate active faults or fractures in the Bosnia and Herzegovina area and understand their role in spatial variability through the analysis of all existing relevant data from geology, seismology, and geodynamics. These data are very important and need to be included in the integrated analysis of space for the needs of

regional and urban planning. It is evident that urban planning, when approached in an integrated manner that considers all aspects and impacts, is potentially the most effective mechanism for mitigating the harmful consequences of many natural hazards. One of the great challenges of today is regional and urban planning resilient to the danger of potential earthquakes, which is insufficiently present in planning practice in Bosnia and Herzegovina.

In the period of former Yugoslavia, a seismological map based on maximal expected intensities was made for the area of Bosnia and Herzegovina, which defined the seismic hazard zones, according to which the calculations of structures for the planned facilities were performed and based on which the seismic risk map was later generated. Based on this map, it was necessary to make seismic micro-zoning maps for each larger urban area, which would give more detailed seismic characteristics of the area with conditions for urbanization and construction. These maps are rarely made, which speaks of the inadequate seismological basis of the territory of Bosnia and Herzegovina from that period. The city of Banja Luka, which was hit by a catastrophic earthquake in 1969, provided a map of seismic micro-regionalization in the 1970s, but today it is unreliable and needs to be updated. In the meantime, NATO seismic hazard maps of the territory of Bosnia and Herzegovina were made in 2016.

Namely, the map redefined seismic zones in such a way that some urban areas of higher seismic risk, such as Banja Luka, were defined as zones of lower hazard, which opens the possibility for initiating spatial planning mechanisms that could endanger the safety of the population from possible earthquakes. The Institute for Standardization of Bosnia and Herzegovina, together with the competent hydrometeorological institutes in Bosnia and Herzegovina, has expressed readiness to update seismic hazard maps while providing new data that are the result of relevant measurements of tectonic processes in Bosnia and Herzegovina.

Therefore, the research that is the subject of this paper is a contribution to supplementing the data on seismic characteristics of the territory, using GNSS technology that can contribute to the creation of seismic maps at the regional level, but also locally, for seismic micro regionalization. Reliable seismic hazard maps and seismic risk maps are necessary for integrated spatial planning, which, depending on the level of detail, will be able to influence land use planning and technical rules for building facilities and create a sustainable built environment.

3. SEISMOLOGY OF THE REGION OF BOSNIA AND HERZEGOVINA

According to current knowledge of its lithofacies development, the geology of Bosnia and Herzegovina is comprised of various sedimentary, igneous, and metamorphic rocks. According to some rough estimates, about 70% of this geologically rich region belongs to the Mesozoic, about 20% can be dated to the more recent Cainozoic, and about 10% to the earliest Palaeozoic eras [3]. Evidence of tectonic activity can be found throughout the region.

Bosnia and Hercegovina is a Balkan country with a high rate of seismicity. The territory of Bosnia and Herzegovina has had a history of devastating earthquakes. Based on the actual earthquakes in the past 100 years, there are several seismic zones in Bosnia and Herzegovina: the Adriatic zone, the zone of External Dinarides, the zone of the Central Dinarides and the Sava-Vardar zone [4]. The northward movement of the African plate and

its collision with Eurasia causes sliding beneath the European continent, makes complex tectonics, and involves the motions of numerous microplates and regional-scale structures.

The devastating earthquakes hit a large area of Bosnian Krajina on October 26, 27 and 31 December 1969. The magnitude of the earthquakes on 26 October and 31 December was 7-8^{o} MCS, and the earthquake that happened on Monday, 27 October, was much stronger. Its strength in an area of about 9 000 km^2 was 7^{o} MCS, on an area of 1 822 km^2 was 8^{o} MCS, and 68 km^2 was 9^{o} MCS. The earthquake hit the area of 15 Krajina municipalities. The municipalities of Banja Luka, Čelinac and Laktaši and parts of neighbouring municipalities suffered the greatest damage [5]. It is the strongest instrumentally recorded earthquake in Bosnia and Hercegovina proper over the past one hundred years. The quake area had a population of over 750,000 in 803 settlements. In the area of the Banjaluka municipality, 36,276 apartments, 131 school buildings, 61 health institutions, 26 cultural institutions, 28 social institutions, and 38 public administration buildings are registered [6]. Out of 224 commercial companies damaged by the earthquake in Krajina, 112 were in the territory of the Banja Luka municipality [7]. Another strong earthquake hit Banjaluka on 13 August 1981 [8].

The geodynamics of the Bosnia and Herzegovina region is not well understood. Geodynamical GNSS studies of friction forces and normal stresses in fault systems are essential to address this issue. These studies build on the current knowledge gained from previous 3D geodynamical GNSS research.

"It is necessary to invest greater efforts in acquiring modern equipment and increasing the number of qualified personnel, as well as 3D monitoring of active tectonic structures and monitoring contemporary trends in seismology. New seismic sensor stations are needed. There is a need for a quick recovery of geosciences, primarily in Bosnia and Herzegovina. The available studies of geodynamic regions in Bosnia and Herzegovina are very sparse.

The low spatial density of GNSS stations used in modern geodynamical studies in Bosnia and Hercegovina does not provide quality data. The permanent GNSS station “SRJV” in Sarajevo is the region’s only permanent GNSS station. Station “SRJV” is a part of the Central European GPS Geodynamic Reference Network (CEGRN), Figure 1. The permanent station “SRJV” is situated on the roof of the Department of Geodesy at the University of Sarajevo. The station became operational on 11 June 1999.

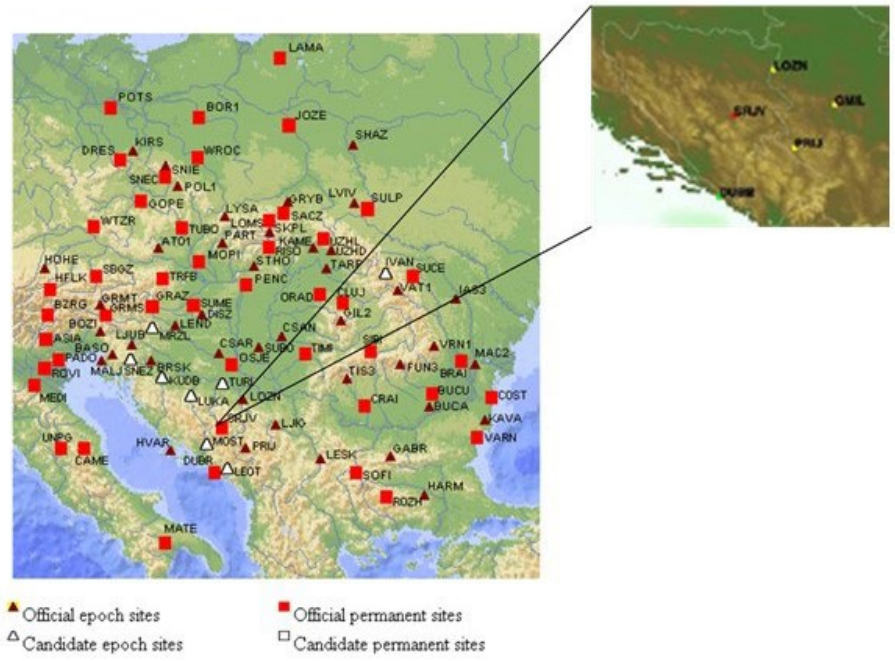

Figure 1. *CEGRN Network [9]*

4. RESULTS OF NUMERICAL RESEARCH

The estimated trend from the time series GNSS station SRJV shows positive values for the horizontal components. The trend shows the increase in the direction of northeastern 28.50 mm/year (Figure 2).

Figure 2. *Ground motion model for GNSS station SRJV (drawing by author)*

Bosnia and Herzegovina have numerous deep and active seismogenic faults. The most complete picture of the tectonic structure in BOSNIA AND HERZEGOVINA was done by Papeš [11]. He has identified deep faults passing through BOSNIA AND HERZEGOVINA, as well as 30 tectonic units. Three main deep faults in the region are distinguished: the Sarajevo Fault, the Banja Luka Fault, and the Konjic Fault. Sarajevo Fault spreads in the direction of NE-SW [11]. Along the transversal deep faults, high seismic activity is identified, while along the Sarajevo Fault (deep fault), the seismic activity is marked from low to moderate level. Sarajevo and Gradiška Faults may experience a series of earthquakes of magnitude M6 on Richter's scale or even higher [11]. Figure 3 shows deep faults, first-order thrusts, second-order thrusts, Tfaults (Thrust fault), Sfaults (Sinistral fault) and Nfaults (Normal fault), and entities the Republic of Srpska, the Federation of Bosnia and Herzegovina and the Brčko District.

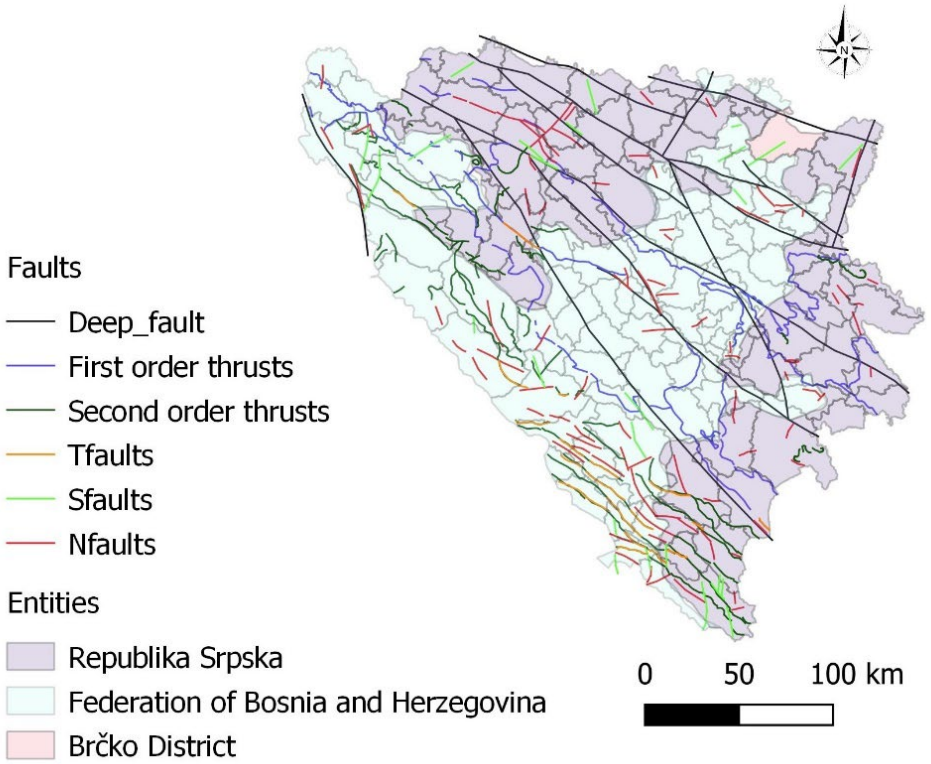

Figure 3. *Map of Bosnia and Herzegovina with deep and active seismogenic faults (drawing by author).*

After that, available historical earthquake catalogues for the region Bosnia and Herzegovina were taken over for the period from 1962 to 2019 year for magnitude 3+ and exported a total of 638 earthquakes [12]. Based on these downloaded data and assessments based on GIS analysis in Qgis, thematic maps are produced showing the area of Bosnia and Herzegovina for magnitude (Figure 4) and depth of earthquakes (Figure 5).

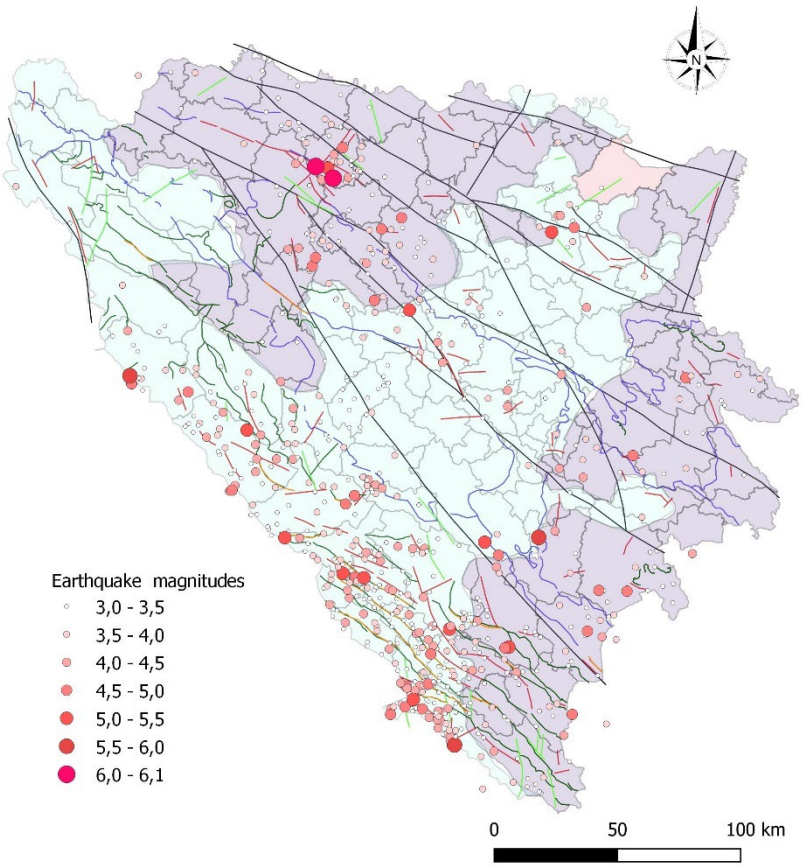

Figure 4. *Map of earthquake magnitude in Bosnia and Herzegovina (drawing by author)*

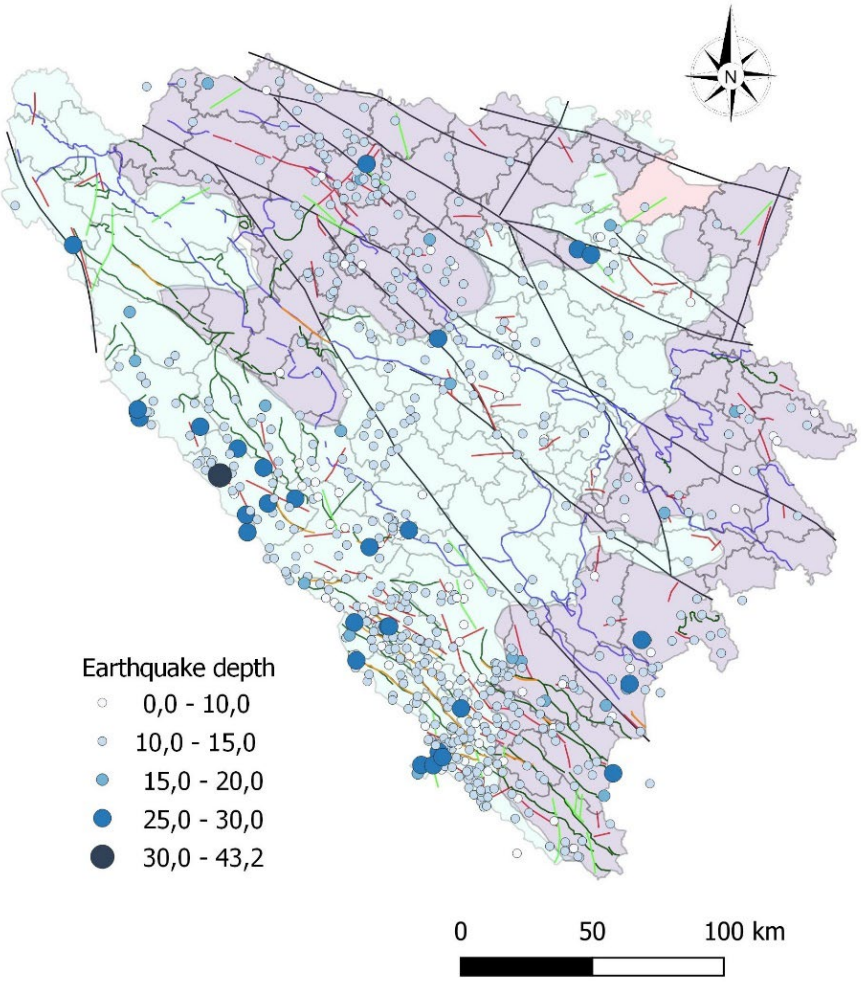

Figure 5. *Map of earthquake depth in Bosnia and Herzegovina (drawing by author)*

Research on the connection between the occurrence of earthquakes and the location of earthquake lines (faults along which earthquakes occur) has shown that they are the strongest historical earthquakes, largely concentrated along the fault zone. Based on the information on seismicity and seismotectonic of Bosnia and Herzegovina, the highest earthquake frequency is in the Herzegovina area, and Livno Canton (the Croatian border and the influence of the Adriatic microplate) and in the north of Bosnia and Herzegovina (Banja Luka).

The permanent danger of catastrophic earthquakes, which occurred relatively often on the territory of Bosnia and Herzegovina and in the immediate vicinity, indicates the necessity to start preventive measures against the harmful effects of earthquakes at the stage of spatial and urban planning and design. Taking into account the specific seismic conditions of the area of the site where facilities are being built by applying the basic principles of seismology, engineering seismology and earthquake engineering in design, it is possible to directly influence the reduction of earthquake consequences to a large extent.

Given that the Banja Luka region has developed a lot urbanistically in the last 20 years and that the city of Banja Luka has a tendency to increase in population, there should not be a reduction in the seismogenic zone in this area. According to Trkulja [14], seismogenic zones in Bosnia and Herzegovina should be followed, as shown in Figure 6.

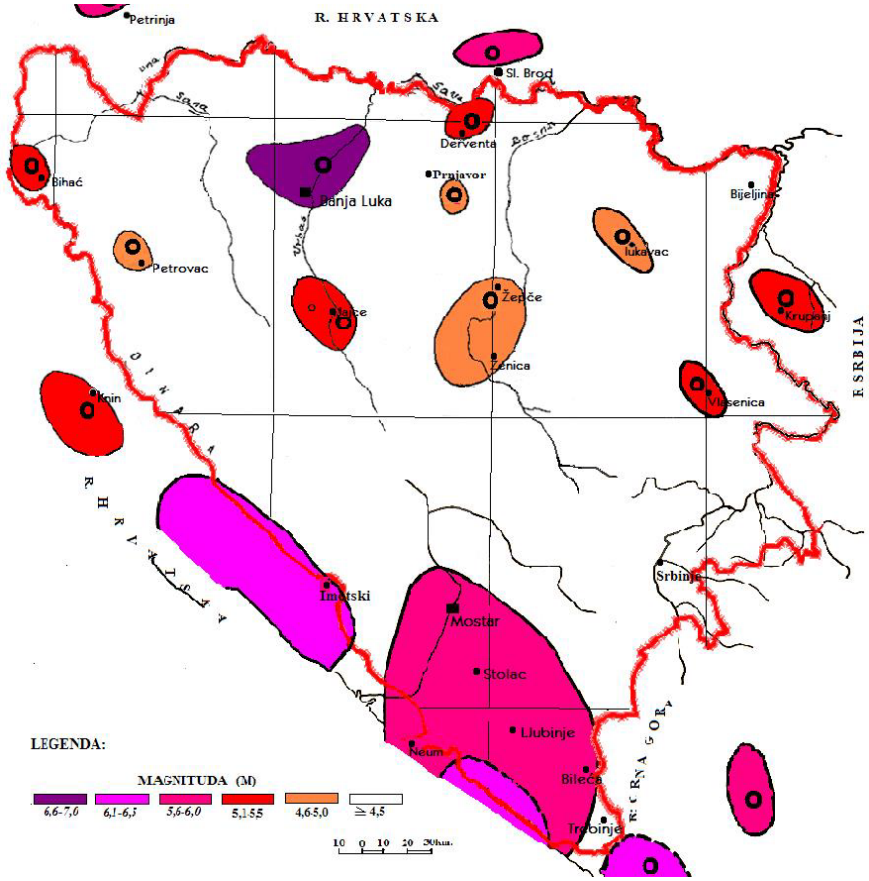

Figure 6. *Map of seismogenic zones in Bosnia and Herzegovina [13]*

5. CONCLUSION

The advanced development of modern geodetic techniques, GNSS, has made a significant contribution to estimating the temporal and spatial change of the earth's surface. Today, GNSS has reached the required accuracy and precision to track surface deformations locally and globally. Today, geodynamics is of key importance in establishing the power of detected and supposed faulting systems in the entire territory of Bosnia and Herzegovina. The Geodynamics of the Bosnia and Herzegovina region has not been sufficiently researched and understood.

Banja Luka and the Livno faults, both in the midsection of the Sarajevo Fault system, should be examined and further researched to be understood. Including regions in Bosnia and Herzegovina in projects, the EUREF (European Reference Frame), and the CERGOP (Central Europe Regional Geodynamics) creates an opportunity for advancement in the field of seismology and earthquake monitoring. Surely, the next steps should follow modern trends in equipment and methodology. One of the steps involves placing new GNSS stations in the

areas of the Banja Luka faults, Livno faults, and the Herzegovina region. New regional and local seismic hazard maps would build on the current knowledge gained from 3D geodynamical GPS studies.

Today, many tectonically active regions are covered by a global real-time GNSS network. In some seismically active regions, the number of GNSS receivers exceeds the seismometers disposed of for earthquake and tsunami monitoring. Recent Developments in High-Rate Geodetic Techniques are invaluable to the rapid evaluation of earthquake hazards. High-rate geodetic data and associated models can help improve ground motion characterization and prediction. Three-dimensional seismic velocity models play an important role in many aspects of seismological research, including strong ground motion modelling, earthquake location, and application of inversion techniques to determine the earth's structure.

It is important to point out that man cannot prevent or eliminate earthquakes because they are natural phenomena related to specific parts of the earth's crust and specific to certain areas. However, by organized and preventive measures, their negative effects can be reduced to a reasonable level.

We can say with certainty that we can fight against the harmful effects of earthquakes only through prevention. This implies that it should be started at the stage of spatial and urban planning by applying mandatory legal regulations in the area of aseismic design and construction so that the effects of earthquakes are mitigated as much as possible. Legal regulation exists. It just needs to be fully respected.

6. REFERENCES

[1] D. Ioane, M. Diaconescu, F. Chitea, G. Garbacea, “Active fault systems and their significance for urban planning in Bucharest, Romania,“ *Springer, Earthquake hazard impact and urban planning*, pp. 15-43, 2014.

[2] S. L. Kramer, “*Geotechnical earthquake engineering.*“ Prentice Hall, Upper Saddle River, N.J., 1996.

[3] S. Čičić, "Geological composition and tectonics of Bosnia and Herzegovina," Sarajevo: Earth Science Institute, 2002.

[4] H. Hrvatović, “Seismotectonic Characteristics of Bosnia and Herzegovina,“ International Conference on Earthquake Engineering, pp. 97–107, Banja Luka, 2009.

[5] Archives of Yugoslavia, Federal Executive Council, Commission for the Assessment of Damage Caused by the Earthquake in Banja Luka and its Surroundings, Report on the Assessment of Damage Caused by the Earthquake in Banja Luka and its Surroundings, Belgrade, May 1970.

[6] ARS, ZZBBK 1969, Proposal of introductory material on events and experiences in the activities of commune authorities in the first days after the catastrophic earthquakes of October 26 and 27, 1969 , 1; AJ, SIV, Commission for the assessment of damage caused by the earthquake in Banja Luka and its surroundings, Report on the evaluation of damage caused by the earthquake in Banja Luka and its surroundings, Belgrade, May 1970, 41.

[7] AJ, SIV, Commission for the assessment of damage caused by the earthquake in Banja Luka and its surroundings , Report on the assessment of damage caused by the earthquake in Banja Luka and its surroundings, Belgrade, May 1970, 10.

[8] N. Ožegović, “BANJALUKA (1969-1991),” Doctoral Dissertation, University of Belgrade, Faculty of Philosophy, Belgrade, 2021.
[9] Interference Monitoring in the Central European GPS Geodynamic Reference Network István Fejes FÖMI Satellite geodetic Observatory Penc, Hungary ESF Workshop on “Active Protection of Passive Radio Services: towards a concerted strategy.” 28-29 October 2004, Cagliari, Italy
[10] M. Bevis, J. Bedford, D. J. Caccamise, “The Art and Science of Trajectory Modelling,“ Geodetic Time Series Analysis in Earth Science, pp. 1-27, 2019.
[11] Papeš, “Tectonic Composition of the Terrritory of Bosnia and Hercegovina. (In Bosnian: Tektonska građa teritorije SR BiH.) Unpublished report for Science Fund of Bosnia-Hercegovina,” Geoinstitut Ilidža, Sarajevo, Bosnia, 1988.
[12] „Search Earthquake Catalog.“ Internet:https://earthquake.usgs.gov/earthquakes/search/, [May 15, 2024].
[13] Drago Trkulja, B. Sikošek, and Vanja Olujić, Earthquakes of Banja Luka Region, 3rd ed. Banja Luka: Zavod za izgradnju, 2009.

AUTHOR'S BIOGRAPHIES

Tanja Đukanović

Tanja Đukanović was born on 22 February 1994 in Nevesinje. She completed her basic academic studies in 2017 at the Faculty of Architecture, Civil Engineering and Geodesy, study program Geodesy, University of Banja Luka, where she also obtained her master's degree in 2021. She is a PhD student at the Faculty of Civil Engineering, University of Belgrade. She has been employed at AGGF since 2019. She is a teaching assistant on a group of course units in the scientific field of geodetic surveying.

Sanja Tucikešić

She was born in Banja Luka on 13 May 1981. She graduated in 2008 from the Faculty of Civil Engineering, University of Belgrade. She obtained her PhD from the Faculty of Civil Engineering of the University of Belgrade in 2020. In her scientific research, she deals with the analysis and modelling of tectonic movements and deformations of the earth's crust using GNSS technology, as well as with calibration and quality control of geodetic instruments and laboratory testing of scales in geodesy, civil engineering and other related areas, as well as volumetric scales. She is employed at the Faculty of Architecture, Civil Engineering and Geodesy as an assistant professor.

Snježana Cvijić-Amulić

Snježana Cvijić Amulić was born on August 9, 1971 in Jajce. She graduated from the Faculty of Science and Mathematics of the University of Novi Sad in 2002 in the Department of Physics. She received her master's degree at the Faculty of Mining and Geology of the University of Belgrade in 2016 (seismic and seismology). She specialized in the analysis, synthesis and interpretation of seismological data. She was additionally educated through several months of international training and courses, participated in several international projects and was part of the working group of the Technical Committee for the development and adoption of the National Annex for the implementation of Eurocode 8.

ТЕКТОНСКА ГЕОДЕЗИЈА КАО ДОПУНА ПОДАЦИМА У СЕИЗМОЛОГИЈИ

Сажетак: Геодезија и њена висока прецизност је важан инструмент за проучавање активне тектонике и презентацију модела кретања чврстих дијелова Земље. Деформације изазване земљотресом представљају битне информације за дефинисање сеизмогених зона. Да би се измјерила брзина деформисања Земљине коре између, током и после земљотреса, морају се извршити прецизна мјерења на зиду самог расједа или на систему повезаних активних расједа. У Босни и Херцеговини је ниска просторна густина ГНСС станица које се користе у савременим геодинамичким студијама. Перманентна ГНСС станица "CPJB", у Сарајеву, једина је стална ГНСС станица у региону. Она је дио ЕУРЕФ Перманенте ГНСС мреже и у том сегменту има ажурне доступне временске серије из ГНСС координата.

Кључне ријечи: *ГНСС станица CPJB, сеизмогени расједи, сеизмогене зоне.*